

University of Rhode Island

DigitalCommons@URI

Open Access Master's Theses

2012

SYNTHESIS AND BIOASSAY OF NOVEL HYBRID ANTIMICROBIAL PEPTIDES (AMPS), DESIGNED TO INCREASE THERAPEUTIC ACTIVITY AND DECREASE HEMOLYSIS

David E. Ryder

University of Rhode Island, ceec55@hotmail.com

Follow this and additional works at: <https://digitalcommons.uri.edu/theses>

Terms of Use

All rights reserved under copyright.

Recommended Citation

Ryder, David E., "SYNTHESIS AND BIOASSAY OF NOVEL HYBRID ANTIMICROBIAL PEPTIDES (AMPS), DESIGNED TO INCREASE THERAPEUTIC ACTIVITY AND DECREASE HEMOLYSIS" (2012). *Open Access Master's Theses*. Paper 98.

<https://digitalcommons.uri.edu/theses/98>

This Thesis is brought to you by the University of Rhode Island. It has been accepted for inclusion in Open Access Master's Theses by an authorized administrator of DigitalCommons@URI. For more information, please contact digitalcommons-group@uri.edu. For permission to reuse copyrighted content, contact the author directly.

**SYNTHESIS AND BIOASSAY OF NOVEL HYBRID
ANTIMICROBIAL PEPTIDES (AMPS), DESIGNED
TO INCREASE THERAPUTIC ACTIVITY AND
DECREASE HEMOLYSIS**

BY

DAVID E. RYDER

**A THESIS SUBMITTED IN PARTIAL FULFILLMENT OF THE
REQUIREMENTS FOR THE DEGREE OF
MASTERS OF SCIENCE
IN
BIOCHEMISTRY**

UNIVERSITY OF RHODE ISLAND

2012

MASTER OF SCIENCE THESIS
OF
DAVID E. RYDER

APPROVED:

Thesis Committee: Linda Hufnagel, PhD
Professor,
Cell and Molecular Biology

Joanna H. Norris, PhD
Associate Professor,
Biological Sciences

Major Professor Lenore M. Martin, PhD
Associate Professor,
Cell and Molecular Biology

Nasser H. Zawia, PhD
DEAN OF THE GRADUATE SCHOOL

UNIVERSITY OF RHODE ISLAND
2012

ABSTRACT

There is currently a critical health issue of global concern; there are many types of bacterial pathogens that have evolved a resistance to many common, conventional antibiotics. *In silico* structural tools can be used to identify antimicrobial peptide (AMP) sequence modifications that result in better antibacterial therapeutics without increasing human erythrocyte hemolysis. Out of the five AMPs designed for this Thesis project, two were minor modifications of an existing Pleurocidin-Dermaseptin (P-DER) hybrid sequence. The *in silico* structural design strategies were used to determine on a biophysical level what made P-DER so effective. The tools included the Chou-Fasman secondary structure algorithm, the Edmondson helical wheel model, and the Hopp-Woods hydrophilicity scale. These design insights were used to model the remaining three AMPs. These novel, hybrid AMPs were created by combining the *N*-terminal region from CEME with the entire sequences of three other AMPs: Ranatuerin 6, VesCP-M and Temporin. Although all five hybrid peptides were synthesized, only the modified P-DER sequences were purified and characterized. The AMPs were tested by varying the concentration of each peptide in contact with the bacteria or human red blood cells (RBC). The dose-dependant cytotoxic and hemolytic effect of those peptides on cells was determined. Screening for bacterial growth inhibition was performed *in vitro* against two species each of representative gram positive and gram negative bacteria. These tests on the AMPs were to see if it was active against a broad spectrum of microbial pathogens that have diverse types of cell surfaces, with the caveat that these AMPs are not suitable for therapeutic use if they cause significant human RBC hemolysis.

ACKNOWLEDGMENTS

I would like to thank Dr. Aftab Ahmed from the University of Rhode Island INBRE lab, and Dr. James Clifton from the Brown University EPSCoR Proteomics Lab for their assistance in characterizing my peptides. I would also like to thank Dr. Lenore Martin for her able assistance and encouragement in the completion of this project.

I would like to thank the following academic associates for all of their input, assistance and encouragement during the process of the completion of this study: Dr. Eric Hall, Mrs. Victoria Hittenger, Dr. Vanina Guidi, Dr. Cynthia Graham Brittan, and Dr. George Dombi.

I would like to acknowledge and thank the following family members for their support, encouragement, and for their belief in my talent: my mother-in-law Mrs. Leona Ilowitz, my cousin, Mrs. Pearl Gershon, and my late uncle, Dr. Eric Koch.

I also would like to thank my dear friends for being there and encouraging me to go on during a long, tedious process: Mr. Jeffrey Wagner, Ms. Deborah Ebbitt, Mr. Scott McCarthy, Mrs. Andrea Charette-Couto, Mr. Scott Smith, Mrs. Jacqueline Blanchette, and the late Dr. Solomon M. Marmor; who provided me with insight and professional knowledge during the initial stages of this project.

This thesis is dedicated to my wife and best friend, Mrs. Betty Ilowitz-Ryder; who has been an interminable proponent of my personal as well as professional goals and has made many sacrifices to allow for their actualization. I could not have accomplished this project without her.

This thesis is also dedicated to the memory of Mr. Sol Mitchell Ilowitz; father, father-in-law, and dear friend, whose desire in life was to have educated children. The continuation of my education and completion of this project is in support of that wish.

TABLE OF CONTENTS

ABSTRACT	ii
ACKNOWLEDGMENTS	iii
TABLE OF CONTENTS	v
LIST OF TABLES	vi
LIST OF FIGURES	ix
CHAPTER 1	1
INTRODUCTION	1
CHAPTER 2	5
REVIEW OF PERTINANT LITERATURE	5
CHAPTER 3	26
MATERIALS AND METHODS	26
CHAPTER 4	51
RESULTS	51
CHAPTER 5	95
CONCLUSIONS.....	95
APPENDICES	101
BIBLIOGRAPHY	132

LIST OF TABLES

TABLE	PAGE
Table 1: Antimicrobial Sequence Design. The first seven antimicrobial peptide sequences were derived from nature. The two listed extant hybrids were made by other research labs. The last five hybrid sequences were novel designs.	3
Table 2: Extant and Novel Antimicrobial Peptide Sequences. This table shows one design strategy for making hybrid AMPs (Jia <i>et al</i>). All sequences were aligned, and color coded to indicate which segments from the natural AMPs are incorporated into the Novel Peptide Hybrids. The first four sequences were derived from nature. Pleurocidin-amide had a C-terminal amide designed to decrease hemolysis; P1 and P1-amide had an N-terminal lysine to increase cationic charge. All the remaining novel sequences were hybrids: P-DER combined portions of Dermaseptin and Pleurocidin; P-CER used Ceratoxin and Pleurocidin; P-M used Pleurocidin and Misgurin; DER-M used Dermaseptin, Pleurocidin and Misgurin; CER-M: used Ceratoxin, Pleurocidin and Misgurin.	16
Table 3: AMP Activity against Fish and Human Pathogenic Bacteria. The peptides made by Jia <i>et al</i> were assayed against representative species of gram positive and gram negative species. The Minimum Inhibitory Concentration (MIC) was expressed as the lowest concentration of AMPs that inhibited overnight bacterial growth by 50%. Results were as follows: Misgurin and CER-M were inactive, Pleurocidin, P1, P-CER, P-M, and DER-M were only active against specific species; Pleurocidin amide, P1 amide and P-DER were broad spectrum active in potency.	17
Table 4: AMP Activity and Human RBC Hemolysis. The peptides made by Strandberg <i>et al</i> were assayed against representative species of gram positive and gram negative species, and the MICs were determined. They were also assayed against Human erythrocytes and the amount required causing 50% hemolysis after 1 hour was determined. PGLa-NH ₂ , the first AMP sequence was from nature. PGLa-OH had exactly the same sequence, but its C-terminus was a free acid. The remaining AMPs were synthetic in design as part of an effort to determine properties that made effective AMPs. MSI-103 used only 4 residue types, but it was nonhemolytic; MAP used only 3 residue types, and it was extremely hemolytic. PGLa-OH and MAP-OH were inactive against the bacterial species; MSI-103-OH and MAP-NH ₂ were only active against specific species; PGLaNH ₂ , and MSI-103-NH ₂ were broad spectrum active. Both of the MAP peptides were hemolytic, so only the PGLaNH ₂ , and MSI-103-NH ₂ sequences were useful at therapeutic doses.	19

Table 5: Template for an Antibacterial Activity Assay. Results were monitored by scanning 96-well plates at 630 nm. The contents were as follows: Media (Mueller-Hinton broth only), Bac (*Escherichia coli*, *Enterococcus faecalis*, *Staphylococcus aureus*, or *Pseudomonas aeruginosa*), Dil (Dilution), AMP (LM7-1 or LM7-2), Antibio (active antibiotic), 6 M NaOH (total cell kill solution). The columns are different experimental conditions; the rows are replicates.

..... 47

Table 6: Typical Setup for a Peptide-induced Hemolysis Assay. The template shows volumes utilized throughout the various experimental runs. All 5 tubes used a standardized concentration of human RBC. The AMP amounts tested varied from tube to tube, with the PBS buffer making up the difference in volume.

..... 49

Table 7: Summary of SPPS Coupling Reactions for Peptide LM7-1. This table shows how many rounds of coupling reactions were required to complete the 27-residue synthetic peptide. The AA position numbers started out at the *N*-terminal. As shown in the middle 3 columns, some Boc amino acids required more than one round of coupling to fully saturate the free amino groups. Eq is equivalents; it indicated how much excess Boc-amino acids were added on each round of coupling relative to the original amount of free amino groups on the resin. AA (mmol) indicated the actual amounts of amino acids used for each coupling reaction. The end dates indicated when an incoming Boc amino acid had fully coupled. Coupling number was the order in which the Boc amino acids were added to the peptide-resin chain; as the synthesis order was reversed from that of enzymatic biosynthesis.

..... 52

Table 8: Summary of Coupling Reactions for Peptide LM7-2. This table shows how many rounds of coupling reactions were required to complete the 27 residue synthetic peptide. The AA positions started out at the *N*-terminus. As shown in the middle 3 columns, some Boc amino acids required more than one round of coupling to fully saturate the free amino groups. Eq is equivalents; it indicated how much excess Boc-amino acids were added on each round of coupling relative to the original amount of free amino groups on the resin. AA (mmol) indicated the actual amount of amino acids used for each coupling reaction. The end dates indicated when an incoming Boc amino acid had fully coupled. Coupling number was the order in which the Boc amino acids were added to the peptide-resin chain as the synthesis order was reversed from that of enzymatic biosynthesis.

..... 59

Table 9: Coupling Efficiency of LM7-1 versus LM7-2. This graph compares how many repeated couplings were required in order to completely attach incoming Boc-AA onto the growing peptide chains of LM7-1 (Blue bars) and LM7-2 (Violet bars). The number of coupling repetitions needed is plotted against peptide sequence numbers from the *N*-terminus to the *C*-terminus.

..... 62

Table 10: MALDI Results and Sample Pooling for LM7-1. The Peptide Rank label indicates how pure the pooled peptide samples were based on MALDI-TOF mass spectrometry results. The Observed m/z indicates the observed mass charge ratios. The Dried Peptide indicates where the samples originated from. The estimated mass of the purified samples is based on visual inspection.

..... 73

Table 11: Sample Pooling for LM7-2. The Peptide Rank label indicates how the peptide samples were pooled based on RP-HPLC peak elution order. The Dried Peptide indicates which HPLC runs the samples originated from that were combined on the final pools. The estimated yields of the purified peptides were defined by weighing them on an electronic balance.

..... 74

Table 12: Minimum Inhibitory Concentrations (MICs) of LM7-1 and LM7-2. The table lists concentration of LM7-1, and LM7-2 sufficient to inhibit 50% of bacterial growth at 24 hours of incubation, as compared to the uninhibited control.

..... 91

Table 13: Minimum Hemolytic Concentrations (HC₅₀) of LM7-1 and LM7-2 at 1 hour. This table lists concentration of LM7-1 and LM7-2 sufficient to lyse 50% human red blood cells (HC₅₀) at 1 hour of incubation.

..... 94

LIST OF FIGURES

FIGURE	PAGE
Figure 1: Generalized Lipopolysaccharide Structure in Gram negative Bacteria. Lipopolysaccharides (LPS) are structural polysaccharides anchored in the outer membrane of gram negative Bacteria, facing in the extracellular direction. LPS is composed of 3 main components: The Lipid A subunit, which is comprised of the fatty acid tail and glucosamine carbohydrate; an invariant Core Polysaccharide region containing phosphate groups; an <i>O</i> -specific polysaccharide outer portion that includes variably repeating polysaccharide chains.	7
Figure 2: Glycerol Teichoic Acid Structure in Gram Positive Bacteria. Teichoic acids are important chelating polysaccharides found in the cell wall of gram positive bacteria. They are composed of alternating phosphate groups, and sugars with amino acid side chains.	8
Figure 3: Phospholipid Structures. Phospholipids are found in all living cells as components of the cell membrane. All have fatty acid tails attached to a glycerol sugar that also links to a head group via a phosphate group. The examples are Cardiolipin (CLP), Phosphatidylglycerol (PG), Phosphatidylcholine (PC), Phosphatidylserine (PS), and Phosphatidylethanolamine (PE).	8
Figure 4: AMP Bacterial Membrane Attack Models. A) Aggregate Pore Model: unstructured AMPs form α -helices in the cell membrane, and aggregate to form multimeric pores. B) Carpet Model: unstructured AMPs form α -helices in the cell membrane and destabilize the cell membrane. C) Torroidal Pore Model: unstructured AMPs form α -helices in the cell membrane and pull the bilayer open.	10
Figure 5: Chou-Fasman Secondary Structural Model of P-DER. The three line graphs show the three common secondary structures: alpha helices (green), beta sheets (red), and beta turns (blue). The likelihood of formation of the secondary structure configuration is plotted against the AMP sequence from the <i>N</i> -terminus to the <i>C</i> -terminus. In this example, P-DER has two strong alpha helical sequences at the <i>N</i> -terminal and <i>C</i> -terminal ends, separated by an unstructured domain.	21

Figure 6: Edmundson helical wheel of P-DER. The top diagram models an *N*-terminal end-on view of an alpha helix. Residues are assigned to 4 different categories: hydrophobic side chains (green), hydrophilic side chains (maroon), acidic side chains (red) and basic side chains (blue). P-DER was strongly amphipathic, with well developed hydrophilic and hydrophobic faces. The bottom diagram models a helical net, which is a side view of an unrolled α -helix.

..... 22

Figure 7: Hopp-Woods Hydrophilicity Scale of P-DER. Hydrophobic to hydrophilic character was plotted against the AMP sequence from the *N*-terminus to the *C*-terminus. In this case, the P-DER AMP had a strongly hydrophilic *N*-terminal region, followed by a more hydrophobic *C*-terminal region.

..... 23

Figure 8: Direct DCC Catalyzed Coupling Protocol. The *N*-Boc-L-amino acid is activated by coupling to *N,N'*-dicyclohexylcarbodiimide, forming the *O*-acyl-isourea leaving group and directly reacts with the free amino group on the peptide-resin. The result is an extended peptide chain.

..... 33

Figure 9: Pre-formed Symmetric Anhydride Protocol. The *N*-Boc-L-amino acid is activated by coupling to *N,N'*-dicyclohexylcarbodiimide, and then the same *N*-Boc-L-amino acid replaces the *O*-acyl-isourea group. The pre-formed symmetric anhydride reacts with the free amino groups, and produces a peptide bond with one of the remaining *N*-Boc-L-amino acid residues as a leaving group. The result is an extended peptide chain.

..... 34

Figure 10: Direct HOBt Coupling Protocol. The *N*-Boc-L-amino acid is pre-activated by coupling to *N,N'*-dicyclohexylcarbodiimide, and then *N*-hydroxybenzotriazole (HOBt) replaces the *O*-acyl-isourea functional group. The exposed amino group reacts with the HOBt active ester to produce a novel peptide bond, and the HOBt leaving group is removed. The result is an extended peptide chain.

..... 35

Figure 11: Direct HBTU Coupling Protocol. In this coupling method, the *N*-Boc-L-amino acid is pre-activated by coupling to 2-(1H-benzotriazole-1-yl)-1,1,3,3-tetramethyluronium hexafluoride phosphate (HBTU). The tetramethyluronium leaving group on the active ester is replaced by HOBt. The exposed amino group reacts with the HOBt active ester to produce a novel peptide bond, and the HOBt leaving group is removed. The result is an extended peptide chain.

..... 36

Figure 12: Generic Gel Filtration Chromatography Plot. In this hypothetical graph, absorbance at 280 nm is plotted against Fraction number. In a typical post-HF cleavage peptide purification run, there are three major volumes produced. The first column “void” volume represents the total liquid excluded from the stationary phase and in the tubing. The second column volume represents the protein products not retained by the gel filtration stationary phase. The third column volume represents protein fragments, HF scavengers and salts retained by the gel filtration stationary phase.

..... 41

Figure 13: Generic Reversed Phase High Performance Liquid Chromatography Sample Peak. In this hypothetical graph, absorbance at 220 nm is plotted against time in minutes. A single, generic protein peak is shown. The peak has background absorbance before the peptide elutes, the leading edge & mid-peak regions contain the purest product, and the peak tail is impure.

..... 43

Figure 14: Spectrophotometer Multiwavelength scan of soluble Hemoglobin from 200-600 nm. In this plot, absorbance is plotted against wavelength in nanometers. The peak maxima at 215 nm, 270 nm and 350 nm correspond to peptide absorption inherent in all large proteins. The peak maxima at 414 nm, 540 nm and 580 nm are specific to oxygenated hemoglobin.

..... 50

Figure 15: Advantages of 1-hydroxybenzotriazole over *O*-acylisourea as a racemization suppressor. This figure shows the possible sites for nucleophilic attack of the lone pair electrons on a free *N*-terminus amine group on two possible coupling reagents. Path 1 shows the preferred location of attack for the amine group lone pair electrons to the carbonyl in the *O*-acylisourea functional group, leading to peptide extension. Path 2 shows an alternate site of attack; the *O*-acylisourea group can draw electrons away from the α -carbon on the Boc-AA, potentially leading to chirality inversion. Path 3 shows the preferred location of attack for the amine group lone pair electrons to the carbonyl in the HOBt active ester functional group, leading to peptide extension. Path 4 shows an unlikely alternate site of attack; the oxybenzotriazole group has reduced electron withdrawing potential compared to the *O*-acylisourea group. Thus, the electrons are less likely to attack the α -carbon on the Boc-AA.

..... 54

Figure 16: LM7-1 Crude Peptide Eluent G-25 Sephadex® Gel Filtration Run.

This graph shows a representative liquid chromatography run that passed a crude LM7-1 AMP wash sample through a 2.5 x 86.0 cm bed of G25 Sephadex® at a flow rate of 0.6 ml/min. The graph compares absorbance at 280 nm versus Fraction number. Note that there are two peaks: the purified LM7-1 Peak A (Fractions 110-143), and the HF scavenger Peak B (Fractions 144-160).

..... 65

Figure 17: LM7-1 Crude Peptide Product G-25 Sephadex® Gel Filtration Run.

This graph shows a crude peptide liquid chromatography run that passed a crude LM7-1 AMP 10% acetic acid extraction sample through a 2.5 x 86.0 cm bed of G25 Sephadex® at a flow rate of 0.6 ml/min. Based on the results shown in Figure 11, the first 80 fractions were discarded and then the remaining fractions were recorded and collected for analysis. The graph compares absorbance at 280 nm versus Fraction number. Note that there are two peaks: the purified LM7-1 Peak A (Fractions 12-41), and the HF scavenger Peak B (Fractions 42-80). As the peptide was concentrated to ~25 mg/ml, the absorbance of the middle of the peaks maxed out the UV detector. Exact peak boundaries were determined by scanning the diluted samples in the off scale regions.

..... 66

Figure 18: LM7-1 Purified by HPLC Preparative Reversed Phase HPLC with a three-step acetonitrile gradient (Run 4). The purified Peak A-2 region (Run # 4) of the LM7-1 AMP eluent from the G-25 column was run through a C₁₈Vydac preparatory, RP-HPLC column (300Å, 2.2 x 25.0 cm, 218 TP) to purify the desired peptide before running bioassays. The flow rate was 2.9 ml/min. The mobile phase gradient consisted of 20%, 35%, and 40% aqueous acetonitrile, followed by a 100% methanol column wash. The graph plots absorbance at 280 nm versus Fraction number.

..... 69

Figure 19: LM7-1 Purified by Preparative Reversed Phase HPLC with a six-step acetonitrile gradient (Run 14). The purified Peak A-2 region (Run 14) of the LM7-1 AMP eluent from the G-25 column was run through a C₁₈Vydac preparatory RP-HPLC column (300Å, 2.2 x 25.0 cm, 218 TP). The mobile phase gradient consisted of 5%, 20%, 25%, 35%, 40% and 70% aqueous acetonitrile. The flow rate was 2.9 ml/min. The graph plots absorbance at 280 nm versus Fraction number.

..... 70

Figure 20: LM7-1 Purified Preparative Reversed Phase HPLC with a six-step acetonitrile gradient (Run 18). The purified Peak A-2 region (Run 14) from the LM7-1 AMP was run through a C₁₈Vydac preparatory RP-HPLC column (300Å, 2.2 x 25.0 cm, 218 TP). The mobile phase gradient consisted of 5%, 20%, 25%, 30%, 35% and 70% aqueous acetonitrile. The flow rate was 2.9 ml/min. The graph plotted absorbance at 280 nm versus Fraction number.

..... 71

Figure 21: Antimicrobial Activity Assay of LM7-1 against *E.coli*. The graph shows Optical density at 630 nm versus time for exposure in hours. The red bars show the uninhibited growth of the bacteria. The remaining bars (orange, green, blue and violet) show the amount of bacterial inhibition observed with increasing concentrations of peptide LM7-1. The error bars display one standard deviation of variance. At the 24 hour time point, compared to the uninhibited *E.coli* growth (‡), the 0.333 µg/ml peptide trial shows a significant (*) difference [0.05>P>0.001], and the 167/333 µg/ml peptide dilutions show extremely significant (**) differences [0.001>P] in bacterial growth.

..... 79

Figure 22: Antimicrobial Activity Assay of LM7-1 against *P.aeruginosa*. The graph shows Optical density at 630 nm versus time for exposure in hours. The red bars show the uninhibited growth of the bacteria. The remaining bars (orange, green, blue and violet) show the amount of bacterial inhibition observed with increasing concentrations of peptide LM7-1. The error bars display one standard deviation of variance. At the 24 hour timepoint, compared to the uninhibited *P.aeruginosa* growth (‡), the 167/333 µg/ml peptide trials show significant (*) differences [0.05>P>0.001] in bacterial growth.

..... 80

Figure 23: Antimicrobial Activity Assay of LM7-1 against *E.faecalis*. The graph shows Optical density at 630 nm versus time for exposure in hours. The red bars show the uninhibited growth of the bacteria. The remaining bars (orange, green, blue and violet) show the amount of bacterial inhibition observed with increasing concentration of peptide. The error bars display one standard deviation of variance. In the 24 hour timepoint, compared to the uninhibited *E.faecalis* growth (‡), the 0.333 µg/ml peptide trial shows a significant (*) difference [0.05>P>0.001], and the 167/333 µg/ml peptide trials show extremely significant (**) differences [0.001>P] in bacterial growth.

..... 81

Figure 24: Antimicrobial Activity Assay of LM7-1 against *S.aureus*. The graph shows Optical density at 630 nm versus time for exposure in hours. The red bars show the uninhibited growth of the bacteria. The remaining bars (orange, green, blue and violet) show the amount of bacterial inhibition observed with increasing concentration of peptide. The error bars display one standard deviation of variance. In the 24 hour timepoint, compared to the uninhibited *S.aureus* growth (‡), only the 333 µg/ml peptide trial shows an extremely significant (**) difference [0.001>P] in bacterial growth.

..... 82

Figure 25: Antimicrobial Activity Assay of LM7-2 against *E.coli*. The graph shows Optical density at 630 nm versus time for exposure in hours. The red bars show the uninhibited growth of the bacteria. The remaining bars (orange, green, blue and violet) show the amount of bacterial inhibition observed with increasing concentration of peptide. The error bars display one standard deviation of variance. In the 24 hour timepoint, compared to the uninhibited *E.coli* growth (‡), the 0.0333 µg/ml peptide trial shows a significant (*) difference [0.05>P>0.001], and the 167/333 µg/ml peptide trials show extremely significant (**) differences [0.001>P] in bacterial growth.

..... 83

Figure 26: Antimicrobial Activity Assay of LM7-2 against *P.aeruginosa*. The graph shows Optical density at 630 nm versus time for exposure in hours. The red bars show the uninhibited growth of the bacteria. The remaining bars (orange, green, blue and violet) show the amount of bacterial inhibition observed with increasing concentration of peptide. The error bars display one standard deviation of variance. In the 24 hour timepoint, compared to the uninhibited *P.aeruginosa* growth (‡), the 0.0333/0.333 µg/ml peptide trials show significant (*) differences [0.05>P>0.001], and the 167/333 µg/ml peptide trials show extremely significant (**) differences [0.001>P] in bacterial growth.

..... 84

Figure 27: Antimicrobial Activity Assay of LM7-2 against *E.faecalis*. The graph shows Optical density at 630 nm versus time for exposure in hours. The red bars show the uninhibited growth of the bacteria. The remaining bars (orange, green, blue and violet) show the amount of bacterial inhibition observed with increasing concentration of peptide. The error bars display one standard deviation of variance. In the 24 hour timepoint, compared to the uninhibited *E.faecalis* growth (‡), the 167/333 µg/ml peptide trials show extremely significant (**) differences [0.001>P] in bacterial growth.

..... 85

Figure 28: Antimicrobial Activity Assay of LM7-2 against *S.aureus*. The graph shows Optical density at 630 nm versus time for exposure in hours. The red bars show the uninhibited growth of the bacteria. The remaining bars (orange, green, blue and violet) show the amount of bacterial inhibition observed with increasing concentration of peptide. The error bars display one standard deviation of variance. In the 24 hour timepoint, compared to the uninhibited *S.aureus* growth (‡), the 167/333 µg/ml peptide trials show extremely significant (**) differences [0.001>P] in bacterial growth.

..... 86

Figure 29: Dose Response Assay of LM7-1/LM7-2 against *E.coli* Growth. The graph shows 24 hours of growth with an Optical density at 630 nm versus LM7-1 (blue line) and LM7-2 (green line) concentration in mg peptide/ml total suspension volume. The error bars display one standard deviation of variance. Only the 0.000333 mg/ml doses of LM7-1 and LM7-2 are extremely significantly (**) different from each other [0.001>P]. The MIC is 0.080 mg/ml for LM7-1, and 0.070 mg/ml for LM7-2.

..... 87

Figure 30: Dose Response Assay of LM7-1/LM7-2 against *P.aeruginosa* Growth. The graph shows 24 hours of growth with an Optical density at 630 nm versus LM7-1 (blue line) and LM7-2 (green line) concentration in mg peptide/ml total suspension volume. The error bars display one standard deviation of variance. The 0.0033 mg/ml the dose of LM7-1 and LM7-2 are significantly (*) different from each other [0.05>P>0.001], and the 0.000333/0.167/0.333 mg/ml doses of LM7-1 and LM7-2 are extremely significantly (**) different from each other [0.001>P]. The MIC is >0.333 for LM7-1, and 0.130 mg/ml for LM7-2.

..... 88

Figure 31: Dose Response Assay of LM7-1/LM7-2 against *E.faecalis* Growth. The graph shows 24 hours of growth with an Optical density at 630 nm versus LM7-1 (blue line) and LM7-2 (green line) concentration in mg peptide/ml total suspension volume. The error bars display one standard deviation of variance. The 0.333 mg/ml doses of LM7-1 and LM7-2 are significantly (*) different from each other [0.05>P>0.001], and the 0.000333/0.00333/0.167 mg/ml doses of LM7-1 and LM7-2 are extremely significantly (**) different from each other [0.001>P]. The MIC is 0.145 mg/ml for LM7-1, and 0.130 mg/ml for LM7-2.

..... 89

Figure 32: Dose Response Assay of LM7-1/LM7-2 against *S.aureus* Growth. The graph shows 24 hours of growth with an Optical density at 630 nm versus LM7-1 (blue line) and LM7-2 (green line) concentration in mg peptide/ml total suspension volume. The error bars display one standard deviation of variance. The 0.333 mg/ml doses of LM7-1 and LM7-2 are significantly (*) different from each other [0.05>P>0.001], and the 0.000333/0.00333 mg/ml doses of LM7-1 and LM7-2 are extremely significantly (**) different from each other [0.001>P]. The MIC is 0.305 mg/ml for LM7-1, and 0.165 mg/ml for LM7-2.

..... 90

Figure 33: Dose Response Assay of LM7-1/LM7-2 Human RBC Hemolysis. The graph displays absorbance at 419 nm (maximum hemoglobin absorbtion) of human red blood cells incubated for 1 hour growth with LM7-1 (blue line) and LM7-2 (green line) versus concentration in mg peptide/ml total suspension volume. There was only one replicate per trial, so there are no error bars or statistical significance displayed.

..... 93

CHAPTER 1

INTRODUCTION

There is an ever growing need to develop new types of drugs that can inhibit or kill antibiotic-resistant bacterial pathogens. Antimicrobial peptides (AMPs) are potentially part of the answer (Jiang *et al*, 2011). Antimicrobial peptides are short proteins that are naturally secreted by many organisms as part of the host defense system against bacteria, fungi, viruses and eukaryotic parasites. The search for undiscovered natural AMP sequences and the development of synthetic AMP analogs has become urgent due to the emergence of resistance to conventional antibiotics by many species of microscopic pathogens (Toke, 2005). In vertebrates, they form a portion of the innate immune system and can be secreted constitutively or when triggered by a specific stimulus. For a variety of reasons, antimicrobial peptides are seen by many microbiologists as an attractive alternative to the chemically unique antibiotics (Zasloff, 2002). Conventional antibiotics typically act on one specific bacterial structural or metabolic process; this gives the bacterial pathogens a pathway to evolve around the drug (Jiang *et al*, 2011). In addition, novel antibiotics are becoming much more expensive to develop and market, and there has been a measurable decline in how many are created annually (Vicente *et al*, 2006). In contrast, many AMPs, regardless of chirality, target a general bacterial structure rather than a specific weak point; this makes it more difficult for pathogens to evolve resistance (Toke, 2005). Many AMPs have a wide range of activity against many pathogenic species, yet do not significantly damage host cells; this is likely due to key structural differences in target cell surfaces. Cationic AMPs are attracted to negatively

charged bacterial cell membrane, and cell wall components; the negative charges are used to chelate divalent cations vital to bacterial metabolism. Many cationic AMPs have the ability to reach and disrupt the cell membrane (Toke, 2005). Many AMPs can additionally cause bacterial cell leakage by forming pores or by disrupting the cell membrane via a membrane coating and destabilization (Zasloff, 2002). Developing new AMP analogs is straightforward because they are polypeptides, and are amenable to automated synthesis. Furthermore, AMPs will not persist in the environment, due to the ubiquity of proteolytic enzymes (Yount *et al*, 2006). Each novel AMP studied is derived from well known, naturally occurring sequences that are demonstrably active antimicrobial peptides. A common design strategy is based on combining the strongly amphipathic, aromatic amino acid containing, *N*-terminal region from one sequence with the more hydrophobic *C*-terminal sequence from other naturally occurring sequences (Boman *et al*, 1989).

Initially, a strongly antimicrobially active, artificial hybrid peptide called P-DER combined the *N*-terminal region of a winter flounder AMP called Pleurocidin, and the *C*-terminal region of a frog AMP called Dermaseptin (Jia, 2000; Cole, 1996). P-DER was selected as a prototype peptide as it had shown impressive results in killing a wide variety of bacterial species at therapeutic doses (Jia, 2000). The P-DER sequence was modified to generate novel sequences. Before the novel variants were synthesized, P-DER was analyzed by three *in silico* tools to determine the important properties of this peptide; these characteristics included the secondary structure, alpha helical amphipathic propensity, and hydrophobic character.

Table 1: Antimicrobial Sequence design. The first seven antimicrobial peptide sequences were derived from nature. The two listed extant hybrids were made by other research labs. The last five hybrid sequences were novel designs.

Categories	Names	Sequences
Natural AMPs	Cercropin A:	H-KWKLFKKIEKVGQNIRDGI IKAGPAVAVVVGQATQIAK-OH
	Dermaseptin:	H-ALWKTMLKKLGTMLHAGKAAALGAAADTISQTQ-OH
	Melittin:	H-GIGAVLKVLTTGLPALISWIKRKRQQ-OH
	Pleurocidin:	H-GWGSFFKKAHVKGKGVGKAALTHYL-OH
	Temporin A:	H-FLPLIGRVLGIL-NH ₂
	Ranatuerin 6:	H-FISAIASMLGKFL-NH ₂
	VesCP-M:	H-FLPIIGKLLSGLL NH ₂
Extant Hybrids	CEME:	H-KWKLFKKIGIGAVLKVLTTGLPALIS-OH
	P- DER:	H-ALWKTMLKKAHVKGKGVGKAALTHYL-NH ₂
Novel Hybrids	LM7-1:	H-ALWKTMLKKAHVGGHVGKAALTHYLN-NH ₂
	LM7-2:	H-ALWKTMLKKAHVKGKGVGKAALTHYLN-NH ₂
	LM7-3 [Rana6-CEME]:	H-FISAIASMLGKFLKWKLFKK-NH ₂
	LM7-4 [Temp-CEME]:	H-FLPLIGRVLGILKWKLFKK-NH ₂
	LM7-5 [VesCP-CEME]:	H-FLPIIGKLLSGLLKWKLFKK-NH ₂

Five novel hybrid sequences are shown in Table 1. All the *in silico* designed peptides displayed broad enough structural transitions to be considered worthwhile to pursue. P-DER was then altered, which produced two novel hybrid sequences called LM7-1 and LM7-2. To create LM7-1, one residue (Lys₁₄ → Gly₁₄) was substituted to increase flexibility at the hinge region and an *N*-terminal amide group was added to reduce hemolytic activity. The more conservative LM7-2 only had the *N*-terminal amide added. The entire sequences of Ranatuerin 6, Temporin A, and VesCP-M were combined with part of the sequence of CEME to make novel sequences LM7-3, LM7-4, and LM7-5, respectively.

The Chou-Fasman algorithm predicted that both LM7-1 and LM7-2 had a noteworthy hinge region, or break, between alpha helical segments. Evidence suggested that there should be a short, unstructured, flexible hinge between the *N*-terminal and *C*-terminal domains, to provide an ideal place for linking distinct segments in the proposed hybrids. The hinge is important, because a completely

α -helical AMP has difficulty impairing bacterial growth (Scotts, 1999; Andreau, 1992). In all five of the novel peptides, the free acidic group at the C-terminal end of the peptide was converted into an amide group; in many cases, this modification increased the antimicrobial activity (Strandberg, 2007).

LM7-1 through LM7-5 were all produced via Solid Phase Peptide Synthesis (SPPS). Due to time constraints, only LM7-1 and LM7-2 were further studied for this thesis project. The AMPs were purified using gel filtration chromatography, and preparative reversed phase high performance liquid chromatography (RP-HPLC). Both AMPs were characterized by liquid chromatography-electrospray ionization-mass spectrometry (LC-ESI-MS). However, due to equipment deficiencies, only LM7-1 was massed using matrix-assisted laser desorption ionization mass spectrometry (MALDI-MS) during peptide purification. Each peptide was tested for inhibitory activity against growth of various pathogenic gram-positive and gram-negative bacteria; the assay determined if the novel peptides were broad spectrum active against microbial pathogens that had different types of cell surfaces. By varying the concentrations of each peptide in contact with the bacteria, the dose-dependent cytotoxic effects of these peptides were determined. As significant RBC hemolysis is a common undesirable side-reaction of many highly active AMPs (like Melittin), LM7-1 and LM7-2 were also tested for hemolysis of human erythrocytes (RBCs).

CHAPTER 2

REVIEW OF LITERATURE

Introduction

Antimicrobial Peptides (AMPs) are diverse, multifunctional components of innate vertebrate immunity. To examine the relevance of AMPs to the Thesis project, this review will be divided into three main strands. The first strand covers features common to antimicrobial peptides, where they are naturally found, and their mode of action. The second strand covers key insights into aspects of hybrid AMP structure and design that led to the formation of the Thesis project. The third strand discusses the specific *in silico* tools used to design the novel AMP sequences. Using these guidelines can improve the design of hybrid, short, alpha-helical, cationic, antimicrobial peptides.

2.1 Antimicrobial Peptide Overview

2.1.1 Antimicrobial Peptide Structure and Pathogenic Targets

These polypeptides form a variety of structural classes: alpha helical, beta sheet, unstructured, and residue rich varieties. Each class has a characteristic shape and amino acid composition: alpha helices form coils, beta sheets form switchbacks, unstructured have a random 3D configuration, residue rich peptides are enriched with combinations of residues that form wedges or polyproline helices. (Yount *et al*, 2006). Although AMPs may share some slight structural similarities, the structures of vertebrate AMPs are not closely related to those of invertebrate and microbial AMPs. There is an enormous diversity of these peptides for two major reasons: there is a large

evolutionary distance between AMPs expressed in different kingdoms, and many AMPs in the same organism have only subtle sequence differences between each other. Although the peptide sequence can vary considerably within these classes of AMPs, there are closely conserved regions that are vital to each classes' function, alongside regions that show considerable sequence variation (Lai and Gallo, 2006).

AMPs can be active against a wide variety of pathogens: gram positive bacteria, gram negative bacteria, protists, fungi and viruses. AMPs serve as a vital part of all mammalian immune systems. In many cases, they are secreted in response to the initial stages of an infection. Many AMPs are immunoattractive as well as antimicrobial, so they play dual roles in organism defense systems. AMPs check pathogenic growth until other immune system responses kick in, and augment an organism's ability to clear infections (Lai and Gallo, 2009).

2.1.2 Alpha-Helical Antimicrobial Peptide Mode of Action

The typical antimicrobial peptide mode of action is to disrupt bacterial cell membranes, and selectively inhibit pathogen growth. Cationic, alpha-helical peptides have a number of positively charged residues (typically 4-10 lysine or arginine residues), which helps to attract them to elements of negatively charged bacterial cell walls (Yount *et al*, 2009). The cell wall components of the bacterial cells include: lipopolysaccharides in gram negative species (Figure 1), and teichoic acids in gram positive species (Figure 2). Once AMPs get past the cell wall and directly interact with the lipid bilayers, many disrupt cell membrane functions, trigger efflux of cellular fluids, and cause eventual cell death. The few known AMPs that do

not act by membrane disruption have a mode of action that involves either impairing cellular enzymes or binding to genetic elements. Unlike conventional antibiotics that target a specific bacterial cellular mechanism, AMPs generally target the overall structures of the bacterial cell membranes. As a consequence, bacteria can more easily evolve resistance mechanisms to get around conventional antibiotics, rather than AMPs; this is another reason AMP research is so vital (Lai and Gallo, 2006). Part of bacterial susceptibility to AMPs is that their cell membranes feature anionic phospholipids, as shown in Figure 3, such as Cardiolipin (CLP), and Phosphatidylglycerol (PG). In contrast, eukaryotic membranes feature zwitterionic or neutrally charged phospholipids, largely Phosphatidylcholine (PC), Phosphatidylserine (PS), and Phosphatidylethanolamine (PE). These latter structures are less susceptible to AMP binding (Yount *et al*, 2006).

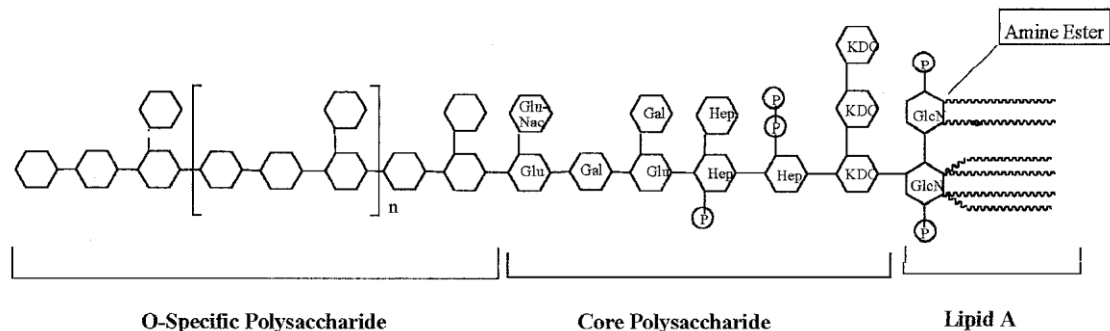


Figure 1: Generalized Lipopolysaccharide Structure in Gram negative Bacteria.

Lipopolysaccharides (LPS) are structural polysaccharides anchored in the outer membrane of gram negative Bacteria, facing in the extracellular direction. LPS is composed of 3 main components: The Lipid A subunit, which is comprised of the fatty acid tail and glucosamine carbohydrate; an invariant Core Polysaccharide region containing phosphate groups; an *O*-specific polysaccharide outer portion that includes variably repeating polysaccharide chains.

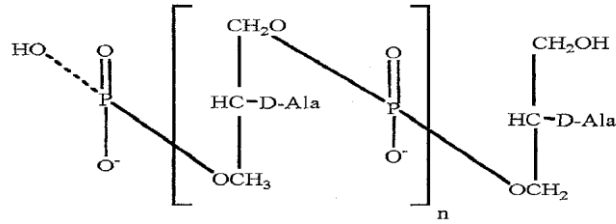


Figure 2: Glycerol Teichoic Acid Structure in Gram Positive Bacteria. Teichoic acids are important chelating polysaccharides found in the cell wall of gram positive bacteria. They are composed of alternating phosphate groups, and sugars with amino acid side chains.

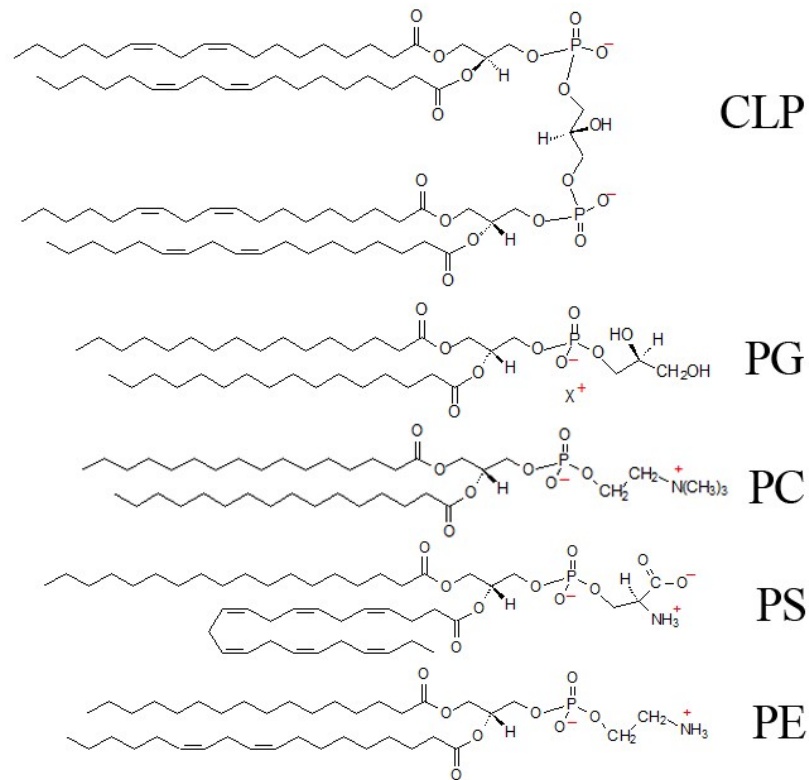


Figure 3: Phospholipid Structures. Phospholipids are found in all living cells as components of the cell membrane. All have fatty acid tails attached to a glycerol sugar that also links to a head group via a phosphate group. The examples are Cardiolipin (CLP), Phosphatidylglycerol (PG), Phosphatidylcholine (PC), Phosphatidylserine (PS), and Phosphatidylethanolamine (PE).

One of the central problems in antimicrobial peptide design is that increasing the amphipathicity of the candidate peptides tends to increase their antimicrobial activity at the same time it increases overall peptide affinity to a broader range of cells. This alteration can lead to hemolysis if the AMPs contact red blood cells. Figure 4 shows the manner by which AMPs induce leaks in bacterial cell membranes, which are hypothesized to be through one of three mechanisms. (A) is the uncommon aggregate pore formation, which forms multimer channels. (B) is the common carpet model arrangement in the bacterial cell membrane, which disrupts the integrity of the bacterial membrane. (C) is the mangainin specific torroidal pore formation, which bends the membrane open (Yount *et al*, 2006).

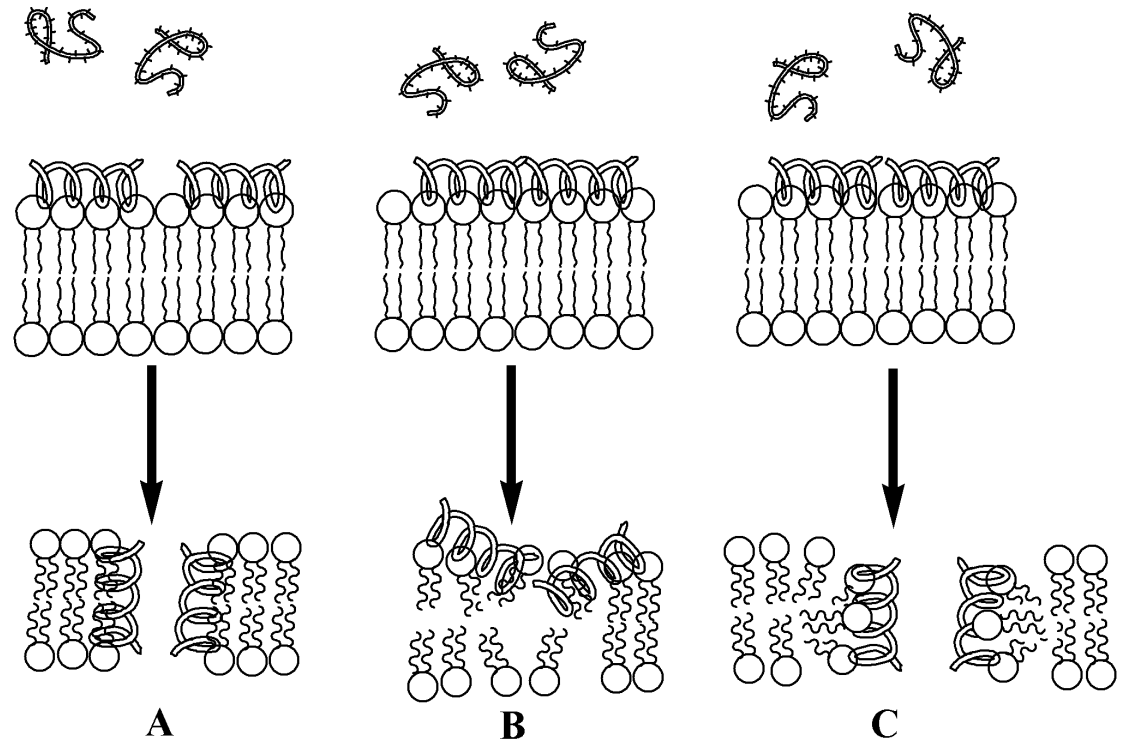


Figure 4: AMP Bacterial Membrane Attack Models. **A)** Aggregate Pore Model: unstructured AMPs form α -helices in the cell membrane, and aggregate to form multimeric pores. **B)** Carpet Model: unstructured AMPs form α -helices in the cell membrane and destabilize the cell membrane. **C)** Torroidal Pore Model: unstructured AMPs form α -helices in the cell membrane and pull the bilayer open.

Within the Alpha helical category of AMPs, the Dermaseptin class also features a characteristic hinge region in the middle of the sequence (highlighted in red):

H-AKWKTML**KKLG**TMALHAGKAALGAADTISQGTQ-OH. The hinge region likely exists because it increases alpha helical flexibility, which potentially allows the peptide to slip through the cell walls of bacteria and contact the inner cell membrane. All of the structural features of AMPs serve important functional roles, as these sequences evolved under selective pressure over long periods of time. As a consequence, excessive tampering with those features can lead to a loss of antimicrobial activity.

Another important property related to conformational flexibility, is that active antimicrobial peptides tend to form stable amphipathic alpha helices only when they contact bacterial cell membranes (Yount *et al*, 2006). Folding is initiated when the hydrophobic amino acid side chains in the peptide insert into the membrane with the hydrophilic face of the peptide pointing back towards the aqueous extracellular environment and the phospholipid head groups (Cole, 1996).

Amphipathic peptides, such as Dermaseptin S, commonly bind sideways on the membrane surface, with a Tryptophan-containing *N*-terminal region that dips further into the bacterial cell membrane than the *C*-terminal region. Dansylating the peptide allows spectroscopic studies to be performed using fluorescent emission from the membrane-bound peptide. In the case of dansylated Dermaseptin S, an AMP orientation parallel to the cell membrane was indicated by a blue-shifted emission spectrum. This peptide orientation is consistent with the “carpet” mechanism (Yount *et al*, 2006).

Multiple AMPs have the ability to increase the permeability of bacterial membranes. By having strongly cationic sequences, the AMPs are selective towards negatively charged bacteria cell membranes, rather than neutrally charged eukaryotic membranes. The main Eukaryotic exception is red blood cell membranes, which contain more anionic phospholipids. The effort to design hybrid peptides that inhibit bacterial growth without being toxic to erythrocytes is a major goal of improved peptide designs (Toke, 2005). Forming a strong amphipathic alpha helix in solution also increases an AMP’s hemolytic potential; one example showed that selective interference with the regular amphipathic profile of Pardaxin and Melittin abolished

their hemolytic potentials without diminishing their antibacterial activities (Toke, 2005).

2.2 Designing Hybrid Cationic Alpha Helical Antimicrobial Peptides

2.2.1 Prior Research into Hybrid Cationic Alpha Helical Antimicrobial Peptides

The antimicrobial peptide CEME was designed and synthesized by Boman *et al.* Their study indicated that the moth AMP Cecropin, had low hemolytic potential, but its antimicrobial activity was too weak to be therapeutically useful. At the same time, they noted that Melittin, a bee venom component, was an extremely hemolytic and amphipathic α -helical peptide. It was also a potent antimicrobial agent as bee venom has evolved to be toxic to the target organism by causing tissue damage and swelling. The Boman group decided to experiment with novel hybrid sequences that combined selectivity-type elements of the moth Cecropin sequence, and potency-type elements of the bee venom Melittin sequence. This was done so that they could potentially harness the potency of Melittin to enhance the antimicrobial activity of Cecropin without having as high a hemolytic potential as Melittin. Under the right conditions, the new hybrid, CEME, proved to be more active than Cecropin itself (Boman *et al.*, 1989).

Boman *et al* assembled a variety of hybrids by mixing and matching varying lengths of Cecropin and Melittin sequences in different arrangements, to arrive at the best combination. Eventually they hit upon an ideal hybrid AMP that had the antimicrobial activity of Melittin without damaging red blood cells. The innovation was that instead of taking a native AMP sequence and changing one residue at a time

to improve its therapeutic properties, they joined larger segments taken from two different, naturally occurring AMP sequences. This highly successful approach was used to design hybrid AMPs, evaluate them using *in silico* tools for structural characteristics common to the active peptides, and synthesize and test them. (Boman *et al*, 1989).

Dermaseptin was one of the two sequences used to make a novel Dermaseptin and Pleurocidin AMP called P-DER; this hybrid AMP was the starting point of the Thesis research. Dermaseptin itself was first isolated and characterized as part of a mixture of AMPs found in the skin and skin secretions of *Xenopus* frogs. Mor *et al* took skin samples, homogenized them, and extracted the mixture of compounds with 10% acetic acid. They then subjected the mixture to three rounds of chromatography (gel filtration, ion exchange and reversed phase HPLC). Groups of already known amphibian AMPs found in their samples included the Bominins and Magainins. They also discovered a novel sequence that wasn't in any of the known groups. The sequence of Dermaseptin was determined using the *N*-terminal Edman degradation method: H-AKWKTMLKKLGTMALHAGKAALGAAADTISQGTQ-OH. They compared the Edman-derived sequence to the ratios of free amino acids yielded by acid hydrolysis, and found the amino acid composition data was compatible between both methods. They termed the novel AMP Dermaseptin. They purified and determined the molecular weight of the isolated AMP using Fast Atom Bombardment-Mass Spectroscopy as 3455.4 [m+H]⁺; they also determined the AMP had no special *N*-terminal, *C*-terminal or side chain modifications. Later, they chemically synthesized the peptide using the Fmoc-type solid phase peptide synthesis (SPPS) method; they

used three rounds of chromatography (gel filtration, ion exchange and reversed phase HPLC) to purify the synthetic product. They demonstrated that the synthesized Dermaseptin was identical to the isolated version in chromatographic properties, mass, and amino acid sequencing results. By varying the hydrophobicity of the solvent, during a Circular Dichroism Spectrometer measurement run, it was found that the peptide favored an alpha-helix conformation in more hydrophobic environments (Mor et al, 1991). They demonstrated the antimicrobial activity of synthetic Dermaseptin by reporting its Minimum Inhibitory Concentration (MIC) against *E.coli* (1.0 µg/ml), *E.faecalis* (5.0 µg/ml), and *S.aureus* (5.0 µg/ml); 100% hemolysis at 1 hour was determined to be 70.0 µg/ml. Dermaseptin is a potent and potentially useful therapeutic AMP (Mor et al, 1994).

Pleurocidin was the other sequence chosen to make the P-DER hybrid peptide, due to its broad spectrum activity, as well as its forming an alpha-helical secondary shape after contact with a membrane. Pleurocidin was part of a mixture of AMPs found in the skin mucosal secretions of the winter flounder, *Pleurocidin americanus*. Cole et al took the skin and mucous samples, extracted the compounds with 10% acetic acid, centrifuged them, and subjected the mixture to two rounds of chromatography (gel filtration, and reversed phase HPLC). After each purification round, they tested the various fractions for antimicrobial activity, and focused their purification efforts on the antimicrobially active fractions. They identified a novel AMP, using peptide sequence analysis with the hinge region is highlighted in red:

H-GWGSFFKKAH**HVGK**HVGKAALTHYL-OH. They termed the novel AMP Pleurocidin. After they isolated and determined the molecular weight of the isolated AMP using

Matrix Assisted Laser Desorption Ionization Mass Spectrometry at 2711 [m+H]⁺, they chemically synthesized it using the solid phase peptide synthesis (SPPS) method. They determined the antimicrobial activity of synthetic Pleurocidin by reporting its Minimum Inhibitory Concentration (MIC) against *E.coli* (6.0-9.0 µg/ml), *P.aeruginosa* (>94.9 µg/ml), *B.subtilis* (3.0-6.0 µg/ml), and *S.aureus* (48.0-94.9 µg/ml) (Cole et al, 1996).

Jia *et al* described the design scheme pioneered by Merrifield *et al* to produce novel antimicrobial peptides for use against bacterial fish pathogens. This hybrid method of creating novel AMPs used entire sequences of one type of peptide paired with selected stretches of other sequences. The first four peptides listed in Table 2 were all natural AMPs that were isolated from 4 different species: Ceratoxin was derived from *Drosophila melanogaster*, Dermaseptin was a skin secretion found in *Phylomedusa sauvagii*, Misgurin was isolated from *Misgurnus anguillicaudatus*, and Pleurocidin was found in the mucal skin secretions of *Pseudopleuronectes americanus*. The remaining eight AMP sequences were the novel AMP designs. Pleurocidin amide was created by adding an amide group to the C-terminal end. P-1 and P-1 amide were peptides that had essentially the same sequence as Pleurocidin and Pleurocidin amide; the only modification was one additional lysine added onto the N-terminus. This alteration increased the net cationic charge, and made the N-terminus more polar. The design of the remaining set of novel AMPs involved a hybrid approach, swapping out entire sections of different natural AMPs to create combined properties that could potentially lead to greater antimicrobial activity. The first hybrid of this type listed was called P-DER, which used the first 9 residues of the N-terminal end of

Dermaseptin and the last 17 residues of the C-terminal end of Pleurocidin. The remaining hybrids also used combinations of Pleurocidin paired with Misgurin and Ceratoxin (Jia et al, 2000).

Table 2: Extant and Novel Antimicrobial Peptide Sequences. This table shows one design strategy for making hybrid AMPs (Jia *et al*). All sequences are aligned, and color coded to indicate which segments from the natural AMPs were incorporated into the Novel Peptide Hybrids. The first four sequences were derived from nature. Pleurocidin-amide had a C-terminal amide designed to decrease hemolysis; P1 and P1-amide had an N-terminal lysine to increase cationic charge. All the remaining novel sequences were hybrids: P-DER combined portions of Dermaseptin and Pleurocidin; P-CER used Ceratoxin and Pleurocidin; P-M used Pleurocidin and Misgurin; DER-M used Dermaseptin, Pleurocidin and Misgurin; CER-M: used Ceratoxin, Pleurocidin and Misgurin.

Categories	Names	Sequences
		1 5 10 15 20 25
Natural AMPs	Ceratoxin:	H-SIGSAFKKALPVAKKIGKAALPIAKAALP-OH
	Dermaseptin:	H-ALWKTMLKKGTMALHAGKAALGAAADTISQTQ-OH
	Misgurin:	H-RQRVEELSKFSKKGAAARRRK-OH
	Pleurocidin:	H-GWGSFFKKAHVKGKGVGKAALTHYL-OH
Novel Peptide Hybrids	Pleurocidin amide:	H-GWGSFFKKAHVKGKGVGKAALTHYL-NH ₂
	P1:	H-KGWGSFFKKAHVKGKGVGKAALTHYL-OH
	P1 amide:	H-KGWGSFFKKAHVKGKGVGKAALTHYL-NH ₂
	P-DER:	H-ALWKTMLKKAHVKGKGVGKAALTHYL-NH ₂
	P-CER:	H-SIGSAFKKAAHVKGKGVGKAALTHYL-NH ₂
	P-M:	H-GWGSFFKKAHVKGKGVGKAALGAAARRRK-OH
	DER-M:	H-ALWKTMLKKAHVKGKGVGKAALGAAARRRK-OH
	CER-M:	H-SIGSAFKKAAHVKGKGVGKAALGAAARRRK-OH

Table 3 shows the antimicrobial activity of the various AMPs against various pathogenic strains of bacteria that infect fish, as well as *Pseudomonas aeruginosa* and *Staphylococcus epidermidis*. The MICs were determined in a 96-well plate using a broth microtiter assay that demonstrated 50% inhibition of bacterial growth as compared to a control using no AMPs (Jia *et al*, 2000). The C-terminal amide on Pleurocidin amide increased the activity by as much as sixteen-fold over native Pleurocidin. The antimicrobial activity of P1/P1 amide only increased against the representative bacterial species up to a two-fold amount. P-DER had the greatest

overall activity of all the hybrid sequences, although it was slightly less active than Pleurocidin-amide. The remaining AMP hybrids were much less active than P-DER (Jia et al, 2000).

Table 3: AMP Activity against Fish and Human Pathogenic Bacteria. The peptides made by Jia *et al* were assayed against representative species of gram positive and gram negative species. The Minimum Inhibitory Concentration (MIC) was expressed as the lowest concentration of AMPs that inhibited overnight bacterial growth by 50%. Results were as follows: Misgurin and CER-M were inactive, Pleurocidin, P1, P-CER, P-M, and DER-M were only active against specific species; Pleurocidin amide, P1 amide and P-DER were broad spectrum active in potency.

		MIC (ug/ml)						
		<i>V. anguillarum</i>	<i>A. salmonicida</i>	<i>S. enterica</i> Serovar Typhimurium Strain: 14028s	<i>S. enterica</i> Serovar Typhimurium Strain: 14028s	<i>P. aeruginosa</i> Strain: K799	<i>P. aeruginosa</i> Strain: Z61	<i>S. epidermidis</i> Strain: C621
Peptide	Misgurin:	>64	>64	>64	>64	>64	>64	>64
	Pleurocidin:	16	2	32	<0.5	64	16	64
	Pleurocidin amide:	2	1	4	<0.5	4	4	4
	P1:	16	2	16	<0.5	64	8	64
	P1 amide:	2	1	2	<0.5	2	2	2
	P-DER:	4	1	4	0.5	4	8	4
	P-CER:	64	8	>64	2	>64	>64	>64
	P-M:	32	1	16	0.5	16	16	16
	DER-M:	>64	2	32	0.5	32	8	32
	CER-M:	>64	32	>64	8	>64	64	>64

2.2.2 Optimizing Hybrid Cationic Alpha Helical Antimicrobial Peptides

As seen in Table 4, Strandberg *et al* noted that the natural sequence PGLa from *Xenopus laevis* was potent; they modified the sequence and generated the novel sequence MSI-103 by simplifying the types of different residues from eight to four. The third AMP was a synthetic, hemolytic peptide called MAP that only had three different types of residues. An active AMP with fewer types of residues simplifies synthesis time and expense. Both the C-terminal free acid (-OH), and amidated (-NH₂) versions of all three peptides were synthesized, purified, and tested for activity

against human pathogens. They discovered a free C-terminal acid residue raised the Minimum Inhibitory Concentrations of four test peptides when compared to identical sequences with C-terminal amidation. This sequence alteration decreased their effectiveness, in some cases by as much as a factor of sixteenfold. In no instance, did adding a C-terminal amide group lower the activity of an AMP. The synthetic sequence MSI-103, with simplified residues as compared to the natural sequence PGLa, was only marginally more effective in amidated form, but exhibited much improved activity in free acid form. At the same time, the additional C-terminal amide group increased the hemolytic potential of the peptides, and then only at a therapeutically-useless high concentration for the MAP sequence, which was hemolytic to start with (Strandberg *et al*, 2007).

Table 4: AMP Activity and Human RBC Hemolysis. The peptides made by Strandberg *et al* were assayed against representative species of gram positive and gram negative species, and the MICs were determined. They were also assayed against Human erythrocytes and the amount required causing 50% hemolysis after 1 hour was determined. PGLa-NH₂, the first AMP sequence was from nature. PGLa-OH had exactly the same sequence, but its C-terminus was a free acid. The remaining AMPs were synthetic in design as part of an effort to determine properties that made effective AMPs. MSI-103 used only 4 residue types, but it was nonhemolytic; MAP used only 3 residue types, and it was extremely hemolytic. PGLa-OH and MAP-OH were inactive against the bacterial species; MSI-103-OH and MAP-NH₂ were only active against specific species; PGLaNH₂, and MSI-103-NH₂ were broad spectrum active. Both of the MAP peptides were hemolytic, so only the PGLaNH₂, and MSI-103-NH₂ sequences were useful at therapeutic doses.

		MIC (ug/ml)				HC ₅₀ (ug/ml)
		<i>E.coli</i> strain: DSM 1103	<i>E.coli</i> strain: DH 5α	<i>B.subtilus</i> strain: ATCC 6633	<i>S.aureus</i> strain: DSM 1104	Human RBCs
Peptide	PGLa-NH₂: H-GMASKAGAIAGKIAKVALKAL-NH ₂	16	8	4	16	800
	PGLa-OH: H-GMASKAGAIAGKIAKVALKAL-OH	>128	>128	32	>128	>1000
	MSI-103-NH₂: H-KIAGKIAKIAGKIAKIAGKIA-NH ₂	8	16	4	8	1000
	MSI-103-OH: H-KIAGKIAKIAGKIAKIAGKIA-OH	8	16	8	128	>1000
	MAP-NH₂: H-KLALKLALKALKALKLA-NH ₂	128	8	4	32	7
	MAP-OH: H-KLALKLALKALKALKLA-OH	>128	>128	>128	>128	11

Jiang of the Hodges research group experimented with the composition of the hydrophobic faces of alpha-helical, amphipathic peptides; they noted that certain gram negative bacteria such as *Pseudomonas aeruginosa* and *Acinetobacter baumannii* have evolved many strains that are resistant to multiple classes of antibiotics. Active antimicrobial peptides could be designed to inhibit bacterial growth, even of the multidrug resistant strains. However, one of the major hurdles of making novel AMPs was the issue of potential hemolysis of human red blood cells; an active AMP that is too hemolytic is not therapeutically useful. A sequence was selected that was

antimicrobially active against strains isolated from living organisms, but was too hemolytic. The research group then made systematic residue changes in an attempt to reduce the hemolytic properties of the peptides without compromising antimicrobial activity. The initial change was the insertion of a positively charged lysine into the center of the hydrophobic face of the α -helix, in a key position they termed the “Specificity Determinant”. More positive charges were added by switching additional neutral residues into lysines; this increased the overall hydrophilicity and positive charge of the polar face of the helix. They then converted selected side chains of amino acid residues from aromatic into aliphatic; having perfectly hydrophobic faces encouraged peptide aggregation and also increased AMP hemolytic activity. Inserting a disruptive, positively charged, polar residue in the “Specificity Determinant” of the hydrophobic face of the helix, curtailed dimer formation, and reduced the effects of hemolysis (Jiang *et al*, 2011).

2.3 Hybrid Cationic Alpha Helical Antimicrobial Peptides *In Silico* Design Strategies

In silico design is useful to aid in peptide design as these tools can evaluate a series of AMPs to determine their potential utility without going through the time and expense to synthesize the prospective sequences.

2.3.1 Chou-Fasman Secondary Structure Algorithm

The first *in silico* tool is the Chou-Fasman secondary structure algorithm; it predicts potential secondary structures based on their amino acid sequences. Using this algorithm, there are three types of secondary structures that are modeled: coiled

alpha helices, ribbon-shaped beta sheets, and 4-residue beta turns. The algorithm assigns a prediction of what secondary structure a given stretch of the protein will form based on residue affinity and composition (Chou and Fasman, 1978). Figure 5 shows a printout of P-DER as modeled by the Peptide Companion® Chou-Fasman algorithm (Lebl, 1994).

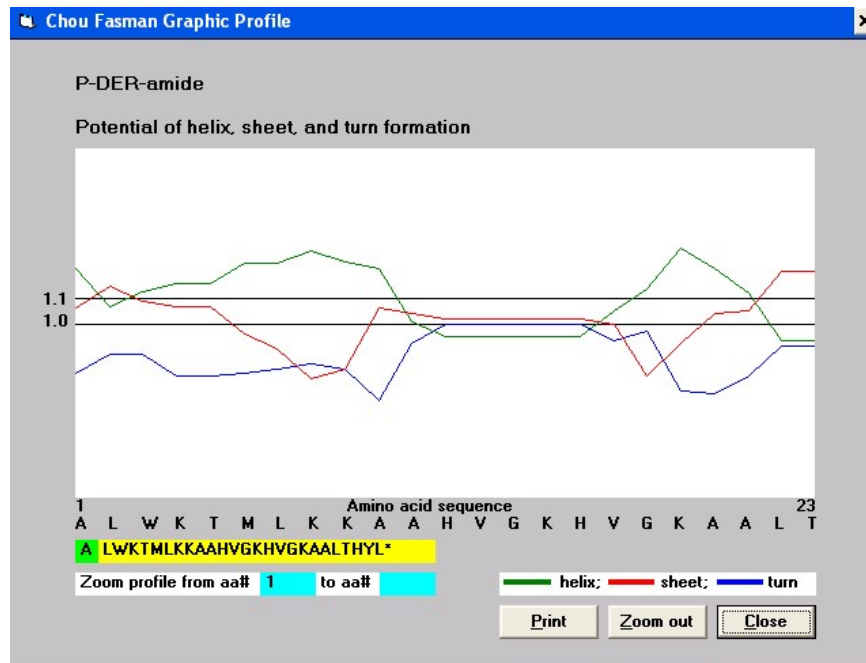


Figure 5: Chou-Fasman Secondary Structural Model of P-DER. The three line graphs show the three common secondary structures: alpha helices (green), beta sheets (red), and beta turns (blue). The likelihood of formation of the secondary structure configuration is plotted against the AMP sequence from the *N*-terminus to the *C*-terminus. In this example, P-DER has two strong alpha helical sequences at the *N*-terminal and *C*-terminal ends, separated by an unstructured domain.

2.3.2 Edmundson Helical Wheel

The second *in silico* tool is the Edmundson helical wheel; it portrays a side view of a potential alpha helix, showing how amphipathic the faces of the helix are (Schiffer and Edmundson, 1967). The model displays an end-on, 2D view of the helix as viewed

from the *N*-terminus. There are 4 different residue types: hydrophobic, neutral polar, acidic and basic. How they are arranged in the model determines how amphipathic the alpha helical AMP is. Figure 6 shows a printout of P-DER as modeled by the Peptide Companion® Edmundson helical wheel (Lebl, 1994).

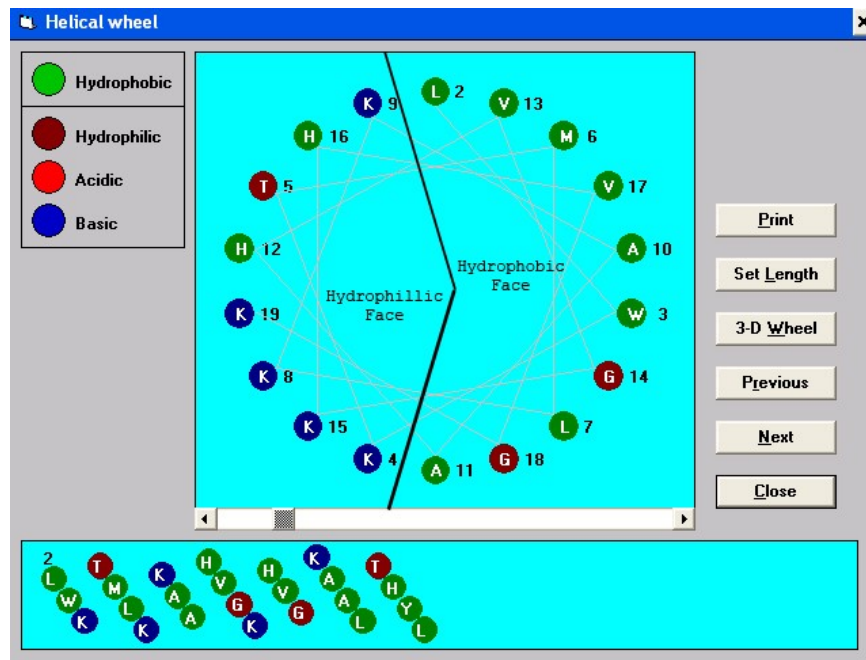


Figure 6: Edmundson helical wheel of P-DER. The top diagram models an *N*-terminal end-on view of an alpha helix. Residues are assigned to 4 different categories: hydrophobic side chains (green), hydrophilic side chains (maroon), acidic side chains (red) and basic side chains (blue). P-DER was strongly amphipathic, with well developed hydrophilic and hydrophobic faces. The bottom diagram models a helical net, which is a side view of an unrolled α -helix.

2.3.3 Hopp-Woods Hydrophilicity Scale

The third *in silico* tool is the Hopp-Woods hydrophilicity scale to model the proposed hybrids in order to evaluate what stretches of a peptide sequence were likely to be hydrophilic or hydrophobic (Hopp and Woods, 1981). All sequences that displayed extreme transitions between hydrophilic and hydrophobic characteristics at

their junctions were judged as being too unpredictable to mimic the natural conformations adopted by natural AMPs, and were rejected. Figure 7 shows a printout of P-DER as modeled by the Peptide Companion® Hopp-Woods hydrophilicity scale (Lebl, 1994).

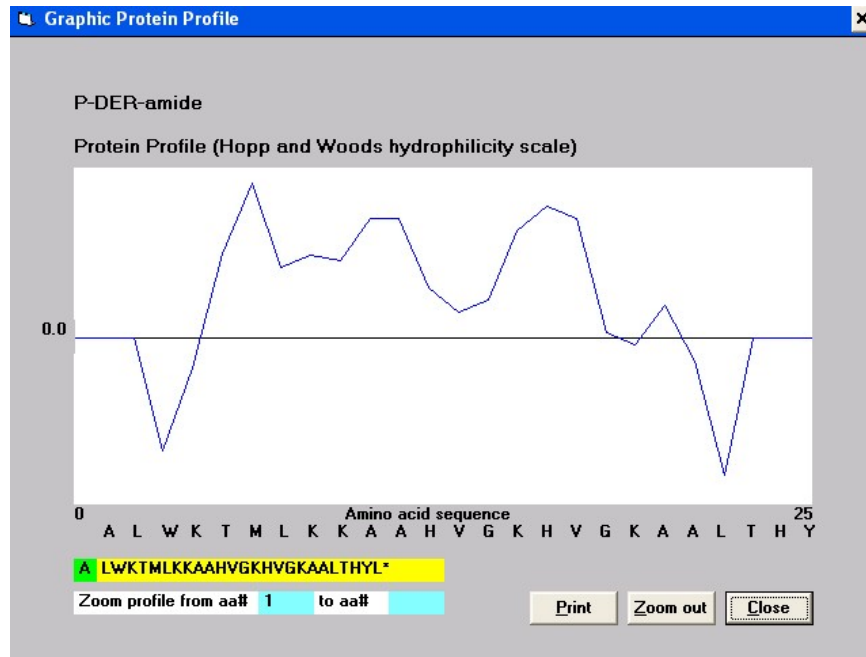


Figure 7: Hopp-Woods Hydrophilicity Scale of P-DER. Hydrophobic to hydrophilic character was plotted against the AMP sequence from the *N*-terminus to the *C*-terminus. In this case, the P-DER AMP had a strongly hydrophilic *N*-terminal region, followed by a more hydrophobic *C*-terminal region.

Summary

The overall strategy used to design the AMPs in this project was to note the biophysical and antimicrobial properties of known and hybrid AMP sequences before the resources were invested on producing them. Due to P-DER being the most potent hybrid AMP from the Jia *et al* experiments, it was used as the starting point for all the novel AMP sequences in this project (Jia *et al*, 2000). P-DER became the initial test

case into how AMP hybrids might be designed to further improve their therapeutic properties. The novel hybrid P-DER derivatives LM7-1 and LM7-2 featured novel C-terminal amidation designed to increase antibacterial activity, without significantly increasing hemolytic potential at potentially therapeutic doses. As a consequence, MBHA resin was used for all of the peptide synthesis, so that when the peptide chains were cleaved off, the AMP would possess a C-terminal amide group (Strandberg et al, 2007). All of the designed peptides in this project used a “Specificity Determinant”. This design strategy is designed so that the nonpolar faces do not easily aggregate to form multimers; such hybrids should exhibit decreased hemolysis. Cationic, alpha-helical AMPs are more effective in penetrating bacterial cell walls when they operate individually as opposed to acting in massed aggregates (Jiang *et al*, 2011). LM7-1 and LM7-2 were designed to be conformationally flexible AMPs, having unstructured secondary structures in an aqueous environment. These AMPs should only form amphipathic alpha-helices when they are in direct contact with a cell membrane. AMP sequences that avoided forming a stable alpha helix when free in solution, and formed a well defined secondary structure when in contact with a membrane surface were used to lower the possibility of unintentional hemolysis (Toke, 2005). Both AMPs also featured an α -helix-hinge- α -helix structural motif; this was an important innovation taken from the design of CEME (Boman *et al*, 1989). When depicted in the Edmundson helical wheel format, it was clear that both peptides had smaller hydrophilic faces compared to their hydrophobic faces; this arrangement contributed to a membrane destabilizing role that would be consistent with the “carpet” model of AMP action on bacterial cell membranes (Toke, 2005). Both LM7-

1 and LM7-2 were hybrid peptides, having *N*-terminal and *C*-terminal sequences drawn from two different natural AMPs. LM7-1 also incorporated a one-residue substitution at position 15 to increase hinge flexibility. These AMP characteristics were also used to design three additional novel hybrids. The design started with the potent hybrid, CEME and combined it with three natural AMPs to create LM7-3, LM7-4 and LM7-5.

The hypothesis for this Thesis Project is that novel, therapeutically useful, hybrid AMP analogues can be generated by linking carefully chosen sequences from one peptide with a region from a different peptide. This goal can be achieved through careful analysis of the helix-forming propensity and amphipathicity of each sequence, and placement of a hinge between the segments such that the activity is not diminished (Andreu, 1992). This hybrid approach should allow the production of many new AMPs that have the efficacy of natural sequences but may circumvent resistance mechanisms that arise in the target bacteria, due to their cationic charges drawing them towards negatively charged bacterial cell wall and cell membrane components.

CHAPTER 3

MATERIALS AND METHODS

3.1 Equipment and Reagents

3.1.1 Equipment

The manual peptide synthesis reaction vessels were purchased from Peptides International (KY, USA). The manual peptide shakers were from St. John's Associates (MD, USA). The heating blocks were from VWR (PA, USA). Borosilicate glass pipettes, 0.5 x 6.0 cm tubes, and magnetic stir bars were from Thermo Fisher Scientific (NH, USA). The HF apparatus, and Kel-F® tubes were from Immuno Dynamics (CA, USA). The 2.5 x 112.0 cm Glass Chromatography column and tubing was from Sigma-Aldrich (MO, USA). The Rabbit Plus peristaltic pump, and automatic pipettes were from Ranin (OH, USA). The in-line UV/VIS detector was from Kratos Analytical (Spectraflow 783, Kyoto, Japan). The fraction collector was manufactured by Gilson (FC 205, WI, USA). The Chart Recorder was made by Linear (Tamil Nadu, India). The RE rotary evaporator and accessories were made by Büchi (Postfach, Switzerland). The automatic 7010 injector valve was manufactured by Rheodyne (CA, USA). The preparatory reversed Phase HPLC column was from Vydac (300 Å, 10 µ, C₁₈, 2.2 x 25.0 cm, 218 TP 152022, IL, USA). The HPLC minipump was from Thermo Separation Products (OR262520, NH, USA). The lyophilizer was from Virtis (PA, USA); the lyophilizing dewars were from Labconco (IL, USA). The MALDI-MS was from Ciphergen (ProteinChip™, CA, USA), and the ESI-MS was from Thermo Fisher Scientific (LTQ Orbitrap Velos, NH, USA). The

Genesys 10UV Scanning Spectrophotometer was from Thermo Scientific (6 carousel, UV-VIS, 190-1100 nm range, NH, USA). The Spectronic 20D was from Milton Roy (PA, USA). The Vmax Kinetic Microplate reader was from Molecular Devices (405/450/570/630 nm, CA, USA). The IEC clinical centrifuge was from International Equipment Corporation (MA, USA). The G10 Gyrotary shaker was from New Brunswick Scientific (NJ, USA). The Petri dishes were from Kard-Valmark (Plastic, 100 x 10 mm, #2900, Ontario, Canada). The -80°C freezer, autoclave, crushed ice machine, cold room, purified (pyrogen-free) water system, high pressure air lines, high pressure vacuum lines were provided by the Cell and Molecular Biology Department at the University of Rhode Island.

3.1.2 Chemical Reagents

All of the solvents except trifluoroacetic acid were HPLC grade; TFA was Technical grade. All of the solid reagents except potassium hydroxide were American Chemical Society standard, KOH was technical grade. The amino acids used were as follows (side chain protecting groups are indicated in brackets): Boc-L-Ala-OH, Boc-L-Arg(Tos)-OH, Boc-L-Asn-OH, Boc-Gly-OH, Boc-L-His(DNP)-OH, Boc-L-Leu-OH, Boc-L-Met-OH, Boc-L-Pro-OH, Boc-L-Ser(Bzl)-OH, Boc-L-Tyr(Bzl)-OH, Boc-L-Thr(Bzl)-OH, and Boc-L-Trp-OH were all purchased from Bachem. In addition, Boc-L-Ile-OH, Boc-L-Lys(2-Chloro-CBZ)-OH, and Boc-Phe-OH were purchased from Peptides International (KY, USA); Boc-L-Val-OH was purchased from The Peptide Institute (Saito, Japan). The p-methylbenzhydrylamine Resin•HCl used for SPPS was from Peptides International

(RMB-1045-PL, 100-200 mesh, 0.40 miliequivalents/g, KY, USA). Calcium gluconate gel was from Attard Minerals (CA, USA). Dichloromethane, *N,N*-diisopropylamine, *N,N*-dimethylformamide, trifluoroacetic acid, *N,N'*-dicyclohexylcarbodiimide, 1-hydroxybenzotriazole, 2-(1H-benzotriazole-1-yl)-1,1,3,3-tetramethyluronium hexafluorophosphate, methanol, 95% isopropanol, potassium chloride, phenol, magnesium sulfate, potassium hydroxide, thiophenol, glacial acetic acid, blue dextran, acetonitrile, *p*-cresol, *p*-thiocresol, formic acid, chloramphenicol, solid potassium hydroxide, Triton® X-100, sodium chloride, sodium phosphate monobasic, sodium phosphate dibasic, MB-3 Amberlite®, G25 Sephadex®, sinapic acid, Mueller Hinton broth, Mueller Hinton agar, Nutrient agar, and Parafilm® were all from Fischer Sigma-Aldrich (MO, USA) or Wilkem (RI, USA). 95% ethanol and absolute ethanol were supplied by the University of RI. Hydrofluoric acid, argon, and nitrogen gasses were supplied by Airgas (RI, USA). Dry ice was supplied by Corp Brothers Inc. (RI, USA).

3.2 Solid Phase Peptide Synthesis (SPPS)

3.2.1 Modes of Solid Phase Peptide Synthesis

SPPS is directly reversed from the direction of enzymatic peptide synthesis; instead of travelling from the *N*-terminus to the *C*-terminus, SPPS elongates the peptide chains in the opposite direction. There are two orthogonal modes of SPPS, based on the choice of protection for the *N*-terminus of the amino acid building blocks. One scheme uses an acid-cleaved *tert*-butyloxycarbonyl (Boc) protecting group and the

other uses a base-cleaved 9-fluorenylmethyloxycarbonyl (Fmoc) protecting group. The Boc method was used for all the peptide synthesis for this Thesis.

SPPS grows the peptide chain out from solid resin support beads. The beads are an essential element to SPPS, because the reaction vessel used for the synthesis has a fritted filter on the bottom that prevents the peptide-bound resin from falling out, while liquid reagents are added and suctioned out freely. The type of support resin chosen depends on what type of *C*-terminal functional group is desired; naturally-occurring peptides may contain a free *C*-terminal acid group or a *C*-terminal amide group. In this case, synthesized peptides were made with a *C*-terminal amide by using 4-methylbenzhydrylamine (MBHA) resin. After the resin is prepared, amino acids are added sequentially to the growing peptide chain in a *C*-terminal to *N*-terminal order. Every amino acid has a Boc protecting group blocking the reactive amino group so that only its *C*-terminus couples with the reactive amino groups on the growing chains. Any reactive side chains of the amino acids are also blocked using labile protecting groups until the peptide elongation is finished. After each coupling cycle has been pushed to completion, the new *N*-terminal Boc group is cleaved off using 50% trifluoroacetic acid (TFA) in dichloromethane (DCM) for 30 minutes, and the coupling cycle is repeated until the peptide is complete. Later, most of the side chains are deprotected at the same time as the anchoring *C*-terminus of the peptide is cleaved from the resin, using anhydrous hydrofluoric acid (HF) at 0°C for 1 hr.

3.2.2 Peptide Synthesis Procedure with Ninhydrin Monitoring

LM7-1 through LM7-5 were synthesized using the Boc method of SPPS. A sample of 2 g of MBHA Resin HL (100-200 mesh)•HCl, with a reported substitution of 0.40 milimoles/g were swollen in dichloromethane (DCM) overnight, and the ninhydrin test was used to quantify the amount of free amino groups on the Resin beads. This determined how many peptide chains could grow on the surface of the beads and dictated how much of any incoming amino acid would be needed to perform a complete coupling reaction.

The quantitative ninhydrin test (Kaiser test) proceeded as follows: 1-2 mg of sample resin was combined with the ninhydrin reagents in a tube, and then incubated in a block heater which was set to 100°C for exactly 10 minutes. A second tube without resin was also set up as a control. In the presence of free amine groups, a blue, light absorbing complex formed; otherwise the solution remained yellow if amines were present at a concentration of <0.01% (Sarin *et al*, 1981). To exactly quantify the free amino groups, the test sample was then filtered to remove the resin. The eluent was diluted to exactly a 10.0 ml total volume with absolute ethanol, and mixed. An aliquot was then scanned at 570 nm to detect the absorption of the Ruhemann's purple pigment. The absorbance was used to calculate the concentration of amine groups in that particular volume according to the published Ruhemann's extinction coefficient, which was $1.55 \times 10^3 \text{ L cm}^{-1} \text{ mol}^{-1}$ (Sarin *et al*, 1981). This specific "loading" value was used to determine the quantity of Boc-amino acid which was needed for a given

coupling reaction. The loading equation to determine mmoles amino groups/g resin is listed below:

$$A = \epsilon c \quad (1)$$

$$A_{570} = \epsilon_{570} \left(\frac{L}{\text{mol} \times \text{cm}} \right) \times l_{\text{cm}} \times c_{\text{mol/L}} \quad (2)$$

$$c_{\text{mmol/L}} = \frac{A_{570}}{(\epsilon_{570} l)} \times \left(\frac{1000 \text{ mmol}}{1 \text{ mol}} \right) \quad (3)$$

$$\text{Resin Loading} = c_{\text{mmol/g}} = c_{\text{mmol/L}} \times \frac{V_{\text{tot,L}}}{\text{mg}_{\text{resin sample}}} \times \left(\frac{1000 \text{ mg}}{\text{g}} \right) \quad (4)$$

$$\text{Loading (in mmol/g)} \times \text{resin mass (in g)} \text{ used in synthesis} = \text{“1 Equivalent”} \quad (5)$$

In all cases, an excess of the Boc amino acids were used to drive the coupling reactions to completion, typically >99.99%. If the ninhydrin test was negative (colorless) after coupling, the synthesis proceeded on to the next residue in the sequence. If it was still positive (blue), then different coupling protocols were used until the incoming Boc amino acid had successfully coupled with all of the available amine groups on the resin beads, resulting in a negative Kaiser test.

The coupling steps were carried out using one of four different coupling protocols as needed, starting with the direct DCC coupling protocol shown in Figure 8. In this coupling method, the carboxylic acid functionality of a *N*-Boc-L-amino acid is activated by coupling to *N,N'*-dicyclohexylcarbodiimide, and then the *N*-Boc-L-amino acid containing the more reactive *O*-acyl-isourea leaving group directly

couples with the free amino group on the growing peptide chain. When the activated Boc-AA is mixed with the peptide resin, the exposed lone pair of electrons on the amino group at the *N*-terminus of the peptide chain attack at the partially positively charged carbonyl carbon on the amino acid, forming a tetrahedral intermediate, followed by elimination of the *O*-acyl-isourea leaving group, with formation of a stable peptide bond. After coupling, the result is the peptide is increased in length by one amino acid. More expensive and reactive coupling reagents were used whenever a positive ninhydrin test showed that the direct DCC coupling protocol did not result in total coupling of the incoming activated Boc-AAs with all of the target growing peptide chains on the resin (<0.01% unreacted amino groups).

To use the protocol, 50% TFA in DCM was used to cleave off the Boc protecting groups, and the peptide resin was washed and neutralized with 20% DIEA in DCM. Then 5 equivalents of Boc-AA were dissolved in a minimal amount of DMF in a clean Erlenmeyer flask and added to the reaction vessel. Afterwards, 5 equivalents of a calibrated solution of exactly 0.5 M DCC in DCM was added to the RV and the direct coupling reaction was run for 90 minutes.

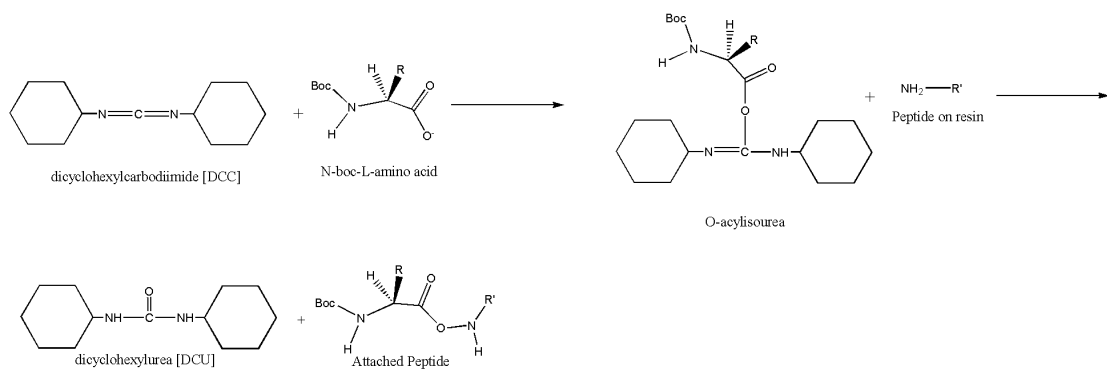


Figure 8: Direct DCC Catalyzed Coupling Protocol. The *N*-Boc-L-amino acid is activated by coupling to *N,N'*-dicyclohexylcarbodiimide, forming the *O*-acyl-isourea leaving group and directly reacts with the free amino group on the peptide-resin. The result is an extended peptide chain.

In the Symmetric Anhydride coupling protocol, as shown in Figure 9, the *N*-Boc-L-amino acid is activated by coupling to *N,N'*-dicyclohexylcarbodiimide, and then an excess of the identical *N*-Boc-L-amino acid replaces the *O*-acyl-isourea functional group. The pre-formed symmetric anhydride is extremely reactive and couples with any free amine groups remaining on the peptide-resin. The exposed lone pair electrons on the amine group at the *N*-terminus of the peptide chain attacks the carbonyl group on the symmetric anhydride, removing one of the *N*-Boc-L-amino acids as a leaving group, and forming a peptide bond with the other one. After coupling, the peptide is increased in length by one amino acid.

To use the Pre-formed, Symmetric Anhydride protocol, the peptide resin was washed with DCM, neutralized with 10% DIEA in DCM, and then drained. Then, 2 equivalents of incoming Boc-AA were dissolved in a minimal amount of DMF in a clean Erlenmeyer flask, and this solution was added to the resin in the reaction vessel.

Afterwards, 1 equivalent of a calibrated solution of exactly 0.5 M DCC in DCM was added to the RV and the Symmetric Anhydride coupling reaction was run for 60 minutes.

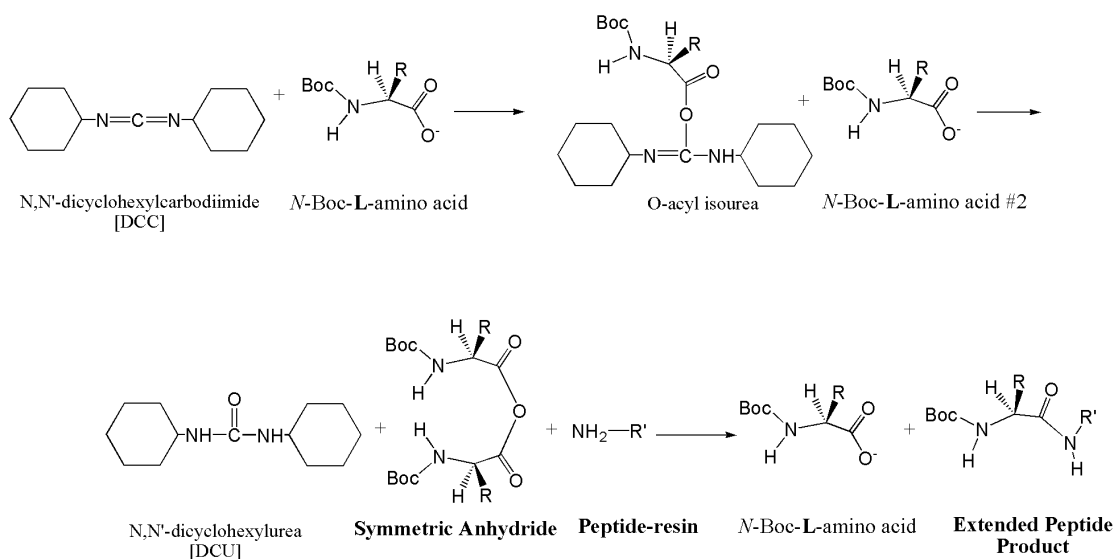


Figure 9: Pre-formed Symmetric Anhydride Protocol. The N -Boc-L-amino acid is activated by coupling to N,N' -dicyclohexylcarbodiimide, and then the same N -Boc-L-amino acid replaces the O -acyl-isourea group. The pre-formed symmetric anhydride reacts with the free amino groups, and produces a peptide bond with one of the remaining N -Boc-L-amino acid residues as a leaving group. The result is an extended peptide chain.

In the Direct HOBt coupling protocol, as shown in Figure 10, the N -Boc-L-amino acid is pre-activated by coupling to N,N' -dicyclohexylcarbodiimide, and then N -hydroxybenzotriazole (HOBt) replaces the O -acyl-isourea functional group. The HOBt Active ester serves to prevent the amino acid from reversing its chirality during coupling. When the HOBt active ester is mixed with the peptide resin, the exposed lone pair of electrons on the amino group at the N -terminus of the peptide chain attacks the carbonyl group on the Boc-amino acid, removing the HOBt as a leaving

group, and forming a peptide bond. After coupling, the peptide is increased in length by one amino acid.

To use the HOBt coupling protocol the peptide resin was washed with DCM, neutralized with 10% DIEA in DCM, and drained. Then, 4 equivalents of Boc-AA and 4 equivalents of HOBt were dissolved using a minimal amount of DMF in a clean Erlenmeyer flask. After the solution was added to the reaction vessel, 4 equivalents of DCC was added to the RV and the coupling reaction was run for 90 minutes.

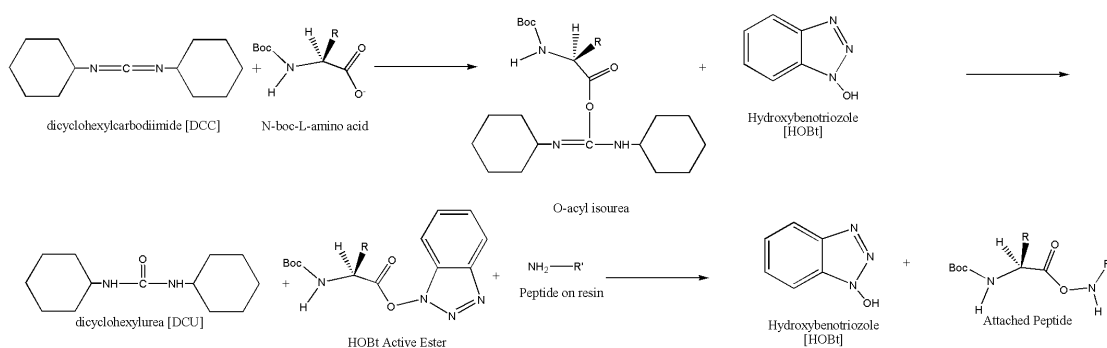


Figure 10: Direct HOBt Coupling Protocol. The *N*-Boc-L-amino acid is pre-activated by coupling to *N,N'*-dicyclohexylcarbodiimide, and then 1-hydroxybenzotriazole (HOBt) replaces the *O*-acyl-isourea functional group. The exposed amino group reacts with the HOBt active ester to produce a novel peptide bond, and the HOBt leaving group is removed. The result is an extended peptide chain.

In the HBTU coupling method, as shown in Figure 11, the *N*-Boc-L-amino acid is pre-activated by coupling to 2-(1H-benzotriazole-1-yl)-1,1,3,3-tetramethyluronium hexafluoride phosphate (HBTU). The ionized acid group of the *N*-Boc-L-amino acid attacks the tetramethyl group and forms a tetramethyluronium active ester. The newly formed *N*-Hydroxybenzotriazole (HOBt) attacks the carbonyl in the ester group, and 1,1,3,3-tetramethylurea acts as a leaving group. When the HOBt active ester is mixed

with the peptide resin, the exposed lone pair electrons on the amine group at the *N*-terminus of the peptide chain attacks the carbonyl group on the Boc-amino acid, removing the HOBt as a leaving group, and forming a peptide bond. After coupling, the peptide is increased in length by one amino acid.

To use the HBTU protocol the peptide resin was washed with DCM, neutralized with 10% DIEA, and drained. Then 5 equivalents of Boc-AA and 5 equivalents of HBTU were dissolved using a minimal amount of DMF in a clean Erlenmyer flask, 10 equivalents of 20% DIEA in DCM was added to the flask, and the mixed flask contents were added to the reaction vessel. The coupling reaction was run for 90 minutes.

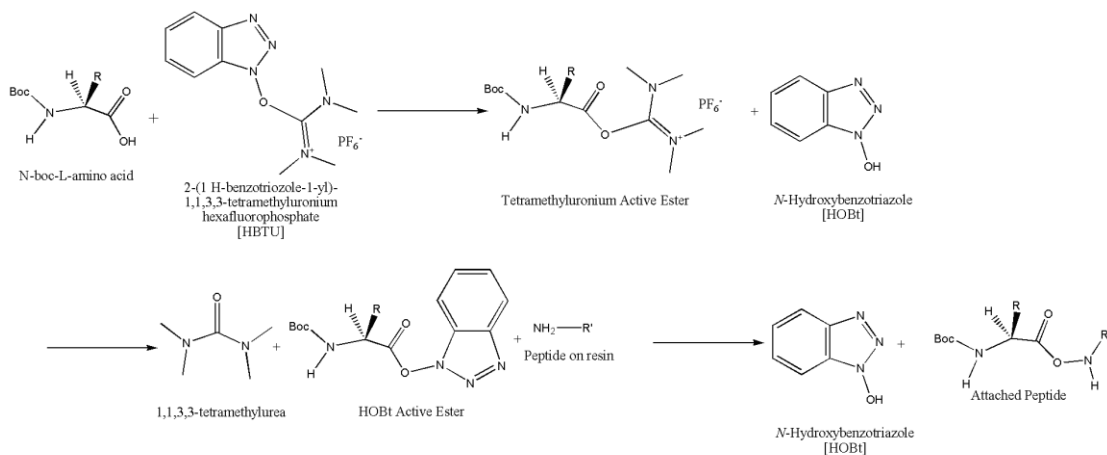


Figure 11: Direct HBTU Coupling Protocol. In this coupling method, the *N*-Boc-L-amino acid is pre-activated by coupling to 2-(1H-benzotriazole-1-yl)-1,1,3,3-tetramethyluronium hexafluoride phosphate (HBTU). The tetramethyluronium leaving group on the active ester is replaced by HOBt. The exposed amino group reacts with the HOBt active ester to produce a novel peptide bond, and the HOBt leaving group is removed. The result is an extended peptide chain.

3.2.3 Histidine-dinitrophenol Removal Protocol

All of the protecting groups attached to the side chains of the Boc amino acids used in the SPPS were labile to hydrofluoric acid cleavage; the lone exception was the dinitrophenol (DNP) protecting group on the side chain of histidine. DNP removal needed to precede HF cleavage; otherwise, the freed DNP molecules might react elsewhere on the peptide. As both LM7-1 and LM7-2 contained Histidines, the DNP groups were removed by using 20 mmol of noxious thiophenol in 5 ml DMF for each mmol of His (DNP) present in the product peptide (0.102 ml/mmol, or 2 ml thiophenol/mmol). The mixture was gently agitated for 1-4 hrs at room temperature, drained, and the peptide-resin was washed with solvents multiple times until the thiophenol and its associated foul odors were removed.

3.2.4 Anhydrous High Hydrofluoric Acid Cleavage Protocol

The *N*-terminal Boc group was removed using TFA: DCM (1:1, 2 + 30 min); this was done before the HF cleavage so that the Boc byproducts would not alkylate any deprotected regions of the peptide. The “DNP-free”, Boc-deprotected peptide-resin was washed with DCM several times and then dried using reduced pressure from a water aspirator.

The peptide-sample was then divided into 2x 1.0 g peptide-resin aliquots and placed them into two separate Kel-F™ HF cleavage vessels, along with a teflon-coated stir bar. The vial lids were added, the lids were covered with Parafilm®, vent holes were poked in the Parafilm®, and the samples were completely dried under high vacuum

with the lyophilizer overnight. Afterwards, a scavenger mixture of 1 ml of p-cresol and 1 ml of p-thiocresol was added to each vial containing the dry peptide-resin (1% v/w).

The HF apparatus was leak-checked with N₂ gas after mounting the peptide-resin (RV) reaction vessels, to ensure the system was closed. The apparatus outlet passed through a 8M aqueous KOH trap to neutralize any excess HF. The HF vials were cooled to -78°C in vacuum dewer flasks containing a slurry of isopropanol and dry ice for 20 minutes, before 10 ml of room temperature HF was distilled into each chilled vial. Once the correct volume of HF was added, the vials were stirred and allowed to warm up to 0°C with an ice-water mixture for 1 hour; the HF cleaved off the peptides from the support resin, and it also removed the remaining side chain protecting groups. When the HF reaction was complete, the vials were allowed to warm up to room temperature, and N₂ gas was used to blow off any remaining HF into the KOH trap, and to dry out the product crude peptides and resin. Suction from a water aspirator was used to completely dry out the resin vessels and apparatus, and then the HF vessels containing resin, scavengers, and crude product peptides were unscrewed from the apparatus.

The organic scavengers from the peptide-resin were extracted with diethyl ether twice, and then the crude peptide was extracted from the solid resin using 10% (v/v) aqueous acetic acid, and any insoluble peptide remnants were further extracted using glacial acetic acid. The 10% and glacial acetic acid extracts with the crude peptide

were lyophilized and the yield of crude peptide was determined. The remaining solid from the extractions was the polystyrene-divinylbenzene support resin.

3.3 Liquid Chromatography Purification

3.3.1 Gel Filtration Liquid Chromatography with a G25 Sephadex® Column

The glass Liquid Chromatography column was fitted with a fritted outlet filter. The column was filled with pre-swollen G25 Sephadex® in 10% (v/v) aqueous acetic acid to form a packed gel filtration bed of 2.5 x 86 cm. Above the column, 10% (v/v) aqueous acetic acid was added via a peristaltic pump from a reservoir. Below the column outlet, the drain line was routed through a preparative flow cell in a UV absorbance detector, which was set to 280 nm to quantify relative amounts of tryptophan present as the peaks eluted. The detector output was recorded on a chart recorder such that the analog chromatogram was annotated with absorbance data readings noted during the run. The eluent was deposited into fraction tubes so that the peptide product peak was collected separately from the synthesis waste. Once the column bed was set up and leak tested, a blue dextran solution was run through the column to determine the column void volume (~160 ml); the dye ran through the column without being retained by the Sephadex® beads.

The crude peptide was then dissolved in 10% (v/v) aqueous acetic acid so the concentration was roughly 25 mg/ml. The liquid in the column was then drained down to just over the top of the Sephadex® bed; a 3 ml sample was layered across the top of the stationary phase bed yielding 75 mg of crude peptide. The sample was

drained into the top of the Sephadex bed, and a head space of 10% acetic acid was added. The peristaltic pump was started, and the eluent was routed through the UV detector.

As shown in Figure 12, the first column “void” volume (~160 ml) was always discarded. The second column volume, which contained the purified peptide, was collected in 13 x 100 mm fraction tubes in 3 ml/tube (160 ml/3 column volumes = 53.3 ml/column volume). The third column volume, with impure peptides and scavengers, was collected separately. The fraction tubes were processed by scanning them individually in a spectrophotometer at 280 nm to determine the true absorbance values where the sample was the most concentrated. The point from where the first peak started to elute to where the absorbance rapidly fell contained the purest peptide product (Peak A); the point where the absorbance fell back down to baseline levels contained impure products (Peak B). Peaks A and B were separately pooled and frozen in a dry ice/isopropanol slurry and added to freeze dryer flasks. After the samples were frozen, the flasks were connected to the lyophilizer; the acetic acid was sublimed off, and the remaining dried, fluffy peptide sample was ready to be purified further.

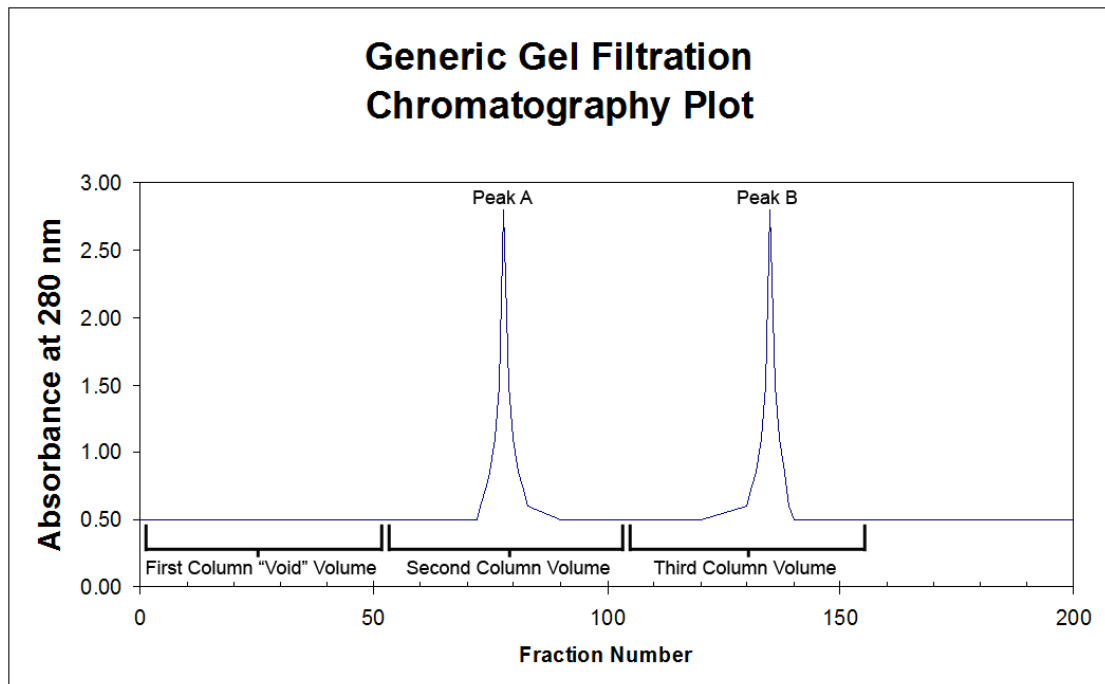


Figure 12: Generic Gel Filtration Chromatography Plot. In this hypothetical graph, absorbance at 280 nm is plotted against Fraction number. In a typical post-HF cleavage peptide purification run, there are three major volumes produced. The first column “void” volume represents the total liquid excluded from the stationary phase and in the tubing. The second column volume represents the protein products not retained by the gel filtration stationary phase. The third column volume represents protein fragments, HF scavengers and salts retained by the gel filtration stationary phase.

3.3.2 Reversed Phase Preparatory High Performance Liquid Chromatography with a C₁₈ Column

All the preparatory RP-HPLC runs were done with a 22 x 250 mm, Vydak 218TP, C18 Reversed Phase column. The mobile phases were stored in bottles of varied concentration ranging from 5% acetonitrile/95% water/0.1% TFA up to 95% acetonitrile/5% water/0.1% TFA. From the reservoir bottle, the mobile phase was run through a pump, and then through a six way Rheodyne 7010 injector valve up into the column. The outlet line from the top of the column was routed through a flow cell with a UV absorbance detector set to 220 nm to detect peptide bonds as the peaks of

interest eluted. The eluent was deposited, 75 drops at a time (3 ml), into fraction tubes so that similar products were later pooled. The UV detector was connected to a chart recorder to provide a paper record of the RP-HPLC run.

The peptide mixtures were dissolved in 10% (v/v) aqueous acetic acid, ensuring that the solution concentration was no higher than 10 mg/ml. The analyte solution was refrigerated at 4°C as a precaution to slow down any peptide degradation until it was injected. Just prior to a RP-HPLC run, up to 5 ml of the peptide sample was loaded into the sample loop in the Rheodyne® high pressure injection valve. Then 5% acetonitrile/95% water/0.1% TFA was run through the column until the baseline absorbance on the UV detector stabilized; the detector was then zeroed. The run was started by switching the valve to inject the loaded peptide product inside the sample loop into the column. For step gradient runs, the reservoir bottles were switched out every time a higher concentration of acetonitrile was required, along with a corresponding annotation written on the chromatogram. At the end of every run, 95% acetonitrile/5% water/0.1% TFA was used to flush any remaining contaminants out of the preparatory RP-HPLC column.

As shown in Figure 13, fraction tubes were processed into groups representing four distinct zones: baseline absorbance outside of peaks, the leading edge & midpeak regions, and the tail end of a peak. Baseline absorbance zones did not contain any usable peptide, due to the low absorption indicating a lack of product. The leading edge and midpeak regions had peptides of the highest purity, due to the fact that these regions of a peak contain components of a very specific hydrophobicity that is

partitioning out of the stationary phase into the mobile phase all at once. The tailing edge frequently had impure products, because overlapping components are partitioning into the mobile phase at a slower rate. Pooled fractions were placed on a rotary evaporator and concentrated until all the acetonitrile was removed, and then the aqueous samples were placed into 15 or 50 ml plastic centrifuge tubes. The pooled, purified samples were frozen in using a dry ice/isopropanol slurry, pinholes were made in the centrifuge tube caps, and the tubes were placed on the lyophilizer in vacuum flasks until all the remaining solvents were sublimed away. The dried, purified peptide samples were saved and frozen at -80°C .

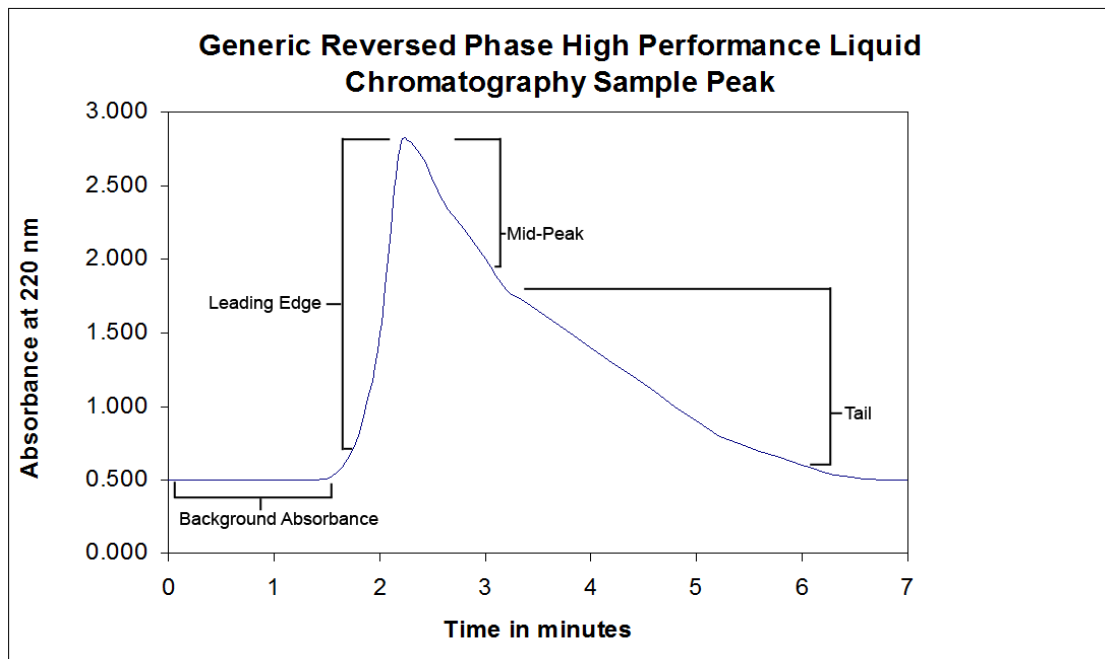


Figure 13: Generic Reversed Phase High Performance Liquid Chromatography Sample Peak. In this hypothetical graph, absorbance at 220 nm is plotted against time in minutes. A single, generic protein peak is shown. The peak has background absorbance before the peptide elutes, the leading edge & mid-peak regions contain the purest product, and the peak tail is impure.

3.4 Mass Spectroscopy

3.4.1 Matrix Assisted Laser Desorption Ionization-Time of Flight Mass Spectrometry

Two $\mu\text{g/ml}$ of a standard protein of known mass was used to calibrate the MALDI-TOF. Single crystals of dried peptides were dissolved in $35\ \mu\text{l}$ of 10% (v/v) aqueous acetic acid. Tenfold dilutions of the samples were made using a diluent mixture (50% acetonitrile/49.95% water/0.05% trifluoroacetic acid). The sample plate was spotted with $1\ \mu\text{l}$ of 10 mg sinapic acid/ml diluent. Then $1\ \mu\text{l}$ of the peptide sample was added within the center of the matrix droplet, and the droplets were air dried. The plate was placed in the MALDI-TOF sample holder and it was exposed to high vacuum conditions. The MW standard was scanned first, and its value was used to correct any deviations from its known mass. The rest of the samples were scanned with the laser beam and the results were averaged and saved. The measured mass/charge (m/z) values of individual HPLC fractions were used as a guide to pool the peptide samples from multiple preparative RP-HPLC runs into appropriate fractions of the synthetic peptide. Samples consisting of single peak with the desired mass were set aside and frozen for use in antimicrobial testing.

3.4.2 Liquid Chromatography-Electrospray Ionization-Mass Spectrometry (ESI-MS)

Single crystals of dried peptides were dissolved in $20\ \mu\text{l}$ of HPLC Buffer A (50% acetonitrile/49.95% water/0.05% formic acid); $1\ \mu\text{l}$ of the dissolved peptide samples were injected into the HPLC column. A fraction of the chromatographic

eluent was diverted into the mass spectrometer where a N₂ sheath gas was added to the flow to “spray” the eluting samples so that some droplets entered the ionization chamber of the MS. The results were recorded in terms of Retention Peaks, Total Ion Chromatograms, and Selected Ion Chromatograms. The electrospray ionization method results in multiply charged peptide. The Mass Spectrometer was then used to determine m/z ratios of multiple peptide peaks having various charges (+1, +2, etc). The m/z ratios were then deconvoluted using software that identifies patterns of peaks which more than likely originated from a single original analyte peak of uncharged mass.

3.5 Antimicrobial Assays

3.5.1 Antimicrobial 96-Well Plate Activity Assay

Mueller-Hinton media and agar was used for antimicrobial broth and plate assays, Nutrient agar was used for maintaining bacterial stocks on slants. 1 loopful of each of the 4 slant species (*Escherichia coli*, *Enterococcus faecalis*, *Staphylococcus aureus*, and *Pseudomonas aeruginosa*) were transferred to separate 150 ml Erlenmeyer flasks containing broth media. The cultures were incubated overnight at 37°C, shaking at 200 RPM. The subcultures were set up by transferring one loopful of each overnight broth culture into fresh, sterile broth media in 150 ml Erlenmeyer flasks. The flasks were incubated overnight again at 37°C, shaking at 200 RPM. Optical Density (OD) was determined by using a Spec20 spectrophotometer set to 630 nm. An uninoculated Mueller-Hinton broth sample was used to zero the absorbance, and then the samples were read by placing 3 ml of the sample into a 13 x100 mm tube, vortexing it, and

inserting the tube into the spectrophotometer. Each subculture was then diluted to a starting OD₆₃₀ of ~0.12.

The 96-well plate was typically set up as shown in Table 5. Each well had a maximum capacity of 300 µl; the plate had 8 rows versus 12 columns. Test peptides LM7-1/LM7-2 were suspended in a solution of filter-sterile Hancock Diluent (0.2% Bovine Serum Albumin in 0.1% Acetic acid) to make an initial working concentration of 5mg/ml, then 1:10 and 1:100 dilutions were also made. Chloramphenicol was used at a working concentration of 0.1 mg/ml; this antibiotic was a control, used to calibrate inhibition of bacterial growth. Using aseptic technique, sterile broth trays were filled with 5 ml of the bacterial suspension at an OD₆₃₀ of 0.12, and mixed with 10 ml of the Muller-Hinton broth to make a “bacterial broth”. The wells in the 96-well plate were then filled up. Each well in columns 2-6, 8-9, and 11 got 150 µl of the bacterial broth. Then Mueller-Hinton media was added: 130 µl to all wells in column 3, 140 µl in all wells in columns 4 + 8 + 9, 300 µl in all wells in columns 1 + 7 + 10. Then, 20 µl of the neat initial AMP solution was added to all wells in Column 3, 10 ul to all wells in column 4, 2 µl of the 1:10 AMP dilution was added to all wells in column 5, and 2 ul of the 1:100 AMP dilution was added to all wells in column 6. Finally, 10 µl of 6M NaOH was added to all wells in column 9, and 10 µl of chloramphenicol was added to all wells in column 8.

Table 5: Template for an Antibacterial Activity Assay. Results were monitored by scanning 96-well plates at 630 nm. The contents were as follows: Media (Mueller-Hinton broth only), Bac (*Escherichia coli*, *Enterococcus faecalis*, *Staphylococcus aureus*, or *Pseudomonas aeruginosa*), Dil (Dilution), AMP (LM7-1 or LM7-2), Antibio (active antibiotic), 6 M NaOH (total cell kill solution). The columns are different experimental conditions; the rows are replicates.

Media only	Bac	Bac AMP Dil	Bac AMP Dil 2	Bac AMP Dil 3	Bac AMP Dil 4	Media only	Bac Chloramphenicol	Bac 6 M NaOH	Media only	Bac	Media only
A1	A2	A3	A4	A5	A6	A7	A8	A9	A10	A11	A12
B1	B2	B3	B4	B5	B6	B7	B8	B9	B10	B11	B12
C1	C2	C3	C4	C5	C6	C7	C8	C9	C10	C11	C12
D1	D2	D3	D4	D5	D6	D7	D8	D9	D10	D11	D12
E1	E2	E3	E4	E5	E6	E7	E8	E9	E10	E11	E12
F1	F2	F3	F4	F5	F6	F7	F8	F9	F10	F11	F12
G1	G2	G3	G4	G5	G6	G7	G8	G9	G10	G11	G12
H1	H2	H3	H4	H5	H6	H7	H8	H9	H10	H11	H12

The 96-well plate reader, and its attached computer was turned on, and the Molecular Devices SoftMax Pro® v.5 program was used to collect the data. The wavelength was set 630 nm, the plate was inserted into the reader, and Optical Density measurements were taken of all 96 wells simultaneously at various time points. In between measurements, the plates were incubated on a shaking platform at 200 RPM at 37°C. Plate readings were done every half hour for the first 3 hours after incubation, and then read again after an overnight incubation. The data files were saved both as X-PDA format (Softmax only) and open source/ASCII X.csv/x.txt format that was imported into Microsoft® Excel for further analysis.

3.5.2 Procedure for Antimicrobial peptide Hemolytic Assay Protocol

Whole human blood samples were drawn from 2 anonymous volunteers into 3.5 ml tubes containing the anticoagulant Heparin to facilitate intact red blood cell isolation. The samples were combined, gently mixed, spun down at 800 x g, the supernatant was discarded, and the cells were resuspended with filter-sterilized PBS Buffer (100 mM NaCl, 80 mM Na₂HPO₄, 20 mM NaH₂PO₄, pH 7.4). The washes were repeated until the supernatant became clear. The washed RBCs were diluted with PBS Buffer to a final concentration of 8% (v/v) of packed cells.

Table 6 shows a typical setup for a Hemolysis Assay. Red blood cells were tested with a total of five different peptide dilutions. The initial peptide concentrations were 5 mg/ml (1.71 mM) for LM7-1 and 5 mg/ml (1.67 mM) for LM7-2. A positive hemolysis control was made by mixing 750 µl of suspended RBC and 750 µl of 0.020% (v/v) aqueous Triton X-100® to osmotically lyse the RBCs. A negative hemolysis control was made by mixing 750 µl of suspended RBC and 750 µl of PBS buffer. All test samples were incubated with mild agitation at 37°C. At selected time points, up to 24 hours, a 60 µl aliquot of each sample was centrifuged at 4000 x g for 10 minutes to pellet the intact RBCs. 50 µl of the test sample supernatant was then diluted tenfold with 450 µl of PBS Buffer, gently vortexed, and read on the Spectrophotometer.

Table 6: Typical Setup for a Peptide-induced Hemolysis Assay. The template shows volumes utilized throughout the various experimental runs. All 5 tubes used a standardized concentration of human RBC. The AMP amounts tested varied from tube to tube, with the PBS buffer making up the difference in volume.

	Tube						
	1	2	3	4	5	(+) Control	(-) Control
LM7-1 AMP (5 mg/ml-1.71 mM) or LM7-2 AMP (5 mg/ml-1.67 mM)	50 μ l	40 μ l	20 μ l	10 μ l	1 μ l		
(8% v/v) RBCs	150 μ l	150 μ l	150 μ l	750 μ l	750 μ l	750 μ l	750 μ l
PBS Buffer 100 mM	100 μ l	110 μ l	130 μ l	740 μ l	749 μ l		750 μ l
0.020% (v/v) aqueous Triton X- 100®						750 μ l	
Total Volume	300 μ l	300 μ l	300 μ l	1500 μ l	1500 μ l	1500 μ l	1500 μ l
AMP Concentration	833 μ g/ml	666 μ g/ml	333 μ g/ml	33.3 μ g/ml	3.33 μ g/ml		
RBC Concentration	4%	4%	4%	4%	4%	4%	4%

The Genesys 10UV Scanning UV-VIS spectrophotometer was warmed up for 30 minutes; a quartz cuvette, which contained PBS buffer as a blank, was inserted into the device. After zeroing the spectrophotometer with the blank, the samples were scanned at 419 nm, which was the largest absorbance peak found in soluble hemoglobin, as shown in Figure 14. The percent hemolysis was calculated using the formula below:

$$\% \text{ Hemolysis} = \left(\frac{\text{Abs}_{\text{Peptide}} - \text{Abs}_{\text{PBSBuffer}}}{\text{Abs}_{0.020\% \text{ Triton X-100}} - \text{Abs}_{\text{PBS}}} \right) \times 100 \quad (1)$$

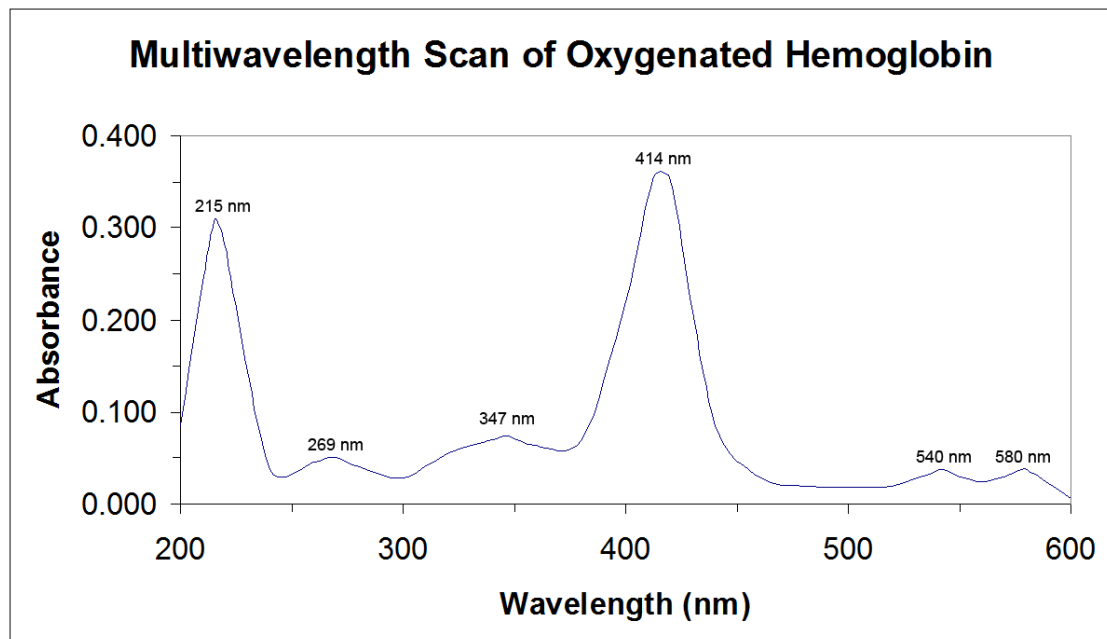


Figure 14: Multiwavelength scan of soluble Hemoglobin from 200-600 nm. In this graph, absorbance is plotted against wavelength in nanometers. The peak maxima at 215 nm, 270 nm, 350 nm, and 414 nm were observed in both oxygenated and deoxygenated hemoglobin. The peak maxima at 540 nm and 580 nm were specific to oxygenated hemoglobin samples.

3.5.3 Data Analysis

The Antimicrobial 96-Well Plate Activity Assays were the only portion of the thesis research done using replicate trials. All of the samples were run with 8 replicates except for the uninhibited bacterial growth samples (16 replicates) and the Mueller-Hinton media only samples (32 replicates). Each dilution of peptide was compared to the uninhibited bacterial growth using an unpaired Student's T-test. Differences were considered significant when $P < 0.05$ (Mather, 1965).

CHAPTER 4

RESULTS

4.1 Solid Phase Peptide Synthesis

4.1.1 Solid Phase Peptide Synthesis Discussion

Solid Phase Peptide Synthesis (SPPS) is a technique which is used to create peptides or alternative medications from amino acid building blocks synthetically, without the need for cells, enzymes, or ribosome's. Although the protected amino acid building blocks are expensive, and the time needed for synthesis is a function of peptide length, SPPS offers several advantages over enzymatic synthesis. SPPS does not take place in living cells, so it avoids the problem of separating the product proteins from the rest of the cellular proteins, the issue of the formation of proteins toxic to the synthesizing organism is avoided, and there are no uncertainties about the contents of the reaction mixtures. It is also easy to incorporate unnatural amino acids and post translational modifications during SPPS, which are more difficult to achieve during peptide synthesis *in vivo*.

4.1.2 Solid Phase Peptide Synthesis of Peptide LM7-1

Table 7: Summary of SPPS Coupling Reactions for Peptide LM7-1. This table shows how many rounds of coupling reactions were required to complete the 27-residue synthetic peptide. The AA position numbers started out at the *N*-terminal. As shown in the middle 3 columns, some Boc amino acids required more than one round of coupling to fully saturate the free amino groups. Eq is equivalents; it indicated how much excess Boc-amino acids were added on each round of coupling relative to the original amount of free amino groups on the resin. AA (mmol) indicated the actual amounts of amino acids used for each coupling reaction. The end dates indicated when an incoming Boc amino acid had fully coupled. Coupling number was the order in which the Boc amino acids were added to the peptide-resin chain; as the synthesis order was reversed from that of enzymatic biosynthesis.

AA Position	AMINO ACID	Eq	aa (mmol)	Eq	aa (mmol)	Eq	aa (mmol)	End Date	Coupling
-	C-term NH ₂	1.0	0.669					-	-
27	N	0.4	0.3	4.0	2.7			7/3/09	1
26	L	5.0	3.4					7/6/09	2
25	Y	5.0	3.4					7/7/09	3
24	H	5.0	3.3	2.0	1.4			7/8/09	4
23	T	5.0	3.4	2.0	1.4			7/9/09	5
22	L	5.0	3.4	2.0	1.3			7/9/09	6
21	A	5.0	3.4					7/13/09	7
20	A	5.0	3.4					7/13/09	8
19	K	5.0	3.3	2.0	1.3	4.0	0.9	7/15/09	9
18	G	5.0	3.3					7/15/09	10
17	V	5.0	3.4	2.0	1.4	4.0	2.7	7/15/09	11
16	H	5.0	3.4	2.0	1.3	1.0	0.7	7/17/09	12
15	G	5.0	3.3	2.0	1.3			7/21/09	13
14	G	5.0	3.3					7/21/09	14
13	V	5.0	3.4					7/21/09	15
12	H	5.0	3.3	1.0	0.2			7/22/09	16
11	A	5.0	3.3					7/22/09	17
10	A	5.0	3.4	2.0	1.3			7/22/09	18
9	K	5.0	3.3	2.0	1.3	1.0	0.7	7/23/09	19
8	K	5.0	3.3	2.0	1.3			7/24/09	20
7	L	5.0	3.4	2.0	1.3			9/22/09	21
6	M	5.0	3.4					9/30/09	22
5	T	5.0	3.3	2.0	1.4	4.0	2.7	10/6/09	23
4	K	5.0	3.3	2.0	1.4	4.0	2.7	11/19/09	24
3	W	5.0	3.1					11/22/09	25
2	L	5.0	3.4					11/24/09	26
1	A	5.0	3.5					12/1/09	27

The summary of the coupling reactions used to synthesize peptide LM7-1 is summarized in Table 7. The 1-hydroxybenzotriazole (HOBt) protocol was the first procedure used to couple the initial Asn²⁷ (*N*-Boc-L-Asn-OH) to the amino-linked beads in the MBHA resin. A racemic suppressor such as HOBt was important because it prevented the incoming Boc-AA from base-catalyzed chirality inversion during an extended overnight reaction. Figure 15 shows the possible sites for nucleophilic attack of the lone pair electrons on a free *N*-terminus amino group on two possible coupling reagents. Path 1 shows the electrons attacking the carbon in the ester group contained within the *O*-acylisourea functional group. This is the intended site of attack, as the Boc-AA will couple to the free amino group, and the DCU leaving group will be removed. Path 2 shows an alternate site of attack; the electrons can attack the α -carbon on the Boc-AA, due to the strong electron withdrawing potential of the *O*-acylisourea group. The loss of the hydrogen on the α -carbon can cause the Boc-AA to potentially reverse chirality before the DCU is removed. Path 3 shows the electrons attacking the carbon in the ester group contained within the HOBt active ester functional group. This is the intended site of attack, as the Boc-AA will couple to the free amino group, and the HOBt leaving group will be removed. Path 4 shows an unlikely alternate site of attack; the electrons are less likely to attack the α -carbon on the Boc-AA, due to the reduced electron withdrawing potential of the oxybenzotriazole group. The initial coupling reaction was inadvertently run 10 times less concentrated than necessary, so it was redone using a higher concentration of the initial Boc-AA. The HOBt protocol used the standard *N, N'*-

dicyclohexylcarbodiimide (DCC) coupling agent, paired with an equimolar amount of the protected amino acid and HOBt.

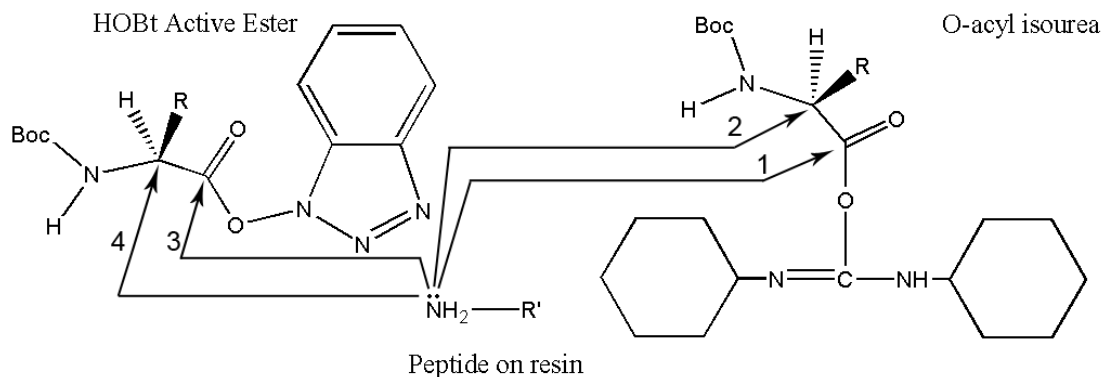


Figure 15: Advantages of 1-hydroxybenzotriazole over *O*-acylisourea as a racemization suppressor. This figure shows the possible sites for nucleophilic attack of the lone pair electrons on a free *N*-terminus amino group on two possible coupling reagents. Path 1 shows the preferred location of attack for the amine group lone pair electrons to the carbonyl in the *O*-acylisourea functional group, leading to peptide extension. Path 2 shows an alternate site of attack; the *O*-acylisourea group can draw electrons away from the α -carbon on the Boc-AA, potentially leading to chirality inversion. Path 3 shows the preferred location of attack for the amine group lone pair electrons to the carbonyl in the HOBt active ester functional group, leading to peptide extension. Path 4 shows an unlikely alternate site of attack; the oxybenzotriazole group has reduced electron withdrawing potential compared to the *O*-acylisourea group. Thus, the electrons are less likely to attack the α -carbon on the Boc-AA.

All of the couplings after the attachment of the first Boc-AA to the resin always started with the Direct DCC catalyzed coupling protocol. It used a fivefold excess of DCC with an equimolar amount of Boc-AA. The DCC reacted to the acidic end of the Boc-AA and made a reactive leaving group that made it far easier for the amino acid to form an amide bond. The DCC ended up as the waste product dicyclohexylurea (DCU).

The next two residues, Leu²⁶ (*N*-Boc-L-Leu-OH), and Tyr²⁵ (*N*-Boc-L-Tyr(OBzl)-OH), coupled with the Direct DCC method. Tyrosine is a Boc-AA that frequently possesses side chain protection, especially during the synthesis of long peptide chains. The hydroxyl group on the side chain has a pK_a of around 10, so it is vulnerable to acylation by TFA or a Boc-AA. Having a Benzyloxy (OBzl) group reduces the chance of acylation, or of the unwanted side reaction of migration of an acyl group to the *ortho* position on the tyrosine ring.

Direct DCC was insufficient to drive the His²⁴ (*N*-Boc-L-His(2,4-DNP)-OH) reaction to completion, as the remaining free amino groups still produced a positive blue pigment during the ninhydrin test. The His²⁴ Boc-AA is a bulky residue, and difficult to dissolve in DMF, especially with the 2,4-dinitrophenol (2,4-DNP) side chain protecting group attached. The 2,4-DNP group is necessary due to the fact that the unprotected side chain of histidine has a pK_a around 6; the aromatic ring is vulnerable to alkylation, and the electron withdrawing imidazole side chain can lead to racemization. With the protecting group attached, the pK_a is lowered to around 3, and the residue side chain is stable during SPPS. Whenever the Direct DCC coupling protocol failed, the Symmetric Anhydride protocol was subsequently employed to completely eliminate any remaining free amino termini.

During the process of utilizing the Symmetric Anhydride protocol, the DCC coupling reagent did not directly catalyze the attachment of the Boc-AA to the peptide-resin. The alternate reaction mechanism was that one equivalent of DCC was used to couple two equivalents of the Boc-amino acid to each other to form a

symmetric anhydride. In the next step of the reaction, the anhydride reacted with the amino end of the peptide to form a slightly longer chain, with one Boc-AA bonding to the chain, and the other ending up as soluble waste along with the DCU. Symmetric anhydrides are extremely reactive, and are effective at coupling sterically hindered or insoluble residues. However, this reaction is never used before Direct DCC for several reasons: half of the Boc-AA reagent is wasted, and at elevated temperatures, the Symmetric Anhydride can react intramolecularly to produce a double Boc-AA coupling. Thr²³ (*N*-Boc-L-Thr(OBzl)-OH) and Leu²² (*N*-Boc-L-Leu-OH) also required a combination of direct DCC and symmetric anhydride couplings to be effective.

Residues Ala²¹ (*N*-Boc-L-Ala-OH) and Ala²⁰ (*N*-Boc-L-Ala-OH) coupled satisfactorily with the Direct DCC Catalyzed Coupling Protocol. The next residue, Lys¹⁹ (*N*-Boc-L-Lys(2-Cl-Z)-OH) did not couple completely with the Direct DCC catalyzed coupling protocol, or Symmetric Anhydride coupling protocol because this yielded positive ninhydrin results. Therefore, the HOBt coupling protocol was used to complete the Boc-AA attachment. This was the same HOBt Coupling Protocol that was used to attach the initial Asn²⁷ residue to the resin. Although the side chain protection on lysine adds to its bulk and reduces solubility in DMF, lysine is a Boc-AA residue that must always be protected during SPPS. A lysine with an exposed side chain amino group can couple with incoming Boc-AAs, creating branched peptides. During this peptide synthesis, 2-chloro-benzyloxycarbonyl (2-Cl-Z) was selected in place of benzyloxycarbonyl (Bzl) as the lysine side protection. Benzyloxycarbonyl,

like *tert*-butyloxycarbonyl (Boc) is labile to TFA cleavage. Adding chlorine to the Bzl group in the *ortho* position reduces side chain protection losses significantly.

During the remainder of the sequence, Gly¹⁸ (*N*-Boc-Gly-OH), Gly¹⁴ (*N*-Boc-Gly-OH), Val¹³ (*N*-Boc-L-Val-OH), Ala¹¹ (*N*-Boc-L-Ala-OH), Met⁶ (*N*-Boc-L-Met-OH), Trp³ (*N*-Boc-L-Trp-OH), Leu² (*N*-Boc-L-Leu-OH), and Ala¹ (*N*-Boc-L-Ala-OH) all coupled in a single reaction with the initial Direct DCC Protocol. With the exception of Tyr²⁵, and Trp³, which were largely aromatic, all the residues that coupled with the first protocol had short chain aliphatic hydrocarbon side chains. Thus, these types of residues were easier to dissolve into solution. None of these residues had side chain protection, as hydrophobic side chains are not susceptible to undesired side reactions.

Two coupling protocols were needed for Gly¹⁵ (*N*-Boc-Gly-OH), His¹² (*N*-Boc-L-His(2,4-DNP)-OH), Ala¹⁰ (*N*-Boc-L-Ala-OH), Lys⁸ (*N*-Boc-L-Lys(2-Cl-Z)-OH), and Leu⁷ (*N*-Boc-L-Leu-OH). Although four of the total residues that coupled on the second protocol were aliphatic, two were polar, and three were positively charged. This seems to indicate that residues with polar and positively charged side chains were more difficult to couple to the peptide chain than other side chain types.

Three coupling protocols were needed for Val¹⁷ (*N*-Boc-L-Val-OH), His¹⁶ (*N*-Boc-L-His(2,4-DNP)-OH), Lys⁹ (*N*-Boc-L-Lys(2-Cl-Z)-OH), Thr⁵ (*N*-Boc-L-Thr(Bzl)-OH), and Lys⁴ (*N*-Boc-L-Lys(2-Cl-Z)-OH). Threonine, like histidine and lysine, is another Boc-AA that requires side chain protection. Unprotected hydroxyl groups in threonine and serine can react with an adjacent amide group to transfer part of the peptide chain onto the side chain, creating an ether linkage. Having a Benzyloxy

(OBzl) group attached blocks this undesired side reaction, although it increases mass and reduces Boc-AA solubility in DMF. Only one of the total residues that coupled on the third protocol were aliphatic, one was polar, and the remaining three were positively charged. This seems to indicate that residues with polar and positively charged side chains were more difficult to couple to the peptide chain than other side chain types.

4.1.3 Solid Phase Peptide Synthesis of Peptide LM7-2

Table 8: Summary of Coupling Reactions for Peptide LM7-2. This table shows how many rounds of coupling reactions were required to complete the 27 residue synthetic peptide. The AA positions started out at the *N*-terminus. As shown in the middle 3 columns, some Boc amino acids required more than one round of coupling to fully saturate the free amino groups. Eq is equivalents; it indicated how much excess Boc-amino acids were added on each round of coupling relative to the original amount of free amino groups on the resin. AA (mmol) indicated the actual amount of amino acids used for each coupling reaction. The end dates indicated when an incoming Boc amino acid had fully coupled. Coupling number was the order in which the Boc amino acids were added to the peptide-resin chain as the synthesis order was reversed from that of enzymatic biosynthesis.

AA Position	AMINO ACID	Eq	aa (mmol)	Eq	aa (mmol)	Eq	aa (mmol)	Eq	aa (mmol)	End Date	Coupling
-	C-term NH ₂	1.0	0.669							-	-
27	N	4.0	0.8	2.0	0.4					1/7/11	1
26	L	5.0	0.9							1/13/11	2
25	Y	5.0	0.9							1/13/11	3
24	H	5.0	0.9	2.0	0.4					1/23/11	4
23	T	5.0	0.9	2.0	0.4					1/30/11	5
22	L	5.0	0.9	2.0	0.4					2/3/11	6
21	A	5.0	0.9							2/15/11	7
20	A	5.0	0.9							2/23/11	8
19	K	5.0	0.9							2/25/11	9
18	G	5.0	0.9	2.0	0.4	4.0	0.7			3/2/11	10
17	V	5.0	0.9							3/4/11	11
16	H	5.0	0.9							3/6/11	12
15	K	5.0	0.9							3/12/11	13
14	G	5.0	0.9							2/21/11	14
13	V	5.0	0.9	2.0	0.4					3/26/11	15
12	H	5.0	0.9							3/28/11	16
11	A	5.0	0.9							3/30/11	17
10	A	5.0	0.9							3/30/11	18
9	K	5.0	0.9							4/1/11	19
8	K	5.0	0.9							4/3/11	20
7	L	5.0	0.9							4/4/11	21
6	M	5.0	0.9							4/6/11	22
5	T	5.0	0.9							4/6/11	23
4	K	5.0	0.9							4/8/11	24
3	W	5.0	0.9	2.0	0.4	4.0	0.7	5.0	0.9	4/27/11	25
2	L	5.0	0.9							4/27/11	26
1	A	5.0	0.9							5/1/11	27

The summary of the coupling reactions used to synthesize peptide LM7-2 is summarized in Table 8. LM7-2 was synthesized under identical conditions to LM7-1 using the same reagents, resin and equipment. Asn²⁷ (*N*-Boc-L-Asn-OH), required the HOBt and Symmetric Anhydride protocols to complete the coupling.

For every Boc-AA residue after that, the Direct DCC Catalyzed Coupling protocol was always used first. Leu²⁶ (*N*-Boc-L-Leu-OH), Tyr²⁵ (*N*-Boc-L-Tyr(OBzl)-OH), Ala²¹ (*N*-Boc-L-Ala-OH), Ala²⁰ (*N*-Boc-L-Ala-OH), Lys¹⁹ (*N*-Boc-L-Lys(2-Cl-Z)-OH), Val¹⁷ (*N*-Boc-L-Val-OH), His¹⁶ (*N*-Boc-L-His(2,4-DNP)-OH), Lys¹⁵ (*N*-Boc-L-Lys(2-Cl-Z)-OH), Gly¹⁴ (*N*-Boc-Gly-OH), His¹² (*N*-Boc-L-His(2,4-DNP)-OH), Ala¹¹ (*N*-Boc-L-Ala-OH), Ala¹⁰ (*N*-Boc-L-Ala-OH), Lys⁹ (*N*-Boc-L-Lys(2-Cl-Z)-OH), Lys⁸ (*N*-Boc-L-Lys(2-Cl-Z)-OH), Leu⁷ (*N*-Boc-L-Leu-OH), Met⁶ (*N*-Boc-L-Met-OH), Thr⁵ (*N*-Boc-L-Thr(OBzl)-OH), Lys⁴ (*N*-Boc-L-Lys(2-Cl-Z)-OH), Leu² (*N*-Boc-L-Leu-OH), and Ala¹ (*N*-Boc-L-Ala-OH) all coupled with the initial Direct DCC Protocol. Eleven of the residues had short aliphatic hydrocarbon side chains, one was aromatic, one was polar, and seven were positively charged. The amino acids with aliphatic side chains tended to be the easiest to couple, as they did not require side chain protection, and were soluble in DMF. The residues with bulky side chain protection coupled easily due to the fact they were not in a disadvantageous position in the sequence.

Two coupling protocols were needed for His²⁴ (*N*-Boc-L-His(2,4-DNP)-OH), Thr²³ (*N*-Boc-L-Thr(OBzl)-OH), Leu²² (*N*-Boc-L-Leu-OH), and Val¹³ (*N*-Boc-L-Val-OH).

Two of the total residues that coupled on the second protocol were aliphatic, two were

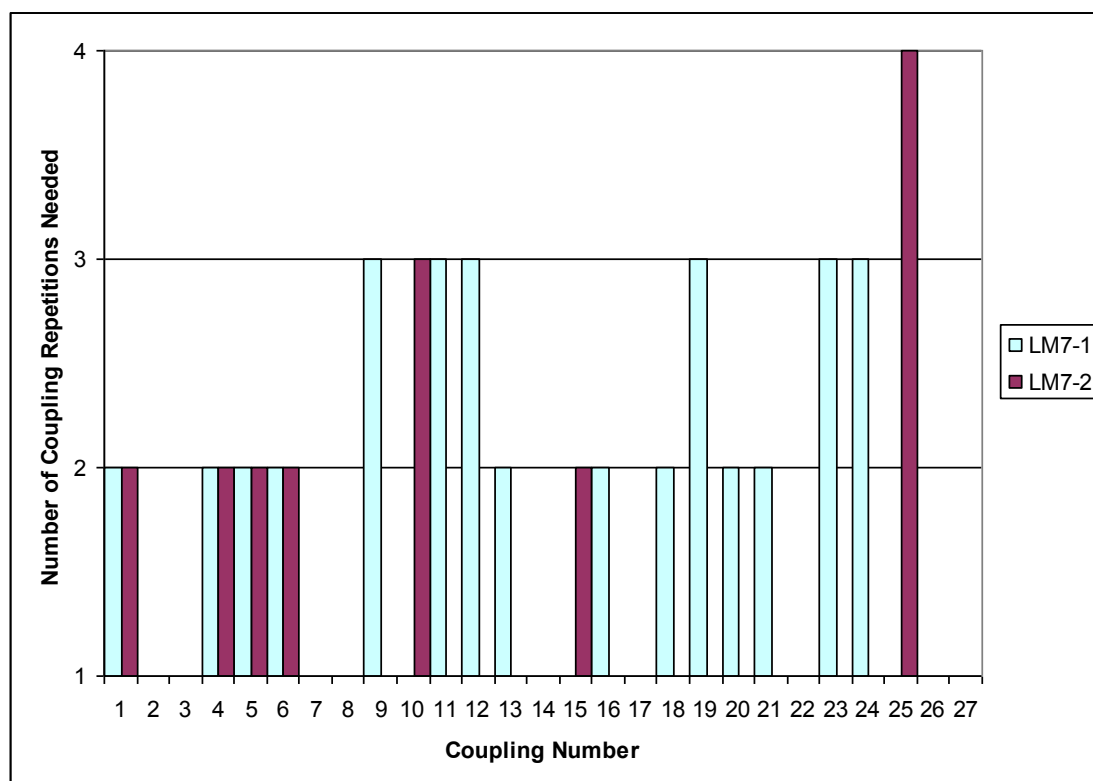
polar, and one was positively charged. Two of the three residues had bulky side chain protection, so it is not surprising that they were more difficult to couple.

Three coupling protocols were needed for Gly¹⁸ (*N*-Boc-Gly-OH). This can be potentially explained by being in a disadvantageous position in the sequence. LM7-1 had a similar coupling difficulty one residue over.

Four coupling protocols were needed for Trp³ (*N*-Boc-L-Trp-OH). The 2-(1H-benzotriazole-1-yl)-1,1,3,3-tetramethyluronium hexafluorophosphate (HBTU) protocol was used due to the failure of the first three protocols. To begin, the HBTU protocol reacted with the Boc-AA using a two step mechanism, and produced a highly reactive leaving group to fully couple the Boc-AA to the peptide chain. The residue that coupled had an aromatic side chain. Trp³ in LM7-1 coupled on the first try, so it is likely that there was difficulty in one of the solvents used during the coupling reaction.

4.1.4 Comparison of Coupling Efficiency of Peptide LM7-1 versus LM7-2

Table 9: Coupling Efficiency of LM7-1 versus LM7-2. This graph compares how many repeated couplings were required in order to completely attach incoming Boc-AA onto the growing peptide chains of LM7-1 (Blue bars) and LM7-2 (Violet bars). The number of coupling repetitions needed is plotted against peptide sequence numbers from the *N*-terminus to the *C*-terminus.



The AMPs LM7-1 and LM7-2 only differed in a single residue; Lys¹⁵ in LM7-2 was replaced with Gly¹⁵ in AMP LM7-1. As shown in Table 9, although there was only one amino acid substitution, there were a variety of differences between the two sequences. LM7-1 had fifteen residues out of twenty seven that required multiple couplings. Upon surveying the results, it was noted that the majority of the “difficult” residues were polar and positively charged; this suggests that those properties increased the difficulty of Boc-amino acid attachment. However, LM7-2 only had seven residues out of twenty seven that required multiple coupling attempts. The side

chain types in LM7-2 were balanced, so no overall pattern can be inferred. With one exception, LM7-1 and LM7-2 had identical AA sequences. Thus, it was likely in the areas where the number of required couplings did not match between the two AMP sequences, that refinement of experimenter technique was responsible for the results, and not the intrinsic difficulty in coupling the sequences themselves. Near the C-terminus of the peptides, at residues His²⁴, Thr²³, and Leu²² the number of repeated coupling steps was the same for both peptides. This implies that the “initiation” region of SPPS possessed the greatest difficulty in attaining full couplings. This finding makes intuitive sense as the initial residues were located closest to the solid resin support, so they would be expected to be the most sterically hindered. Alternatively, this difficulty could possibly be due to the formation of an alpha-helical type in the highly conserved C-terminal sequence, despite the lack of an aqueous solvent during SPPS.

4.2 Liquid Chromatography

4.2.1 Liquid Chromatography Overview

Liquid Chromatography is a purification technique which is used to separate out the desired pure peptide product from shorter failure peptide sequences, and all other contaminants. When proteins are manufactured by SPPS and cleaved off the resin support, chemical contaminants must be first removed so that the product peptide can be thoroughly purified. The two types of liquid chromatography listed below are usually sufficient for synthetic peptide purification for antimicrobial assays when used sequentially. Gel filtration liquid chromatography is used to separate protein products

from synthesis reagents and byproducts immediately following HF resin-cleavage. Preparatory Reversed Phase High Performance Liquid Chromatography is then used to isolate the pure peptide. The purity of the peptide is assessed with Mass Spectrometry, and then the isolated peptide can be used in antimicrobial assays and other tests.

4.2.2 Gel Filtration Liquid Chromatography Discussion

Sephedex® is a dextran derived, cross-linked mixture of polysaccharide beads that are manufactured at varying pore sizes to exclude all analytes above a certain cutoff volume; all biopolymers below this cutoff are retained in inverse proportion to their overall hydrated volume. In this case, G25 Sephedex® will typically exclude the AMPs above the 5 kDa range, and retain the low mass scavengers and reagents left over following the HF cleavage step. For many peptides, the use of this polysaccharide stationary phase after Solid Phase Peptide Synthesis will separate the peptide from other synthesis by products, and yield an adequately pure sample for biological studies.

4.2.3 Gel Filtration Liquid Chromatography Results

It was observed that both crude product peptides LM7-1 and LM7-2 behaved very similarly during preliminary purification on the Gel Filtration Chromatography column, which was run after the final side chain deprotection peptide-resin cleavage steps were completed. The yellow mixture of peptides and synthesis by products rapidly transited the column and separated out into two visible yellow bands. The

eluent was monitored by UV detection, at 280 nm and 300 nm; which also indicated a two peaked chromatogram which was divided into Peak A and Peak B pools for further analysis. As the G25 column stationary phase was designed to exclude >5kDa peptides such as LM7-1 and LM7-2, these products traveled unrestrained through the column and eluted directly after the void mobile phase volume had passed through the apparatus. The leading edge and peak region of Peak A, as seen in Figure 16, likely contained the purest peptide sample. The tailing end of Peak A was assumed to contain a mixture of pure peptide and possibly shorter failure sequences. The B Peak Region contained very little full-length peptide, and consisted of a large proportion of synthesis waste by products.

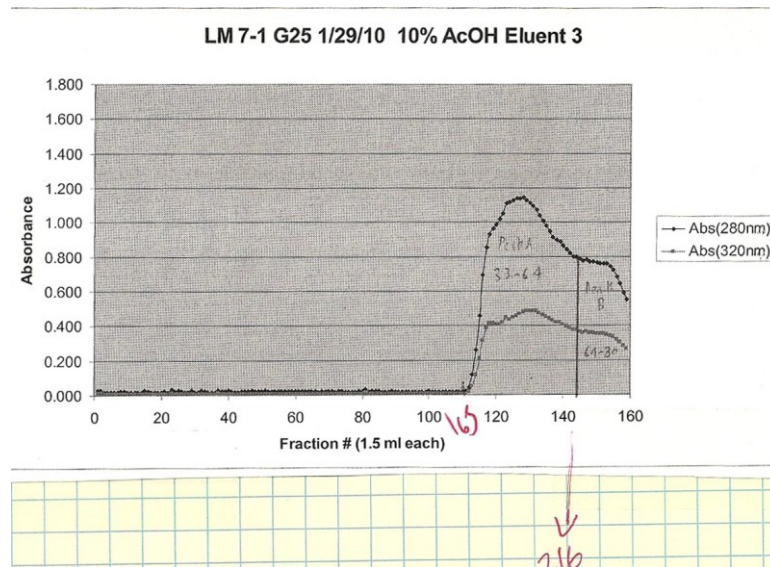


Figure 16: LM7-1 Crude Peptide Eluent G-25 Sephadex® Gel Filtration Run. This graph shows a representative liquid chromatography run that passed a crude LM7-1 AMP wash sample through a 2.5 x 86.0 cm bed of G25 Sephadex® at a flow rate of 0.6 ml/min. The graph compares absorbance at 280 nm versus Fraction number. Note that there are two peaks: the purified LM7-1 Peak A (Fractions 110-143), and the HF scavenger Peak B (Fractions 144-160).

As the concentration of dissolved peptide in the post hydrofluoric acid cleavage protocol 10% acetic acid wash was low, and the subsequent runs used concentrated solutions prepared from dried crude peptide product. This is shown in Figure 17. Again, the two yellow bands were visibly resolved in the column, although the larger concentration of peptides in the eluent maxed out the UV detector used to monitor peaks during the chromatogram run. When necessary, fraction tubes that showed maximized absorbance on the UV flow cell were removed, diluted, and individually run on a spectrophotometer to determine precisely where the pure peptide peak (with the largest peptide bond absorbance) was precisely located.

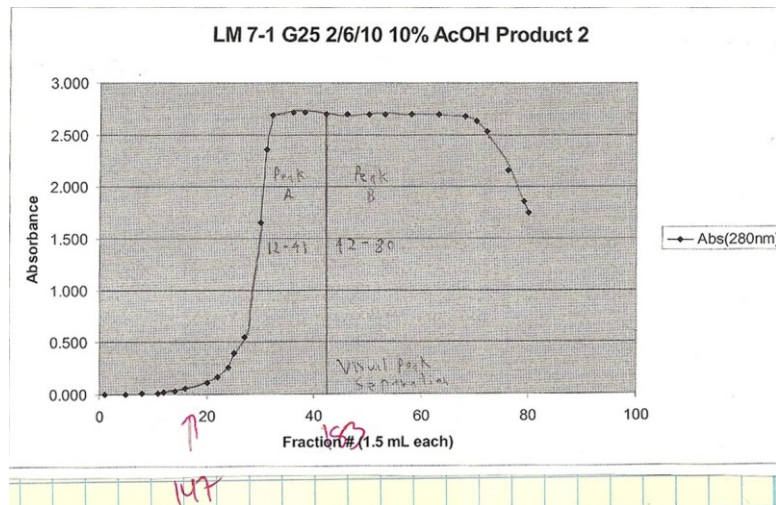


Figure 17: LM7-1 Crude Peptide Product G-25 Sephadex® Gel Filtration Run. This graph shows a crude peptide liquid chromatography run that passed a crude LM7-1 AMP 10% acetic acid extraction sample through a 2.5 x 86.0 cm bed of G25 Sephadex® at a flow rate of 0.6 ml/min. Based on the results shown in Figure 11, the first 80 fractions were discarded and then the remaining fractions were recorded and collected for analysis. The graph compares absorbance at 280 nm versus Fraction number. Note that there are two peaks: the purified LM7-1 Peak A (Fractions 12-41), and the HF scavenger Peak B (Fractions 42-80). As the peptide was concentrated to ~25 mg/ml, the absorbance of the middle of the peaks maxed out the UV detector. Exact peak boundaries were determined by scanning the diluted samples in the off scale regions.

4.2.4 Preparatory High Performance Liquid Chromatography Discussion

Reversed Phase High Performance Liquid Chromatography (RP-HPLC) is a high resolution separation technique that can be used to purify many different types of chemicals. When used for proteomic applications, the main focus of these applications is on short peptides from 4-40 amino acid residues in length. RP-HPLC uses a non-polar stationary phase paired with a more polar mobile phase. The stationary phase contains silica beads with covalently bonded C₁₈ hydrocarbon chains to present a hydrophobic surface for the analyte to adsorb. The mobile phase is mixture of polar water, nonpolar acetonitrile and the hydrophobic counterion trifluoroacetic acid (TFA). The pressurized mixture is pumped in through a control valve, into the base of the column, up out through the top, and then through a UV detector to a fraction collector. Initial conditions for RP-HPLC include a mobile phase of 5% acetonitrile/95% water/0.1% TFA. Under these conditions the injected peptide and associated synthesis byproducts will adsorb tightly to the C₁₈ hydrocarbon chains within the stationary phase. During a run, the amount of acetonitrile is increased by incremental steps. When the mobile phase hydrophobicity, increases to the point that it matches a component of the sample, the product will then partition into solution and elute off the column and into the mobile phase. Because no two components in a sample mixture have identical hydrophobicities; under the correct gradient conditions, complex multi-peptide mixtures can be eluted as separate purified peaks.

4.2.5 Preparatory High Performance Liquid Chromatography on a C₁₈ Reversed Phase Column Results

Both LM7-1 and LM7-2 AMPs were run through a RP- HPLC C₁₈ column that used an acetonitrile/water/TFA mobile phase. By ramping up the acetonitrile (ACN) concentration in discrete steps, substances of increasing hydrophobicity eluted as separate peaks. For LM7-1, the exact character of the hydrophobicity of the crude Peptide Peak A was unknown. Thus, small samples were then run through the prep column as to develop a method which produces a maximum number of peaks with baseline resolution during a given run.

Figure 18 shows an early example of a peptide run through a preparative RP-HPLC column with only three mobile-phase gradient steps, and they were characterized by the following mixtures of acetonitrile and water, with 0.1% TFA as an ion-pairing additive: 20% acetonitrile (0:00-22:00 min), 35% acetonitrile (22:01-40:00 min), and 40% acetonitrile (40:00-55:00 min). There was a final wash step of 100% methanol (55:01-66:00 min). Only four peaks were noted in the resulting chromatogram, and the middle two were poorly resolved. The larger peaks had several components hidden within them, as the mass spectroscopy results indicated that none of the eluted peaks contained a single mass.

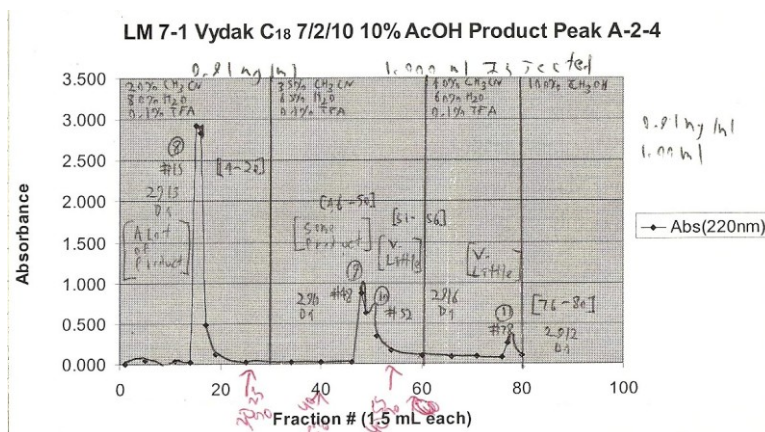


Figure 18: LM7-1 Purified by HPLC Preparative Reversed Phase HPLC with a three-step acetonitrile gradient (Run # 4). The purified Peak A-2 region (Run # 4) of the LM7-1 AMP eluent from the G-25 column was run through a C₁₈Vydac preparatory, RP-HPLC column (300Å, 2.2 x 25.0 cm, 218 TP) to purify the desired peptide before running bioassays. The flow rate was 2.9 ml/min. The mobile phase gradient consisted of 20%, 35%, and 40% aqueous acetonitrile, followed by a 100% methanol column wash. The graph plots absorbance at 280 nm versus Fraction number.

Figure 19 shows an example of a preparatory Reversed phase HPLC peptide run with six steps in the gradient, and they were characterized by the following mixtures of acetonitrile and water: 5% acetonitrile (0:00-15:00 min), 20% acetonitrile (15:01-18:00 min), 25% actonitrile (18:01-25:00 min), 35% acetonitrile (25:01-40:00 min), 40% acetonitrile (40:01-52:00 min), and 70% acetonitrile (52:01-66:00 min). Eight peaks were noted in the resulting chromatogram, and only two of them contained multiple masses. Mass spectroscopy analysis of these peaks indicated the presence of complex samples, indicating that further HPLC methods development should be done to further resolve the hidden peaks.

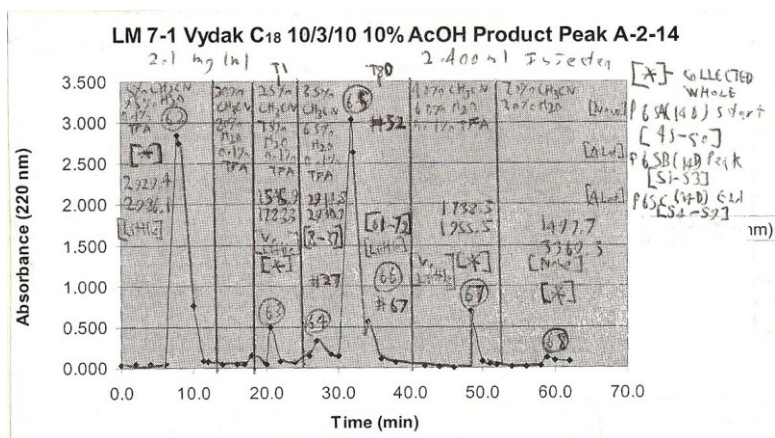


Figure 19: LM7-1 Purified by Preparative Reversed Phase HPLC with a six-step acetonitrile gradient (Run 14). The purified Peak A-2 region (Run 14) of the LM7-1 AMP eluent from the G-25 column was run through a C₁₈Vydac preparatory RP-HPLC column (300Å, 2.2 x 25.0 cm, 218 TP). The mobile phase gradient consisted of 5%, 20%, 25%, 35%, 40% and 70% aqueous acetonitrile. The flow rate was 2.9 ml/min. The graph plots absorbance at 280 nm versus Fraction number.

Figure 20 shows an example of a preparative RP-HPLC run with six steps in the gradient: 5% acetonitrile (0:00-12:00 min), 20% acetonitrile (12:01-18:00 min), 25% acetonitrile (18:01-22:00 min), 30% acetonitrile (22:01-42:00 min), 35% acetonitrile (42:01-58:00 min), and 70% acetonitrile (58:01-66:00 min). There are eight peaks, and only two of them remain poorly resolved. Most notably, several of the peaks contained only a single peptide based on mass spectroscopy results. The RP-HPLC purification method for this peptide was deemed optimized, and similarly eluting peaks were then pooled for both peptides LM7-1 and LM7-2.

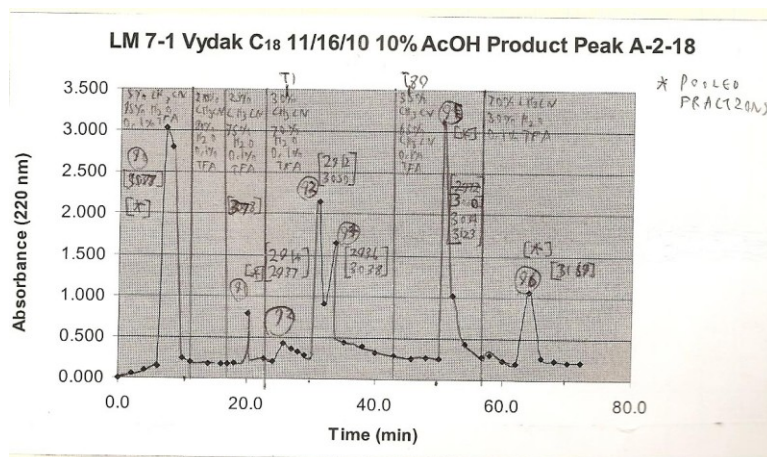


Figure 20: LM7-1 Purified Preparative Reversed Phase HPLC with a six-step acetonitrile gradient (Run 18). The purified Peak A-2 region (Run 14) from the LM7-1 AMP was run through a C₁₈Vydac preparatory RP-HPLC column (300Å, 2.2 x 25.0 cm, 218 TP). The mobile phase gradient consisted of 5%, 20%, 25%, 30%, 35% and 70% aqueous acetonitrile. The flow rate was 2.9 ml/min. The graph plots absorbance at 280 nm versus Fraction number.

4.3 Mass Spectroscopy

4.3.1 Matrix Assisted Laser Desorption Ionization-Time of Flight Discussion

Matrix Assisted Laser Desorption Ionization-Time of Flight (MALDI-TOF) is a gentle and accurate mass spectrometry technique used to determine the charge/mass ratio for intact peptides. Mass spectrometry requires ionization of sample molecules, which must enter the gas phase so they can be accelerated into a trajectory that migrates along the TOF detector tube based on the relative mass/charge ratios. MALDI, unlike many other forms of mass spectrometry, ionizes large peptides without fragmenting them. The peptide samples are first dried in a laser-absorbing matrix that surrounds the sample molecules. The matrix protects the peptide from the laser, and so the peptide is ejected into the gas phase in an intact form. The exact time

required for ions to travel through a long tube before they hit the detector provides accurate m/z data.

4.3.2 Matrix Assisted Laser Desorption Ionization-Time of Flight Results and Sample Pooling

Table 10 shows the Ciphergen SELDI protein chip mass spectroscopy results. All the dried LM7-1 peptide fractions from the prep HPLC runs were subjected to a second round of pooling peptides according to similar mass composition. The three pooling categories were: pure peptides, impure peptides and peaks containing non-target sequences. The first column of Table 10 has the label used for the 3 sample types: 1/P-FR (Pure Fractions), 2/IMP-FR (Impure Fractions), and 3/JK-FR (Junk Fractions). The masses listed indicate the approximate target mass/charge used to determine where each sample was to be pooled. The second column indicates all the observed mass/charge ratios observed, rounded to the nearest Dalton/z. The third column indicates which dried peptide samples from prep RP-HPLC runs were combined to make each of the three final peptide pools. The three symbol code refers to previously pooled peptides, the longer code indicates individual peptide fractions, and the waste code indicates that some peptides were indeed isolated from non-peak regions. The fourth column indicates the estimated yield (by visual inspection) of the lyophilized final peptide pools, ready for biological assays.

Table 10: MALDI Results and Sample Pooling for LM7-1. The Peptide Rank label indicates how pure the pooled peptide samples were based on MALDI-TOF mass spectrometry results. The Observed m/z indicates the observed mass charge ratios. The Dried Peptide indicates where the samples originated from. The estimated mass of the purified samples is based on visual inspection.

Pure Peptide Rank/Label	Observed m/z	Dried Peptide	Estimated Mass
1/P-FR 2912 2934/2970	2912, 2913, 2914, 2915, 2934, 2936, 2937, 2970, 2971	6A-3, 6A-4, 6B-1, 6B-2, 6B-5, A-2-17C (P84), A-2-17H (P89), A-2-18C (P92)	~15 mg
2/IMP-FR 2912 2934/2970 3000+	2910, 2911, 2912, 2913, 2914, 2915, 2929, 2932, 2933, 2934, 2936, 2967, 2968, 2969, 2970, 2971, 3000, 3002, 3004, 3005, 3034, 3038, 3050, 3058, 3060, 3108, 3106, 3110, 3124, 3140	2B-2, 6B-3, 6B-4, A-2-17D (P85), A-2-17E (P86), A-2-17F (P87), A-2-17G (P88), A-2-18D (P93), A-2-18E (P94), A-2-19C (P99), A-2-19D (P100), A-2-19E (P101), A-2-19F (P102), A-2-19G (P103A), Waste 6, Waste 9	~95 mg
3/JK-FR Everything except: 2912 2934/2970	1725, 1980, 2854, 2985, 3000, 3007, 3017, 3034, 3035, 3036, 3077, 3079, 3091, 3093, 3094, 3116, 3118, 3123, 3126, 3128, 3169, 3174, 3185	4A-2, 6A-5, A-2-17A (P82), A-2-18A (P90), A-2-18B (P91), A-2-18F (P95), A-2-18G (P96), A-2-19A (P97), A-2-19G (P103B), A-2-19H (P104), A-2-19I (P105), Waste 7, Waste 8, Waste 10	~55 mg

Table 11 shows the LM7-2 pooling results. Determining the mass of the peptides purified during preparatory HPLC runs for LM7-2 was difficult due to the lack of usable results from the INBRE core lab's new instrument, the Shimazu Axima MALDI-TOF, so the samples were simply pooled by HPLC elution times instead. The first column in Table 11 has the labels for the 8 sample patterns obtained from the LM7-2 prep HPLC runs: Peak A, Peak B, Peak C, Peak D (peak leading edge and

top), Peak D tail (peak tail), Peak E (peak leading edge and top), Peak E tail (peak tail). Any samples that did not yield peptide sample after lyophilization were counted as discards. The second column indicates which dried peptide samples were combined to make the eight pooled peptide samples. The third column indicates the mass of the pooled, and lyophilized peptide fractions.

Table 11: Sample Pooling for LM7-2. The Peptide Rank label indicates how the peptide samples were pooled based on RP-HPLC peak elution order. The Dried Peptide indicates which HPLC runs the samples originated from that were combined on the final pools. The estimated yields of the purified peptides were defined by weighing them on an electronic balance.

Pure Peptide Rank/Label	Dried Peptide	Mass
LM7-2 Peak A	A-7A (P30)	1.0 mg
LM7-2 Peak B	A-1A tail (P1-2), Pre A-2B (P6-), A-2B (P6), A-3B (P11), Pre A-4B (P16-), A-4B (P16), Pre A-5B (P21-), A-5B (P21), Pre A-6B (P26-), A-6B (P26)	0.6 mg
LM7-2 Peak C	A-1B (P2), A-1B tail (P2-3), A-2C (P7), A-3C (P12), A-4C (P17), A-5C (P22), A-6C (P27), A-7C (P32)	1.5 mg
LM7-2 Peak D	A-1C (P3), A-2D (P8), A-3B (P13), A-4D (P18), A-5D (P23), A-6D (P28), A-7D (P33)	2.7 mg
LM7-2 Peak D tail	A-1C tail (P3-4), A-2D tail (P8-9), A-3D tail (P13-14), A-4D tail (P18-19), A-5D tail (P23-24), A-6D tail (P28-29), A-7D tail (P33-34)	7.1 mg
LM7-2 Peak E	A-1D (P4), A-2E (P9), A-3E (P14), A-4E (P19), A-5E (P24), A-6E (P29), A-7E (P34)	13.9 mg
LM7-2 Peak E tail	A-1D tail Fr (P4+), A-1D tail pool (P4+), A-2E tail Fr (P9+), A-3E tail (P14+), A-4E tail (P19+), A-5E tail (P24+), A-6E tail (P29+), A-7E tail (P34+)	21.9 mg
LM7-2 Discards	Pre A-1A (P1-), A-1A (P1), Pre A-2A (P5-), A-2A (P5), A-2E tail pool (P9+), Pre A-3A (P10-), A-3A (P10), Pre A-3B (P11-), Pre A-4A (P15-), A-4A (P15), Pre A-5A (P20-), A-5A (P20), Pre A-6A (P25-), A-6A (P25), Pre A-7A (P30-), Pre A-7B (P31-), A-7B (P31)	-

4.3.3 Liquid Chromatography-Electrospray Ionization-Mass Spectrometry

Discussion

Liquid Chromatography-Electrospray Ionization-Mass Spectrometry (LC-ESI-MS) is an accurate mass spectrometry technique used to determine charge/mass ratio for peptides and other analytes. The samples are typically injected into a LC column that resolves the sample into separate peaks, which individually enter into the mass spectrometer. This technique also acts as a check for purity, as fewer peaks indicate less contamination in the sample. Once in the spectrometer, the samples are ionized by an evaporation nebulizer and accelerated in an electric field. As they circle in a vacuum chamber around an electrode in the detector area, their characteristic frequency can be measured to determine their m/z ratios. Differing numbers of positive charges on an identical the peptide sample yield a closely related family of m/z ratios that can be deconvoluted to produce an overall mass for each peptide in the sample.

4.3.4 Liquid Chromatography-Electrospray Ionization-Mass Spectrometry

Results

LM7-1 (1P-FR) and LM7-2 (Peak E) were subjected to Liquid Chromatography-Electrospray Ionization-Mass Spectrometry using a Linear Trap Quadrupole Orbitrap Velos Mass Spectrometer at the EPSCoR Brown University Proteomics lab.

LM7-1 Results:

Calculated monoisotopic mass:	2913.63 Da
Observed m/z:	1457.825, 972.219, 729.416, 583.734, 486.615, 417.242, 365.211
Deconvoluted observed mass:	2913.638 (+/- 0.006) Da

Based on the LC-MS results, only a single major mass peak was isolated by prep HPLC. All of the multiple-charged m/z peaks are consistent with a single peptide mass of 2913.638 Da. As the calculated mass for the amino acid sequence of the peptide and the measured masses were identical, this indicated the LM7-1 peptide was successfully synthesized, and purified to homogeneity.

LM7-2 Results:

Calculated monoisotopic mass:	2984.70 Da
Deconvoluted observed mass:	2984.675 (+/- 0.001) Da 2914.633 (+/- 0.001) Da

Based on the LC-MS results, a major mass peak and a minor mass peak were present in the peptide sample. The calculated mass of 2984.675 Da, based on the desired amino acid sequence was the major observed product, along with a failure sequence of mass 2914.633 Da that possessed a mass consistent with a product peptide having a deleted alanine residue. As the calculated and measured masses were very close for at least one of the AMPs in the product mixture, the LC-MS results indicated that LM7-2 was mostly purified. However, the pooled peptide product tested in later assays contained small amounts of a shorter failure sequence as well.

4.4 Antimicrobial Activity Assay

4.4.1 Antimicrobial Activity Assay Discussion

A bioactivity assay is a method used to measure the ability of antibiotics and antimicrobial peptides to inhibit bacterial growth in the log phase. Any diminishment or elimination of normal bacterial growth indicates that the compound being assayed is active against the test bacteria. A common type of screening assay examples is an exponentially growing bacterial culture monitored in a 96-well plate. Overall bacterial cell density is charted by measuring optical density (light scattering at 630 nm) using a plate reader spectrophotometer to scan cultures over a 24 hour time course.

4.4.2 Antimicrobial Activity Assay Results

For comparison, graphs of the results of the antimicrobial assays against four different bacterial strains all have the same general format. Not graphed were control data showing the inhibition of bacterial growth in either chloramphenicol or NaOH. The mean ODs of the Mueller Hinton media only scans was subtracted from all the other data sets to eliminate the light scattering effect of the growth media itself prior to graphing. On the left side of each time point, the bar represents the OD of an inoculum of bacteria in Mueller Hinton Broth which models unrestrained growth. The next four bars show the effect of increasing concentrations of the manufactured peptides. The time between monitoring steps was an interval of ~30 min, except for prior to the last step, which was obtained at the 24 hour mark.

The antimicrobial effectiveness of LM7-1 against the two gram negative bacterial strains is shown: *E.coli* in Figure 21 and *P.aeruginosa* in Figure 22. These bacterial species were chosen as they were frequently cited as human pathogens. In the *E.coli* assay, all doses of the LM7-1 peptides were effective at inhibiting bacterial growth at the 3 hour time point; the two higher doses of the LM7-1 peptides inhibited bacterial growth at the 24 hour time point. In the *P.aeruginosa* assay, the two higher doses of the LM7-1 peptides inhibited bacterial growth at the 2 hour time point; no doses of the LM7-1 peptides inhibited bacterial growth at the 24 hour time point. This suggested that LM7-1 was active against *E.coli* and *P.aeruginosa* for the first few hours of incubation; however, LM7-1 was only active against *E.coli* at 24 hours post-treatment. This data suggested that LM7-1 was effective against *E.coli*.

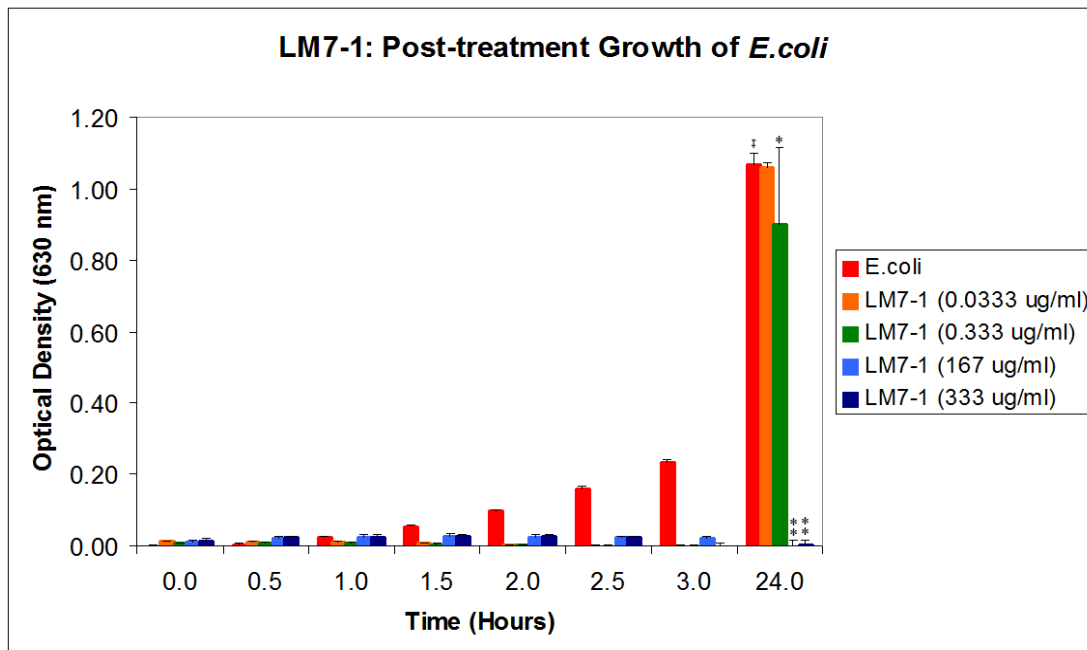


Figure 21: Antimicrobial Activity Assay of LM7-1 against *E.coli*. The graph shows Optical density at 630 nm versus time for exposure in hours. The red bars show the uninhibited growth of the bacteria. The remaining bars (orange, green, blue and violet) show the amount of bacterial inhibition observed with increasing concentrations of peptide LM7-1. The error bars display one standard deviation of variance. At the 24 hour time point, compared to the uninhibited *E.coli* growth (‡), the 0.333 $\mu\text{g/ml}$ peptide trial shows a significant (*) difference [$0.05 > P > 0.001$], and the 167/333 $\mu\text{g/ml}$ peptide dilutions show extremely significant (**) differences [$0.001 > P$] in bacterial growth.

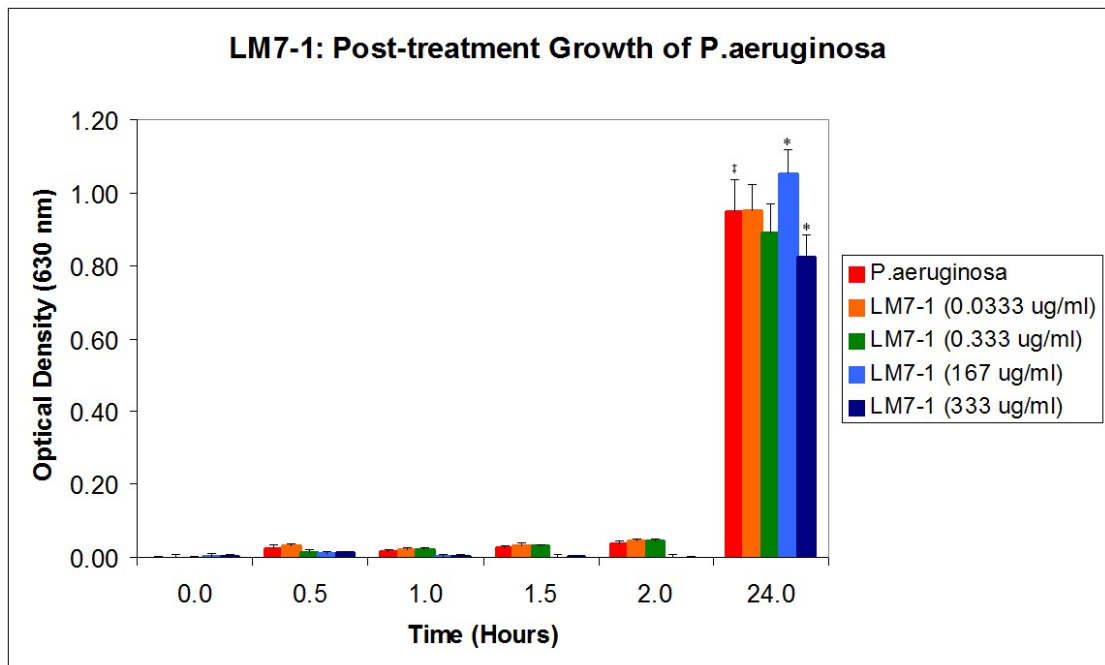


Figure 22: Antimicrobial Activity Assay of LM7-1 against *P.aeruginosa*. The graph shows Optical density at 630 nm versus time for exposure in hours. The red bars show the uninhibited growth of the bacteria. The remaining bars (orange, green, blue and violet) show the amount of bacterial inhibition observed with increasing concentrations of peptide LM7-1. The error bars display one standard deviation of variance. At the 24 hour timepoint, compared to the uninhibited *P.aeruginosa* growth (\ddagger), the 167/333 $\mu\text{g/ml}$ peptide trials show significant (*) differences [$0.05 > P > 0.001$] in bacterial growth.

The antimicrobial effectiveness of LM7-1 against the two gram positive strains is shown: *E.faecalis* in Figure 23 and *S.aureus* in Figure 24. These bacterial species were chosen as they were frequently cited as human pathogens. In the *E.faecalis* assay, the two most concentrated samples of the LM7-1 peptides were effective at inhibiting bacterial growth at the 3 hour time point; the two higher doses of the LM7-1 peptides inhibited bacterial growth at the 24 hour time point. In the *S.aureus* assay, the two higher doses of the LM7-1 peptides inhibited bacterial growth at the 3 hour time point; only the highest dose of the LM7-1 peptides inhibited bacterial growth at

the 24 hour time point. This suggested that LM7-1 was active against both *E.faecalis* and *S.aureus* for the first few hours of incubation; however, LM7-1 only remained active against *E.faecalis* at 24 hours post-treatment. This data suggested that LM7-1 was effective against *E.faecalis*.

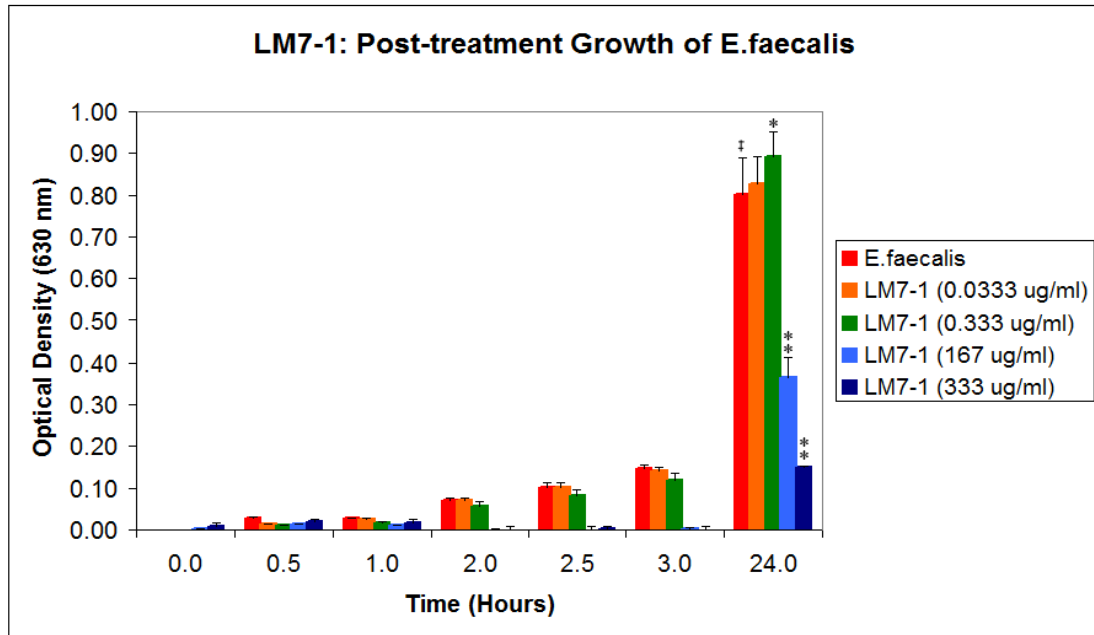


Figure 23: Antimicrobial Activity Assay of LM7-1 against *E.faecalis*. The graph shows Optical density at 630 nm versus time for exposure in hours. The red bars show the uninhibited growth of the bacteria. The remaining bars (orange, green, blue and violet) show the amount of bacterial inhibition observed with increasing concentration of peptide. The error bars display one standard deviation of variance. In the 24 hour timepoint, compared to the uninhibited *E.faecalis* growth (\ddagger), the 0.333 $\mu\text{g/ml}$ peptide trial shows a significant (*) difference [$0.05 > P > 0.001$], and the 167/333 $\mu\text{g/ml}$ peptide trials show extremely significant (**) differences [$0.001 > P$] in bacterial growth.

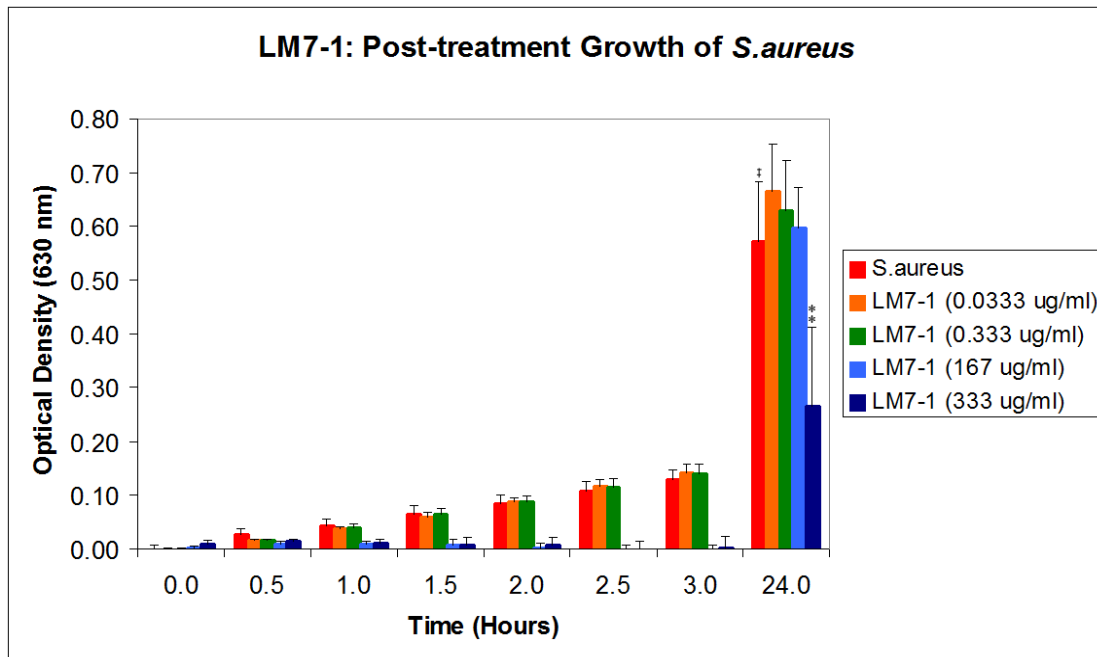


Figure 24: Antimicrobial Activity Assay of LM7-1 against *S.aureus*. The graph shows Optical density at 630 nm versus time for exposure in hours. The red bars show the uninhibited growth of the bacteria. The remaining bars (orange, green, blue and violet) show the amount of bacterial inhibition observed with increasing concentration of peptide. The error bars display one standard deviation of variance. In the 24 hour timepoint, compared to the uninhibited *S.aureus* growth (\ddagger), only the 333 $\mu\text{g/ml}$ peptide trial shows an extremely significant (**) difference [$0.001 > P$] in bacterial growth.

The antimicrobial effectiveness of LM7-2 against the two gram negative bacterial strains is shown: *E.coli* in Figure 25 and *P.aeruginosa* in Figure 26. In the *E.coli* assay, all doses of the LM7-2 peptides were effective at inhibiting bacterial growth at the 3 hour time point; only the two higher doses of the LM7-2 peptides continued to inhibit bacterial growth at the 24 hour time point. In the *P.aeruginosa* assay, no doses of the LM7-2 peptides significantly inhibited bacterial growth at the 3 hour time point; however, the two higher doses of the LM7-2 peptides significantly inhibited bacterial growth at the 24 hour time point. The inconclusive results at the 3

hour time point was likely due to the inherent background absorption of the yellow-colored peptide itself at high concentrations. This suggested that LM7-2 was active against *E.coli* for the first few hours of incubation; however, LM7-2 was active against both *E.coli* and *P.aeruginosa* at 24 hours post-treatment. This data suggested that LM7-2 was broad spectrum effective against gram negative bacteria.

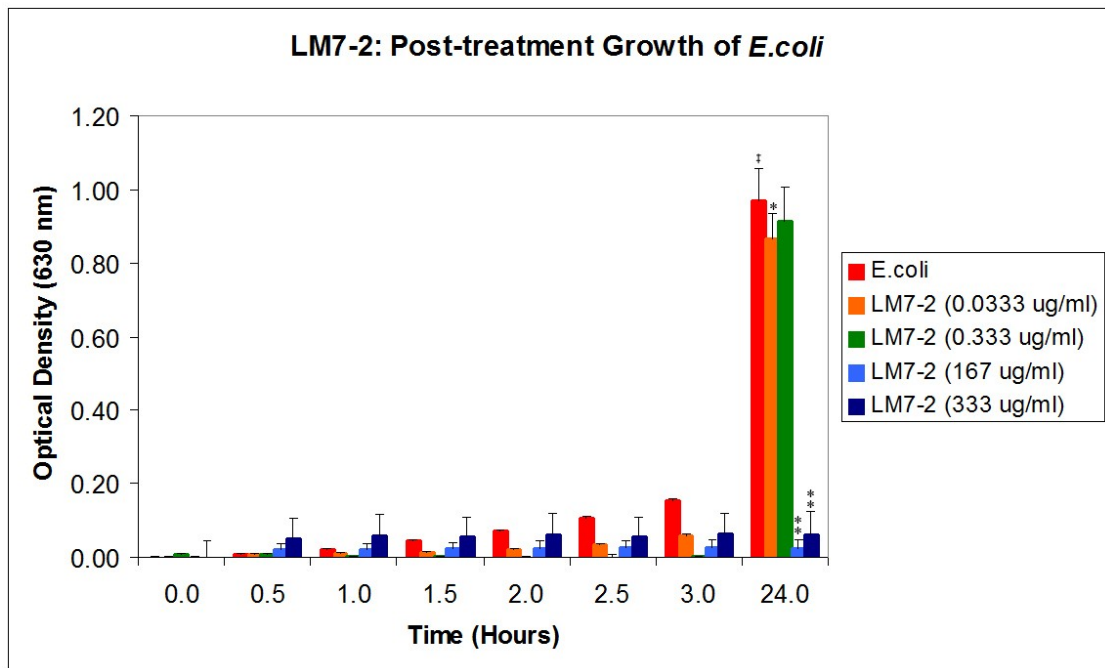


Figure 25: Antimicrobial Activity Assay of LM7-2 against *E.coli*. The graph shows Optical density at 630 nm versus time for exposure in hours. The red bars show the uninhibited growth of the bacteria. The remaining bars (orange, green, blue and violet) show the amount of bacterial inhibition observed with increasing concentration of peptide. The error bars display one standard deviation of variance. In the 24 hour timepoint, compared to the uninhibited *E.coli* growth (‡), the 0.0333 $\mu\text{g/ml}$ peptide trial shows a significant (*) difference [$0.05 > P > 0.001$], and the 167/333 $\mu\text{g/ml}$ peptide trials show extremely significant (**) differences [$0.001 > P$] in bacterial growth.

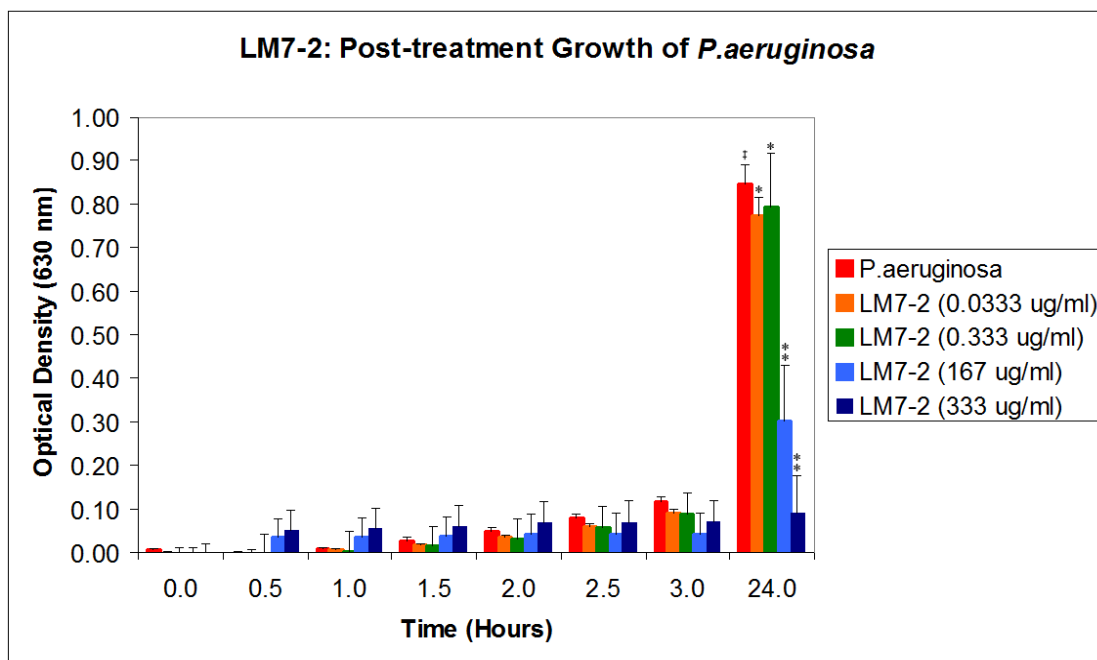


Figure 26: Antimicrobial Activity Assay of LM7-2 against *P.aeruginosa*. The graph shows Optical density at 630 nm versus time for exposure in hours. The red bars show the uninhibited growth of the bacteria. The remaining bars (orange, green, blue and violet) show the amount of bacterial inhibition observed with increasing concentration of peptide. The error bars display one standard deviation of variance. In the 24 hour timepoint, compared to the uninhibited *P.aeruginosa* growth (†), the 0.0333/0.333 $\mu\text{g/ml}$ peptide trials show significant (*) differences [$0.05 > P > 0.001$], and the 167/333 $\mu\text{g/ml}$ peptide trials show extremely significant (**) differences [$0.001 > P$] in bacterial growth.

The antimicrobial effectiveness of LM7-2 against the two gram positive strains is shown: *E.faecalis* in Figure 27 and *S.aureus* in Figure 28. In the *E.faecalis* assay, the two most concentrated samples of the LM7-2 peptides were effective at inhibiting bacterial growth at the 3 hour time point; and continued to significantly inhibit

bacterial growth at the 24 hour time point. In the *S.aureus* assay, the two higher doses of the LM7-2 peptides inhibited bacterial growth at the 3 hour time point, and continued to inhibit bacterial growth at the 24 hour time point. This data suggested that LM7-2 was broadly effective against gram positive bacteria, at both early and late stage post-treatment.

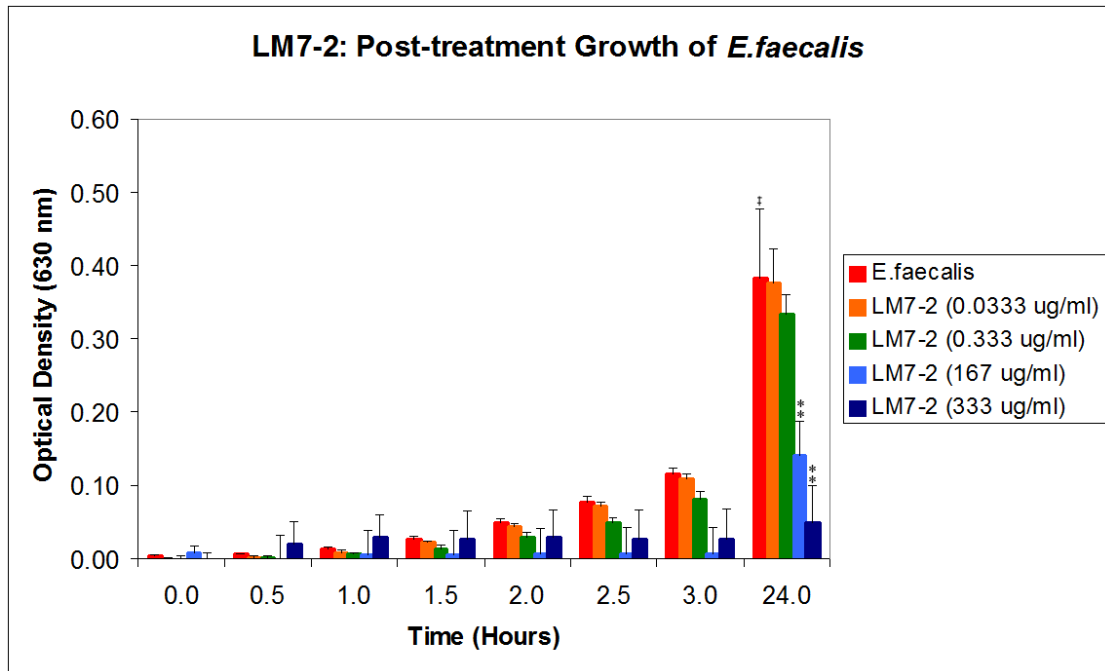


Figure 27: Antimicrobial Activity Assay of LM7-2 against *E. faecalis*. The graph shows Optical density at 630 nm versus time for exposure in hours. The red bars show the uninhibited growth of the bacteria. The remaining bars (orange, green, blue and violet) show the amount of bacterial inhibition observed with increasing concentration of peptide. The error bars display one standard deviation of variance. In the 24 hour timepoint, compared to the uninhibited *E. faecalis* growth (‡), the 167/333 $\mu\text{g/ml}$ peptide trials show extremely significant (**) differences [$0.001 > P$] in bacterial growth.

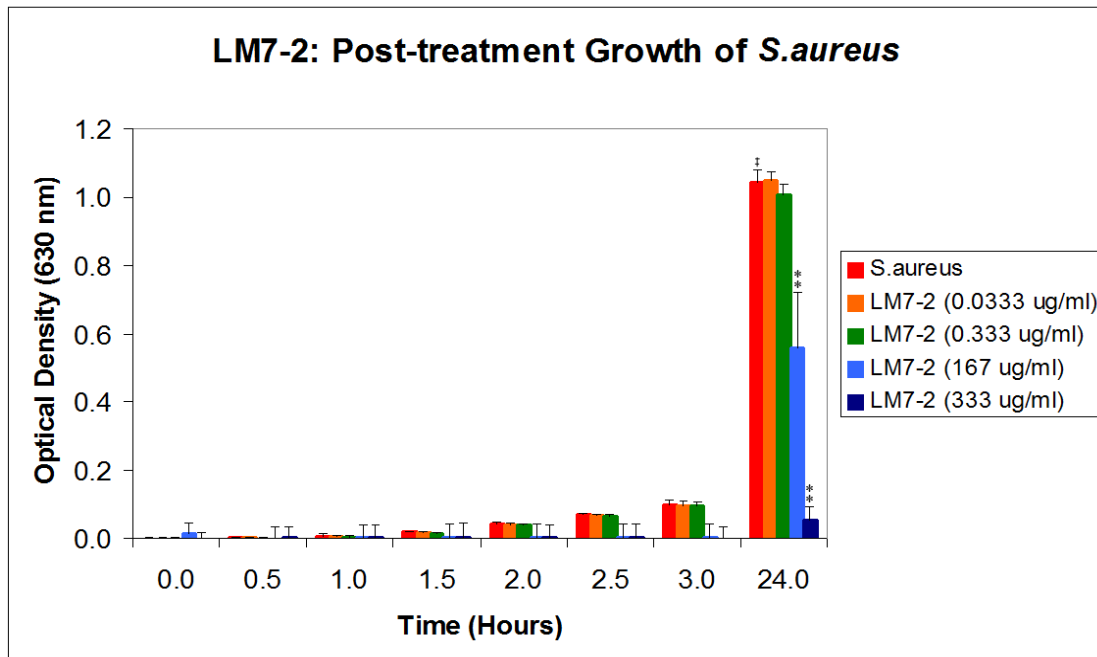


Figure 28: Antimicrobial Activity Assay of LM7-2 against *S.aureus*. The graph shows Optical density at 630 nm versus time for exposure in hours. The red bars show the uninhibited growth of the bacteria. The remaining bars (orange, green, blue and violet) show the amount of bacterial inhibition observed with increasing concentration of peptide. The error bars display one standard deviation of variance. In the 24 hour timepoint, compared to the uninhibited *S.aureus* growth (\ddagger), the 167/333 $\mu\text{g/ml}$ peptide trials show extremely significant (**) differences [$0.001 > P$] in bacterial growth.

4.4.3 Minimum Inhibitory Concentration of LM7-1 and LM7-2

The Minimum Inhibitory Concentration (MIC) was defined by the Jia group as a concentration of peptide sufficient to inhibit 50% bacterial growth for 24 hours as compared to the uninhibited control (Jia *et al*, 2000). Figures 29-32 list the Dose Response Comparison of LM7-1 and LM7-2 inhibition of growth for the 4 bacterial species: *E.coli* in Figure 29, *P.aeruginosa* in Figure 30, *E.faecalis* in Figure 31, and *S.aureus* in Figure 32. *E.coli* was the most susceptible bacteria, as it showed equal vulnerability to both peptides, and had low MIC values. *P.aeruginosa* demonstrated

strong resistance to LM7-1 and moderate resistance to LM7-2. *E.faecalis* was more inhibited by LM7-2 than LM7-1. *S.aureus* was more strongly inhibited by LM7-2 than LM7-1.

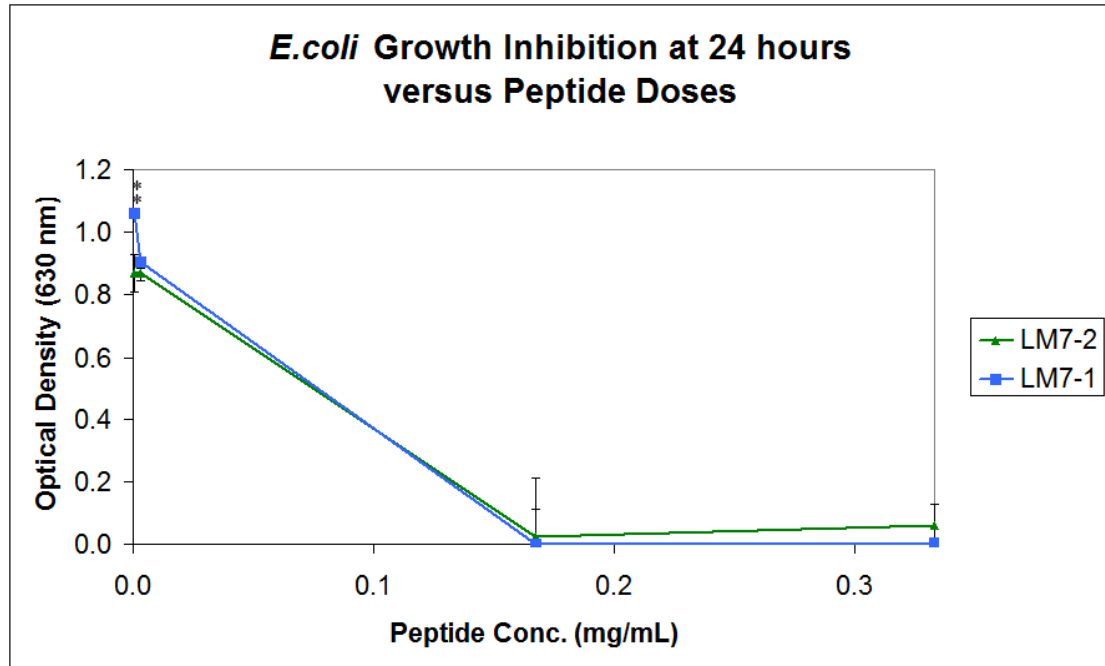


Figure 29: *E.coli* Growth Inhibition at 24 hours versus Peptide Doses. The graph shows 24 hours of bacterial growth monitored by Optical density at 630 nm versus LM7-1 (blue line) and LM7-2 (green line) concentrations in mg peptide/ml total culture volume. The error bars display one standard deviation of variance. Only the 0.000333 mg/ml doses of LM7-1 and LM7-2 are extremely significantly (**) different from each other [0.001>P]. The MIC is 0.080 mg/ml for LM7-1, and 0.070 mg/ml for LM7-2.

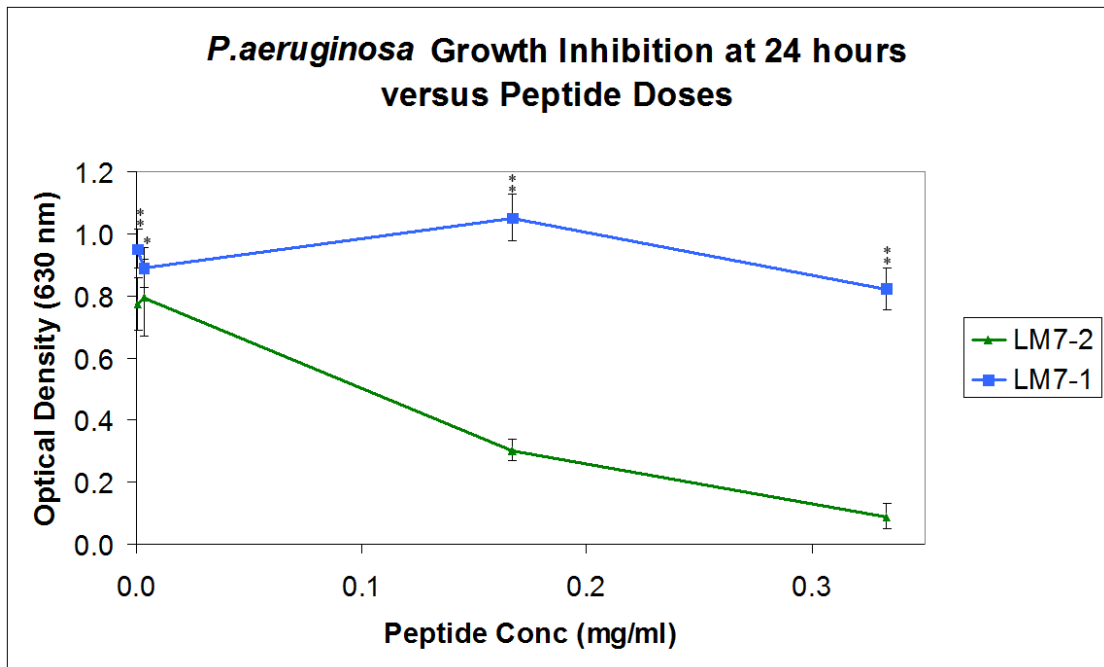


Figure 30: *P.aeruginosa* Growth Inhibition at 24 hours versus Peptide Doses. The graph shows 24 hours of bacterial growth monitored by Optical density at 630 nm versus LM7-1 (blue line) and LM7-2 (green line) concentrations in mg peptide/ml total culture volume. The error bars display one standard deviation of variance. The 0.0033 mg/ml the dose of LM7-1 and LM7-2 are significantly (*) different from each other [$0.05 > P > 0.001$], and the 0.000333/0.167/0.333 mg/ml doses of LM7-1 and LM7-2 are extremely significantly (**) different from each other [$0.001 > P$]. The MIC is >0.333 for LM7-1, and 0.130 mg/ml for LM7-2.

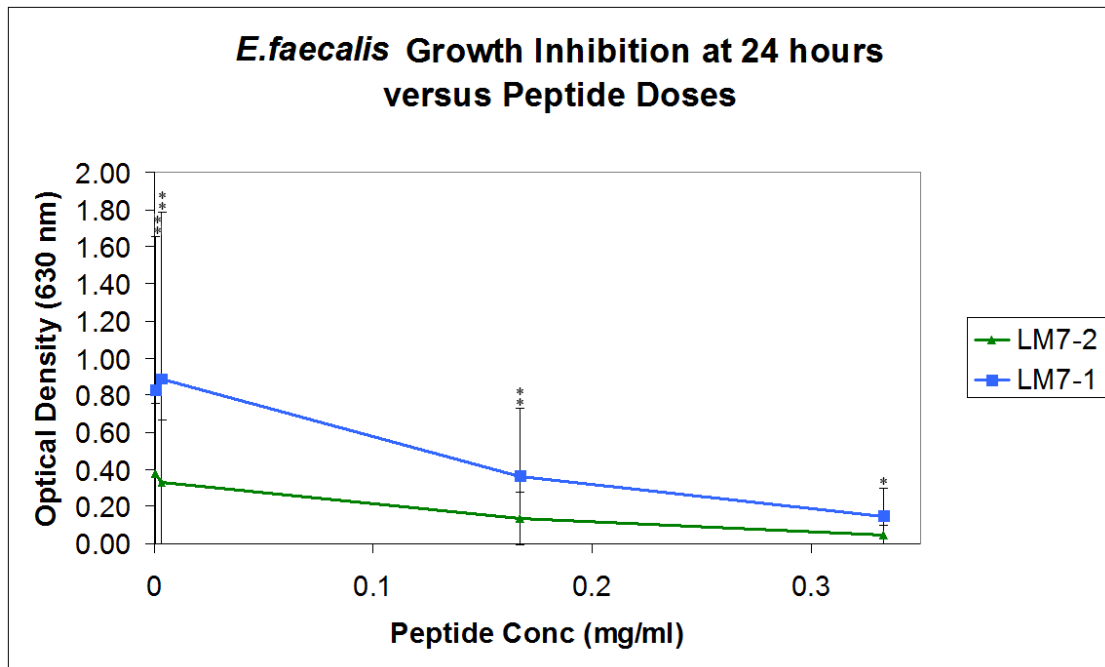


Figure 31: *E. faecalis* Growth Inhibition at 24 hours versus Peptide Doses. The graph shows 24 hours of bacterial growth monitored by Optical density at 630 nm versus LM7-1 (blue line) and LM7-2 (green line) concentrations in mg peptide/ml total culture volume. The error bars display one standard deviation of variance. The 0.333 mg/ml doses of LM7-1 and LM7-2 are significantly (*) different from each other [$0.05 > P > 0.001$], and the 0.000333/0.00333/0.167 mg/ml doses of LM7-1 and LM7-2 are extremely significantly (**) different from each other [$0.001 > P$]. The MIC is 0.145 mg/ml for LM7-1, and 0.130 mg/ml for LM7-2.

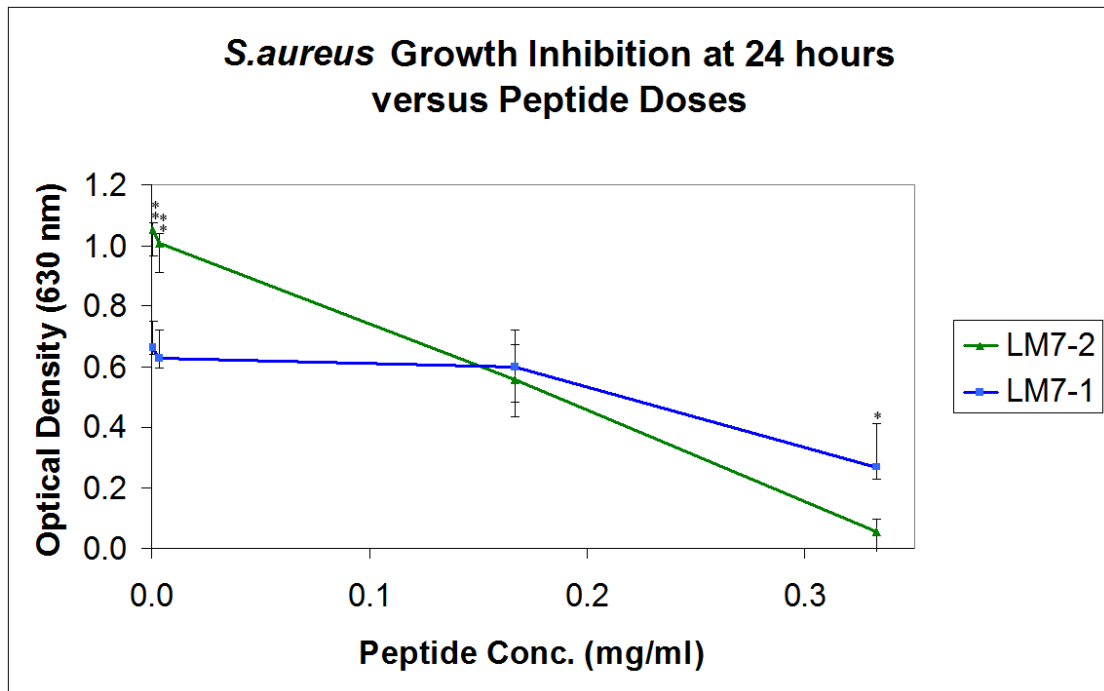


Figure 32: *S.aureus* Growth Inhibition at 24 hours versus Peptide Doses. The graph shows 24 hours of bacterial growth monitored by Optical density at 630 nm versus LM7-1 (blue line) and LM7-2 (green line) concentrations in mg peptide/ml total culture volume. The error bars display one standard deviation of variance. The 0.333 mg/ml doses of LM7-1 and LM7-2 are significantly (*) different from each other [$0.05 > P > 0.001$], and the 0.000333/0.00333 mg/ml doses of LM7-1 and LM7-2 are extremely significantly (**) different from each other [$0.001 > P$]. The MIC is 0.305 mg/ml for LM7-1, and 0.165 mg/ml for LM7-2.

To calculate the MIC values for LM7-1 and LM7-2 against the four pathogenic bacterial species, the maximum Optical density was divided in half, and the corresponding peptide concentration was obtained from the dose response plotted curves in Figures 29-32. Table 12 shows the MIC results, which indicate that LM7-2 (P-DER) was a more active peptide antibiotic than LM7-1 against most strains tested. The lower the MIC, the more effective the AMP was at inhibiting bacterial growth over a 24 hour period. Based on these results, LM7-1 was shown to be a

therapeutically useful growth inhibitor for use against *E.coli* (MIC=80 µg/ml), and *E.faecalis* (MIC=145 µg/ml). Based on these results, LM7-1 appeared to be largely ineffective against *P.aeruginosa* (MIC>333 µg/ml), and *S.aureus* (MIC=305 µg/ml) in cell culture assays. The LM7-2 sequence, although only different in one of its 27 amino acid residues, was shown to be therapeutically useful against *E.coli* (MIC=70 µg/ml), *P.aeruginosa* (MIC=130 µg/ml), *E.faecalis* (MIC=130 µg/ml), and *S.aureus* (MIC=165 µg/ml). Overall, LM7-2 was a more active, broad spectrum antimicrobial peptide than LM7-1 was. Both chloramphenicol and NaOH trials were effective at completely inhibiting bacterial growth of all 4 bacterial species over a 24 hour period.

Table 12: Minimum Inhibitory Concentrations (MICs) of LM7-1 and LM7-2. The table lists concentration of LM7-1, and LM7-2 sufficient to inhibit 50% of bacterial growth at 24 hours of incubation, as compared to the uninhibited control.

		Minimum Inhibitory Concentrations (MICs) in mg/ml			
		Gram (-) <i>E.coli</i>	Gram (-) <i>P.aeruginosa</i>	Gram (+) <i>E.faecalis</i>	Gram (+) <i>S.aureus</i>
Peptide	LM7-1	0.080±0.004	>0.333	0.145±0.007	0.305±0.007
	LM7-2	0.070±0.009	0.130±0.015	0.130±0.026	0.165±0.012

4.4.4 Hemolysis Assay Discussion

A hemolytic assay is a method used to determine if useful therapeutic doses of Antimicrobial peptides (AMPs) will potentially exert toxic effects by lysing human red blood cells. Red blood cells are known to be sometimes vulnerable to cationic α -helical AMPs because their anionic cell membranes have many similarities to anionic bacterial cell membranes. AMPs are considered too dangerous for use in humans if they cause significant RBC lysis at or near therapeutic concentrations. As the

membrane lipid compositions of red blood cells have been shown to vary widely between mammalian species, it is more predictive to use human RBCs in hemolysis assays rather than the more commonly used sheep RBCs.

4.4.4 Hemolysis Assay Results for LM7-1 and LM7-2

Human RBCs were collected from three anonymous volunteers at the URI student health services laboratory, then washed and isolated. At high enough doses, Peptides LM7-1 and LM7-2 caused hemolysis of human RBCs. The point at which a concentration of peptides lysed 50% of the RBC at 1 hour into the assay was recorded as the HC_{50} dose. Figure 33 indicated that LM7-1 was slightly more hemolytic than LM7-2; however both caused lysis of RBC at very low concentrations.

The HC_{50} dose seemed to be unusually low, and is possibly due to inconsistencies in the Hemolysis Assay itself. The method development for setting up this hemolysis assay was difficult. The literature lists many varying and mutually inconsistent methods of determining the HC_{50} dose. Many of the methods suggested scanning the hemoglobin absorption at the 540 nm, which although conveniently in the visible range, was wildly inconsistent depending on whether the hemoglobin was oxygenated or not. Some doses of the peptide caused hemoglobin to visibly shift color from red to red-brown, implying deoxygenation of the hemoglobin. The only hemoglobin absorption peak that did not vary depending on oxygen concentrations was the 419 nm peak. Another issue was that some of the concentrations of the positive control of Triton X-100 suggested in the literature caused complete lysis of the RBCs as well as hemoglobin degradation, which meant that 100% lysis did not necessarily equal

maximum hemoglobin absorption. Other variables included spontaneous RBC lysis, which anticoagulant was used during the collection process, the sample error using only small volumes, and single replicate trials.

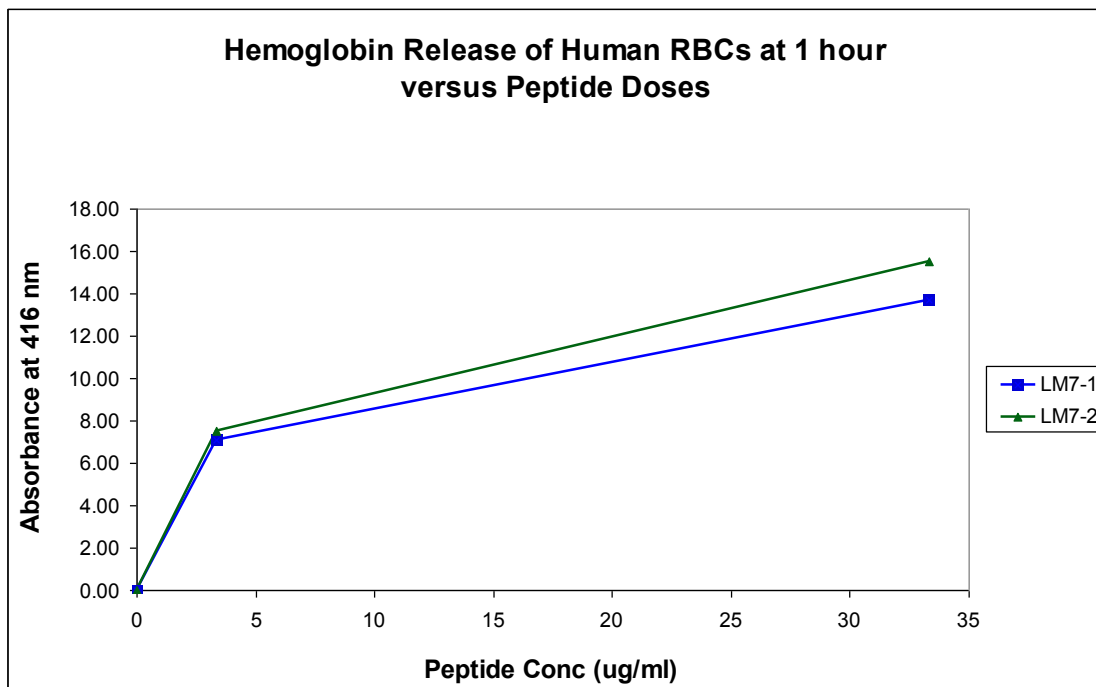


Figure 33: Dose Response Assay of LM7-1/LM7-2 Human RBC Hemolysis. The graph displays absorbance at 419 nm (maximum hemoglobin absorption) of human red blood cells incubated for 1 hour in PBS Buffer (pH 7.2, 4% RBC packed cell volume) with the added LM7-1 peptide (blue line) or LM7-2 peptide (green line). The graph shows released hemoglobin absorption at 419 nm versus peptide concentration in μg peptide/ml total suspension volume. There was only one replicate per hemolysis trial, so there are no error bars.

Table 13 lists the exact HC_{50} values obtained in these experiments. The result shows that although LM7-1 was active in inhibiting growth of 2 different types of bacteria, and LM7-2 was active in inhibiting growth of 4 different types of bacteria, both AMPs were too hemolytic to be therapeutically useful.

Table 13: Minimum Hemolytic Concentrations (HC_{50}) of LM7-1 and LM7-2 at 1 hour. This table lists concentration of LM7-1 and LM7-2 sufficient to lyse 50% human red blood cells (HC_{50}) at 1 hour of incubation.

Peptide		Minimum Hemolytic Concentration (HC_{50}) in mg/ml
	LM7-1	0.016
	LM7-2	0.017

CHAPTER 5

CONCLUSIONS

The design of alpha helical, amphipathic, antimicrobial peptides are straightforward if the correct features are incorporated into the design, particularly with the aid of *in silico* design tools. Based on primary literature research, the following cationic, α -helical properties were important: an α -helix that only forms in a membrane, the presence of a flexible hinge region, a polar face smaller than the nonpolar face, C-terminal amidation to increase activity, a positively charged residue in the middle of the nonpolar face to reduce aggregation/hemolysis, and a shortened sequence to reduce chemical synthesis time and production expense. Although the initial attempt at modifying an extant sequence only involved one amino acid change, the major goal was to design more dramatic novel hybrids by mixing and matching extant sequences to engineer the desired peptide properties. All of the novel sequences were evaluated using *in silico* tests to predict physical properties, probable effectiveness, and to eliminate unsuitable candidates for human therapeutic use. The Edmonton Helical Wheel was used to predict the amphipathic profile for the AMPs, the Chou-Fasman Algorithm was used to predict secondary structure, and the Hopp-Woods Hydrophilicity Scale was used to predict the transition zone between the N-terminal and C-terminal α -helical regions. These tools were initially used to evaluate the P-DER hybrid AMP sequence. Attempts were made to tweak the sequence to improve its antimicrobial activity without raising its hemolytic index. Then, using *in silico* tools to incorporate the important features found in naturally-occurring, cationic, α -helical AMPs, 20 novel hybrid AMPs were designed by mixing and matching

segments of such active AMPs. Thus, the use of the *in silico* toolset was used to arrive at the calculated data profiles used in generating novel, hybrid peptide sequences. The prospective sequences were evaluated and narrowed down to 3 novel hybrid sequences that conformed to the best calculated profiles of active AMPs. These sequences then became designated hybrids LM7-3, LM7-4, and LM7-5.

The Solid Phase Peptide Synthesis (SPPS) for this project was completed manually to monitor the challenges encountered in this type of synthesis so that the procedures could be adjusted as necessary. These challenges included determining whether certain Boc-amino acid types and locations within a particular sequence makes them more difficult to attach to the peptide-resin than others. Refinement of the SPPS technique and acquired experience led to greater coupling efficiency during the second synthesis (LM7-2). During SPPS of LM7-1, 15 out of 27 residues required multiple coupling attempts before succeeding. Peptide LM7-2 differed by one residue (Lys¹⁵ → Gly¹⁵), but thanks to improved coupling strategies, only 7 out of 27 residues required multiple coupling steps to succeed. Six of those multiple couplings were a common problem sequence region in both LM7-1 and LM7-2, which implied that the remaining extra coupling steps required to synthesize LM7-1 were more than likely due to inexperience. The HF cleavage yielded a significant amount (>2g) of crude AMPs for biological tests. Manual SPPS was laborious, so now that the difficult sequences have been identified, any future related derivative sequences can be synthesized on an automated peptide synthesizer that can run the coupling reactions over many hours without extensive human intervention. Generally, as long as the

peptide-resin sample is tested regularly with the ninhydrin test to confirm complete coupling of every residue, automated SPPS is likely to be superior to manual SPPS.

The use of Gel Filtration was effective in removing gross impurities from the peptide product, as the Sephadex beads separated the peptide sequences from the much less massive reagent by-products and HF scavengers. Multiple runs were needed to fine-tune the final LM7-1 purification, by developing an appropriate step gradient protocol on the Preparatory Reversed Phase HPLC for the peptide. Eventually, pure peptide peaks were reproducibly eluted from the column, and the correct peptide masses were later confirmed with MALDI-TOF and LC-ESI mass spectrometry. The established prep HPLC gradient was later also used to purify related peptide LM7-2, as its hydrophobic properties were nearly identical to those of LM7-1.

Molecular weight determinations by MALDI-TOF mass spectrometry, were then used extensively during purification of LM7-1, to determine appropriate post-HPLC peak pooling. However, when the INBRE lab switched to a more current MALDI-TOF machine, despite many hours of effort, the replacement unit failed to provide any comparable data for LM7-2 peptide pooling. Therefore, it became a less precise method of pooling peaks solely by HPLC elution times was used for LM7-2. Mass spectroscopy using LC-ESI-MS confirmed the correct masses purified for LM7-1 (2913.638 Da) and LM7-2 (2984.675 Da); these measured values corresponded to the calculated values obtained for the monoisotopic weights of the desired AA sequences.

The antimicrobial activity assay for significant inhibition of normal bacterial growth for 24 hours post-treatment demonstrated a clear difference in antimicrobial

activity between LM7-1 and LM7-2. LM7-1 was active against gram negative bacteria, such as *E.coli*, but not against *P.aeruginosa*. LM7-1 was active against gram positive bacteria such as *E.faecalis*, but less active against *S.aureus*. LM7-2 was more active against gram negative *E.coli*, and *P.aeruginosa* than LM7-1. LM7-2 was more active against gram positive *E.faecalis* and *S.aureus* than LM7-1. This data suggests the alteration from (Lys¹⁵ → Gly¹⁵) lowered the AMP's activity in a "broad spectrum effect" simultaneously against all the bacterial species. A possible explanation for this outcome was that the extra glycine made it more difficult for LM7-1 to form an alpha-helical conformation at the bacterial cell membrane surface. Potentially, the additional lysine positive charge was essential in targeting the AMP against all bacterial membranes more effectively. Inhibitory activity was diminished against both gram positive and gram negative species, so it is unlikely that subtle differences in cell wall architecture between of the two classes of bacteria were the main issues in determining the specificity of the peptides.

Although the protocol for the hemolytic assay is still in development, the preliminary data suggested that the two peptides could both be highly hemolytic under specific assay conditions, which limits their effective therapeutic doses. Human blood was used instead of sheep's blood as the red blood cells of the two species differ in terms of cell membrane lipid structure. Due to the fact that all of the AMPs were designed to be human therapeutics, it was necessary go through the extra inconvenience to obtain fresh human RBCs. Although LM7-1 and LM7-2, when tested, failed to clear the hemolysis test, it is still possible that repeating the hemolysis assay using other types of animal blood cells might yield a better result. These AMPs

could potentially be useful for veterinary applications even if they prove toxic to humans.

The next three AMPs in this family, LM7-3, LM7-4 and LM7-5 have been designed, synthesized and cleaved from the resin. In an extension of the current project, they would be subjected to the same purification procedures, massed and evaluated using antimicrobial and RBC hemolytic assays. In the future, the hemolysis assays should be run well before the antimicrobial activity assays, as hemolytic AMPs are useless as therapeutics due to the fact that the peptides would kill host RBCs before inhibiting the growth of invading pathogenic bacteria. LM7-3 through LM7-5 could potentially display novel and useful biological effects, as they were designed using *in silico* tools. The *in silico* tools allow multiple designs to be compared to identify peptides candidates having the following desired properties: formation of an α -helix/hinge/ α -helix conformation in membranes, a partly amphipathic sequence, and a gradual transition from a more hydrophilic *N*-terminal region to a more hydrophobic *C*-terminal region. By using these criteria to rapidly narrow down prospective hybrid peptides from distinct species of organisms with novel sequences, the best candidates can be readily identified and screened for desired biological effects.

In sum, if properly employed, this hybrid approach to AMP design using novel criteria to evaluate sequence modifications has great potential to unlock the power of AMPs to treat drug-resistant bacterial infections. It is likely that sequence modifications of known AMPs could be more effective against a wide variety of types of bacteria, without simultaneously harming human RBCs via hemolysis. The natural extension of this project is to evaluate via antimicrobial activity assays as well as

hemolytic assays whether the novel hybrid peptides LM7-3, LM7-4 and LM7-5 can distinguish between bacteria and RBCs better than LM7-1 and LM7-2 did. My conclusion is that the incremental residue alteration made in LM7-1 may have increased its hemolytic properties by disrupting essential sequence motifs that prevent peptide self-aggregation. Using intact stretches of native AMP sequences to create hybrid AMPs without disrupting essential residue patterns found within naturally evolved sequences should increase antimicrobial activity and possibly reduce hemolysis. AMPs have evolved for millions of years; retaining portions of the intact sequences and recombining them is more likely to preserve their activities against pathogenic bacteria, as opposed to single residue modification. The *in silico* design of novel hybrid AMPs holds great potential for generating novel therapeutic effects, and the improved understanding of poorly characterized sequence motifs encoded within the native sequences of AMPs clearly requires new software tools and more experimental data on what works to increase desirable features.

APPENDIX A: ABBREVIATIONS

AMP: antimicrobial peptide

AMU: atomic mass units

Boc: *tert*-butyloxycarbonyl

CFU: colony forming units

Da: Daltons

DCC: *N, N'*-dicyclohexylcarbodiimide

DCM: dichloromethane

DCU: *N, N'*-dicyclohexylurea

DMF: *N, N*-dimethyl formamide

GUI: graphics user interface

HC₅₀: minimum hemolytic concentration

HF: hydrofluoric acid

HBTU: 2-(1H-benzotriazole-1-yl)-1,1,3,3-tetramethyluronium hexafluorophosphate

HOBt: 1-Hydroxybenzotriazole

LC-ESI-MS: liquid chromatography-electrospray ionization-mass spectrometry

LPS: lipopolysaccharide

MALDI-MS: matrix assisted laser desorption ionization - mass spectrometry

MBHA resin: 4-methyl benzhydrylamine styrene divinylbenzene copolymer

MIC: minimum inhibitory concentration

MW: molecular weight

OD: optical density

RP-HPLC: reversed phase high performance liquid chromatography

SPPS: solid phase peptide synthesis

TFA: trifluoroacetic acid

TOF: time of flight

UV: ultraviolet

APPENDIX B:
***IN SILICO* RESEARCH: ANTIMICROBIAL PEPTIDE EDITABLE
DATABASE (AMPED) PROJECT REPORT**

B.1 Introduction

The AMPED project team was composed of: Lenore Martin, Project Manager and Professor of Biochemistry; Daniel Ducharme, Computer Scientist and David Ryder, Biochemist.

The primary rationale behind the AMPED project was to install an expert peptide analysis system, possessing upgraded features as compared to existing peptide analysis programs. A side goal was to develop collaborative relationships between scientists and programmers. A desirable outcome was having the ability to generate a specific database with searchable, stored fields along with expert peptide analysis systems that were on par with if not better than the Peptide Companion® program (Lebl, 1992). However, due to time constraints, only the expert systems were coded and the editable database was set aside for a future project.

Peptide Companion®, is an old DOS program written for Windows 3.1 and used on all of the operating systems since. This program was outlined as an exemplar as to what features could be improved with the creation of the AMPED program; it has many useful features, including an editable storage for sequences, and extensive tools such as Chou-Fasman, HPLC prediction, Molecular weight and many other features. However, the program has not been updated since 1992, and it cannot be modified. It

has never been updated for the newer operating systems, and has not been reissued with the newer algorithms. Another issue with Peptide Companion® is that the proprietary code means that the exact steps the algorithms take is unknown. For example, the Peptide Companion® version of the Chou-Fasman algorithm only shows the likelihood of forming various secondary structures as line graphs. The algorithm was unable to evaluate the entire length of the peptide, and always skipped the last six residues.

Peptide tools are an important element with peptide researchers looking for accurate, complete and reliable information about the antimicrobial peptides of interest. Along with sequence information, accurate, and well-documented bioinformatic implementation of common algorithms is a vital component of a well designed program. The AMPED expert system has the advantage of being open source, as well as being transparent. All the algorithms used would be explicitly cited and described in detail.

B.2 Problem Definition

The intention of the AMPED project was to create a database to hold data from a variety of websites, and then designing tools to operate on that data. The toolset was to be designed as open source using clearly published algorithms to allow for easy validation of the tools. Each tool was to be tested by comparing it to both hand calculated results and to the output of Peptide Companion®.

The program was to be written in C++ since that was an strong language with a full feature set and could interface with any database that was later chosen. At first the database was decided to be programmed in MySQL because of its cross-platform compatibility. However, due to graphic user interface (GUI) issues on Windows, the program was switched to PostGreSQL which is also compatible with all major operating systems but had a much better feature set for Windows.

The expert peptide analysis systems were geared to research groups that synthesized, purified and assayed the effectiveness of Antimicrobial Peptides. The most fundamental system needed was a peptide molecular average/monoisotopic weight function. The raw data was obtained from the NIST Physics laboratory and programmed in (NIST Website, 2010). In addition, the program was designed to provide percentages of each amino acids within the sequence using simple string searches and tabulations.

The second expert system was the use of the Chou-Fasman algorithm to determine predicted protein secondary structure (Chou, 1978). It took a great deal of effort to produce secondary structure predictions that reflected the Peptide Companion's® models. Once refinements were made, the results were judged to be at least equal to the older program. It was decided that the step by step output of the Chou-Fasman algorithm would be valuable to the peptide chemist, especially as concerning questionable sequence assignments.

B.3 AMPED Project Results

At this point both tools are operational and have their tabular data stored in the database. The Amino Acid and Molecular Composition has been hand verified and both the percent and molecular weight were confirmed to be correct. The AMPED Chou-Fasman algorithm does correctly follow the published algorithm and enforces parameters (such as having a minimum of five residues in a beta sheet) better than the existing Peptide Companion® tool.

As currently designed, the Expert Systems on the AMPED program features:

- 1) Command Line Sequence input featuring manual or Copy/Paste input.
- 2) Peptide Analysis:
 - (a) Predicted Molecular Weight (Monoisotopic or Average) can be calculated.
 - (1) In addition, it lists number/percent [x.xx] of each of the following elements: (C/H/O/N/S/Cl).
 - (b) Amino Acid Composition can be determined.
 - (1) Program will Count number/percent [x.xx] of each of the 20 standard amino acids.
- 3) Chou-Fasman Algorithm:
 - (a) Find all groups of 4 contiguous Alpha Helix formers with six residues having an average $P_a > 1.03$.
 - (b) Extend each helix in both directions until the average P_a falls below 1.03 or a Proline is found not at the *N*-terminus end of the helix.

- (c) Find all groups of 3 contiguous Beta Sheet forming residues with five residues having an average $P_b > 1.00$.
- (d) Extend each sheet in both directions until the average P_b falls below 1.00.
- (e) Find all groups of 4 residues that form a turn with an average $P_t > 1.00$ and a probability > 0.000075 .
- (f) Compare overlapping regions of Alpha and Beta and where $P_a > P_b$ mark as Alpha; otherwise mark as Beta.
- (g) Test the length ensuring that each run still meets the requirements of step a and c. If it fails the test, remove it. If the opposite structure has been removed in step f, restore it and repeat step g.

B.4 Future Work and Conclusions

Although the AMPED program is functional, there are clear avenues for future revision and expansion. There are many other expert peptide analysis systems that can be added such as prediction of amino acids from molecular weight, helical wheel projections and accounting for post-translational modifications to the sequence (Schiffer, 1967). Another important layering is that of having a web-enabled GUI that can be accessed by other research groups in order to use the database as well as its peptide expert analysis systems. However, having these extra layers are only essential if the output is a chart or drawing.

In sum, the creation and collaboration required producing a functional and useful Editable database that can further research goals, although challenging and complex, is worthwhile.

B.5 Chou-Fasman Algorithm

1) α -helix formation:

(a) Read off the P_a values for 6 residues at a time. If 4 out of 6 residues in a row average larger than 1.03, then an alpha helix can be nucleated.

A Proline residue can only be at the *N*-terminal end of the sequence.

(b) Extend until the average P_a value drops below 1.03. If the average P_a is larger than P_b for the same stretch, then the region is an α -helix.

2) β -sheet formation:

(a) Read off the P_b values for 5 residues at a time. If 3 out of 5 residues in a row average larger than 1.05, then a beta sheet can be nucleated.

(b) Extend until the average P_b value drops below 1.05. If the average P_b is larger than P_a for the same stretch, then the region is a β -sheet.

3) β -turn formation:

(a) Read off 4 residues in a row. If the P_t values average larger than 1.00, then a beta turn can be formed. If the average P_t for the stretch is greater than the P_a or P_b values for the same sequence, then a beta turn can form.

(b) To determine the precise start of the turn, find the products of f_i , f_{i+1} , f_{i+2} and f_{i+3} for the residue of interest and each of the downstream residues in sequence. If the product exceeds 7.5×10^{-5} , then a good initiation site for a beta-turn is assumed. The highest initiator with the possible beta-turn stretch is nominally judged to be the first residue in the turn.

APPENDIX C:

MARTIN LAB STANDARD OPERATING PROCEDURES FOR CATIONIC ALPHA HELICAL ANTIMICROBIAL PEPTIDE SYNTHESIS, PURIFICATION, CHARACTERIZATION, AND ACTIVITY ASSESSMENT

C.1 Solid Phase Peptide Synthesis

C.1.1 Solid Phase Peptide Synthesis Procedure

1. Swell the methoxybenzhydryl (MBHA) resin used for SPPS dichloromethane overnight in dichloromethane (DCM), and assess the amount of free amino groups using a quantitative ninhydrin test. This test will determine how much of any given amino acid is needed to perform a coupling. For any given coupling, use an excessive amount of the *tert*-butyloxycarbonyl (Boc) amino acids in order to drive the reaction to completion.
2. Couple the first amino acid to the resin by using a Direct DCC catalyzed 1-hydroxybenzotriazole (HOBt) coupling protocol without the reagent trifluoroacetic acid (TFA), using the Boc amino acid, *N,N*'-dicyclohexylcarbodiimide (DCC), and HOBt. Check if the reaction has been completed by performing a ninhydrin test. If it has coupled, proceed to the next residue; if it hasn't, switch to a different coupling protocol. There are many different protocols available to couple Boc amino acids to growing peptide chains. A sample order is the Preformed Symmetric Anhydride Protocol, Direct DCC Catalyzed Coupling Protocol, and Direct HBTU Catalyzed Coupling Protocol.

3. Any subsequent Boc amino acid residues should be coupled and if a ninhydrin check proves positive, switch to a different protocol until the Boc amino acid is fully coupled. A useful order is Direct DCC Catalyzed Coupling Protocol, Preformed Symmetric Anhydride Protocol, Direct DCC catalyzed HOBt, and Direct HBTU Catalyzed Coupling Protocol.
4. Once the synthesis is complete, the peptide-resin can have the histidine side groups deprotected; then the sequence can be cleaved with hydrofluoric acid, and characterized.

C.1.2 Solid Phase Peptide Synthesis Coupling Protocols

Protocol #1: Direct *N, N'*-dicyclohexylcarbodiimide Coupling Protocol after acid deprotection of the amino acid group of the growing chain with trifluoroacetic acid

1. Make sure the resin is fully swollen in DCM solvent solution in a glass reaction vessel (RV) fitted with a fritted filter prior to coupling. The frit prevents the solid phase resin from escaping when the reagents are drained out of the RV. The reaction vessel should be mounted on a shaker to ensure complete mixing. Wash with DCM three times, and completely drain the RV of wash solvent after each wash step.
2. Add a solution of 50% TFA/50% DCM, with a volume sufficient to fully suspend the peptide resin and let the reaction vessel shake for 90 seconds, to allow the resin to swell up to its maximum volume in this reagent. Drain off the TFA/DCM mixture and add a fresh amount of the acid deprotecting

reagent. Allow the reaction vessel to shake for 90 minutes to ensure the TFA solution completely cleaves off all the Boc protecting groups, and then drain off the excess reagent. Warning: this step is when the RV is most likely to leak through the threads of its Teflon cap. TFA is also a volatile, dangerous acid; it presents both a contact and inhalation hazard. Neutralize all TFA after use.

3. Wash the resin thoroughly with six washes of DCM, followed by two 90-second washes of the basic solution (20% diisopropylethylamine (DIEA)/80% DCM) to neutralize any residual TFA, as well as to restore the ionized amine salts back to a reactive, deprotonated, “free-base” form. Complete the series of post-Boc deprotection with six more rounds of DCM washes.
4. Weigh out a five equivalents of the Boc-amino acid and dissolve the protected amino acids in a minimal amount of DMF; then add the solution to the reaction vessel. Do not drain.
5. Measure out volumetrically, a five equivalents of DCC in a calibrated ~0.50 M stock solution prepared fresh in DCM. Add the solution to the RV, but do not drain.
6. Add sufficient additional DCM to fully suspend the resin, Boc-amino acid and coupling reagent and start the shaker to couple for at least 90 minutes. After 90 minutes, the reaction should be completed; using an aspirator vacuum, drain out the leftover reagents and solvent.
7. Do four post-coupling resin washes with DCM, followed by two 90-second washes with 10% DIEA/90% DCM, and finally six more washes with DCM.

Leave the peptide-resin fully suspended, swollen, and shaking in solvent after the final wash until the next procedure is begun.

8. Perform a ninhydrin check to verify that all the free amino groups on the resin-bound growing chains have reacted completely with the incoming Boc amino acid. Repeat the coupling reaction with the same Boc-amino acid if the ninhydrin test is positive, or go onto coupling the next amino acid in the sequence if the ninhydrin test is negative.

Protocol #2: Preformed Symmetric Anhydride Coupling Protocol without without prior trifluoroacetic acid deprotection of the amino group

1. Fully swell the peptide resin in DCM prior to performing any coupling step to expose the maximum number of peptide chains to the coupling reagents as possible. Wash with a DCM solution three times to initiate the procedure, and fully drain the RV after each wash.
2. Weigh out a two equivalents of the Boc amino acid to be coupled, with the amount of free amine groups on the growing peptide chains attached to the solid phase resin. Dissolve the Boc-AA in a minimal amount of DMF in a small, dry, glass Erlenmeyer flask. Measure out volumetrically, 1 equivalent of DCC in a calibrated ~0.50 M stock solution prepared fresh in DCM. Add the DCC solution to the flask to allow the DCC to catalyze coupling of the Boc amino acid to itself, which produces the reactive, preformed symmetrical anhydride of the incoming Boc-amino acid. After allowing the reaction to

proceed for 5-10 minutes, add the symmetric anhydride solution to the RV, but do not drain.

3. Add sufficient additional DCM to fully suspend the resin, the activated preformed symmetrical anhydride of the Boc-amino acid and coupling reagent, then start the shaker to couple for at least 60 minutes. After the reaction completes, use an aspirator vacuum to drain out the leftover reagents and solvent.
4. Do four post-coupling resin washes with DCM, followed by two 90-second washes with 10% DIEA/90% DCM, and finally four more washes with DCM. Leave the peptide-resin fully suspended, swollen, and shaking in solvent after the final wash until the next procedure is begun.
5. Perform a ninhydrin check to verify that all the free amino groups on the resin-bound growing chains have reacted completely with the incoming Boc amino acid. Repeat the coupling reaction with the same Boc-amino acid if the ninhydrin test is positive, or go onto coupling the next amino acid in the sequence if the ninhydrin test is negative.

Protocol #3: Direct 1-hydroxybenzotriazole Coupling Protocol without prior trifluoroacetic acid deprotection of the amino group

1. Fully swell the peptide resin in DCM prior to performing any coupling step to expose the maximum number of peptide chains to the coupling reagents as possible. Wash with a DCM solution three times to initiate the procedure, and fully drain the RV after each wash.

2. Weigh out four equivalents of the Boc amino acid to be coupled. Equivalents are calculated as the amount of free amino groups at the ends of the growing peptide chains attached via their *C*-terminal ends onto the MBHA resin.
Weigh out four equivalents of the racemization suppressor, HOBt. Dissolve the coupling reagents together in a minimal amount of dimethylformamide (DMF) solvent and add the mixture to the reaction vessel. Mix, but do not drain.
3. Volumetrically measure out four equivalents of a calibrated DCC solution in DCM and add it to the reaction vessel. Be careful to avoid skin contact, as DCC is an extremely strong allergen. Mix, but do not drain.
4. Add sufficient additional DCM to just barely suspend the resin and reagents so they mix efficiently in the RV, and then start the shaker, and allow the first coupling reaction to proceed at RT for at least 90 minutes. After the reaction is complete use a vacuum to filter out the leftover coupling reagents with a water aspirator trap.
5. Following each coupling reaction, use four washes of each of the following reagents: DCM, DMF, methanol, and again DCM. This will ensure that residual reagents and soluble by products are eliminated, leaving only the resin and its attached amino acid chains behind.
6. Perform a ninhydrin check to verify that all the free amino groups on the resin-bound growing chains have reacted completely with the incoming Boc amino acid. Repeat the coupling reaction with the same Boc-amino acid if the ninhydrin test is positive (any degree of blue coloration is observed), or go

onto coupling the next amino acid in the sequence if the ninhydrin test is negative (pure yellow solution).

Protocol #4: Direct 2-(1H-benzotriazole-1-yl)-1,1,3,3-tetramethyluronium hexafluorophosphate (HBTU) Coupling Protocol without prior trifluoroacetic acid deprotection of the Boc group on the amino acid

1. Swell the peptide resin in DCM prior to coupling to expose the maximum number of peptide chains possible. Wash with DCM four times, and drain the reaction vessel after each wash.
2. Weigh out a five equivalents of the Boc amino acid. Dissolve the Boc-amino acid in a minimal amount of DMF in a small, dry, glass Erlenmeyer flask. Weigh out five equivalents of HBTU and add it in to the same mixture, followed by a ten equivalents of 20% DIEA/80% DCM to activate the HBTU. Pour the mixture into the reaction vessel.
3. Add sufficient DCM to suspend the resin and reagents and start the shaker for at least 60 minutes. After the reaction is complete, drain out the leftover reagents using vacuum filtration.
4. Do four resin washes of DCM, followed by two 90 second washes of 10% DIEA/90% DCM, and finally four washes of DCM. Leave the peptide-resin suspended and shaking after the final wash.
5. Perform a ninhydrin check to verify if all the free amino groups on the resin have reacted with the Boc amino acid. Repeat the next coupling if the

ninhydrin is positive, or proceed to the next amino acid coupling if the ninhydrin is negative.

C.1.3 Ninhydrin Free Amine Verification

1. The ninhydrin test is used to indicate the presence of free amine groups; either on SPPS resin directly, or on attached, *N*-terminal unprotected peptides bound to the resin. This particular test uses a combination of three reactive reagents to perform the test. Ninhydrin forms a blue, light absorbing complex with the amine group, KCN serves as a reducing agent, and pyridine displaces ninhydrin from the resin so the ninhydrin can enter the solution and be detected with a spectrophotometer.
2. Ninhydrin uses two solutions, labeled Reagent A and B. To make Reagent A, 40 g of phenol is added to 10 ml of absolute ethanol and gently heated to dissolve the phenol. Add, stir, and filter out 4 g of MB-3 Amberlite® resin. In a separate flask, dissolve 65 mg of KCN in 100 ml of water. Remove a 2 ml aliquot, and dilute it to 100 ml using pyridine. Add, stir and filter out 4 g of MB-3 Amberlite resin. Combine the phenol and KCN/pyridine solutions. To make Reagent B, dissolve 2.5 g of ninhydrin in 50 ml of absolute ethanol, and store it under nitrogen.
3. Take out a 2-5 mg sample of peptide/resin and place it into a small tube. Add 4 drops of ninhydrin Reagent A, and 2 drops of ninhydrin reagent B to the sample tube and to an empty control tube. Place the sample tubes in a block heater set to 100°C for exactly 10 minutes to allow the reaction to complete.

4. Take out the sample tubes, allow them to cool, and then add some isopropanol and agitate the tubes to thoroughly mix the contents. Any pure yellow color in the liquid is the natural color of the unreacted ninhydrin reagents and is interpreted as a negative result. Any reaction of free amines to the reagents will add a blue color to the sample. The more intense the color is, the more free amine groups are in the sample.
5. If an exact quantification of free amine groups is required, filter the sample with 60% ethanol through a glass pipette stuffed with glass wool, and dilute it out to 10.0 ml in a volumetric flask. Place the sample in a quartz cuvette in a spectrophotometer set to 570 nm to detect the absorption of the blue pigment. The concentration will be proportional to the absorbance.

C.1.4 Histidine-dinitrophenol Removal Protocol

1. This protocol is used to remove the dinitrophenol (DNP) side chain protection from histidine. Swell the Boc-protected peptide resin in DMF for several minutes in a glass solid phase reaction vessel. Drain the DMF. Add fresh DMF at a ratio of 5 ml DMF per gram of peptide-resin.
2. Without draining the solvent, add 20 mmol thiophenol (0.102 ml/mmol, or 2 ml) for each mmol of His (DNP) present in the product peptide. Stir (or shake) the mixture for four hours at room temperature. The solution should turn bright yellow as DNP is removed.
3. Drain thoroughly, and wash the resin three times with (DMF) and dichloromethane (DCM), followed by four washes of 1:1 Methanol/DCM and

DCM. A small amount of intensely yellow colored DNP-thiophenol may remain adsorbed to the peptide-resin. After standard wash procedures, the peptide-resin may still be slightly yellow, but the sulfurous odor should be completely gone. The used thiophenol solution, and any apparatus that touched it should be immersed in a 10% bleach solution and stored in the hood until the smell is dispersed.

4. Remove the *N*-terminal Boc group with 50% TFA in DCM before the HF Cleavage.

C.1.5 Anhydrous High Hydrofluoric Acid Cleavage Protocol

1. At the end of SPPS, immediately prior to the peptide-cleavage step, the *N*-terminal Boc protecting group should be removed using 50% TFA in DCM followed by a ninhydrin test to confirm free amine groups are exposed. It is also used to verify the amount of free *N*-terminal amine that is present on the peptide-resin product.
2. Dry the deprotected peptide-resin by washing with DCM several times and then vacuum filter it until it is dry and flaky. Then transfer up to 1.0 g peptide-resin into each of the two Kel-F® HF cleavage vessels followed by a teflon-coated stir bar. Add the bumper lids with the o-ring ridges facing up. Cover the lids with parafilm and poke holes to allow vapors to escape. Place the HF vials upright in a vacuum flask and lyophilize the peptide-resin samples at room temperature overnight.

3. Break the vacuum, remove the HF vials containing the dry peptide-resin, and add HF scavengers. For a typical peptide, use a cleavage mixture of 10:1:1 HF/p-cresol/p-thio cresol (v/v/v). Plan for 5 ml of HF for every 0.5 g of peptide-resin mass. **WARNING:** hydrofluoric acid (HF) is extremely toxic and can cause bone damage if it absorbed through the skin. Keep a 26% MgSO₄ solution on hand to soak and wash affected areas; also have a calcium gluconate gel to apply topically or inject on the burn site to neutralize the acid. Seek medical attention at once if you suspect you have been burned.
4. Check the KOH trap to make sure it contains adequate base to neutralize any excess HF. The phenolphthalein dye indicator should be orange (pH >8). Leak test the HF apparatus using N₂ gas after mounting the peptide-resin (RV) reaction vessel(s) to ensure the system is closed. Chill the HF vials to -78°C in vacuum dewer flasks using an isopropanol slurry, and dry ice for at least 20 minutes before attempting to distill HF into the vessels. Once HF is distilled into the cleavage flask, the peptide-resin should turn red.
5. Once HF is delivering properly through the system, monitor the volume of HF condensed into each RV by lowering the jacks supporting the dewars and holding a flashlight behind the RV so the HF level may be observed. If the correct volume of liquefied HF is present, stop the HF flow, flush the system with N₂ gas, and begin stirring the HF vessels vigorously, maintaining the HF vessels temperature at 0°C with an ice-water mixture for 1 hour.
6. After 1 hour at 0°C, carefully open the 3-way valves on the apparatus so the N₂ gas blows the HF into the KOH trap at a rate that does not “bump” the resin up

into the apparatus. N₂ gas is used to drive out HF and dry the peptides and resin, one vessel at a time. When all the HF has been removed, use the water aspirator system to completely dry out the resin vessels and apparatus.

7. Unscrew the HF vessels containing resin, scavengers, and product peptide from the apparatus. Extract the scavengers from the peptide and resin with diethyl ether twice; then extract the peptide from the resin using 10% aqueous acetic acid (v/v). The acetic acid will dissolve the peptide and the solution can be filtered, separating out the solubilized peptide solution from the insoluble resin beads. Follow with “safety extracts” using glacial acetic acid, in case the peptide is very insoluble, then dry and set aside the resin as waste. Lyophilize the 10% and glacial acetic acid extracts and determine the yield of crude peptide obtained.

C.2 Liquid Chromatography Purification

C.2.1 Gel Filtration Liquid Chromatography with a G25 Sephadex Column

1. Sephadex® is a dextran derived, cross-linked mixture of polysaccharide beads that are manufactured at varying pore sizes to exclude all analytes above a certain cutoff mass; all substances below the cutoff are retained in inverse proportion to the overall mass. For most peptides, using this compound after Solid Phase Peptide Synthesis will separate the large peptides from the low mass synthesis byproducts.
2. The column using the Sephadex® must use size G25 at the most, otherwise the 5 kDa peptide will be retained by the beads. Any mixture of G15, G10 can be

used with G25 as long as the beads are thoroughly mixed. The beads should be always kept wet in a 10% aqueous acetic acid (v/v), which can be added via a peristaltic pump from a reservoir.

3. The drain line from the column should be routed through a flow cell in a UV absorbance detector set to 280 nm to note tryptophan absorbance as the peaks elute. If the peptide does not contain tryptophan, 220 nm can detect the absorbance of the peptide bonds themselves. The eluent should be deposited into fraction tubes so that the peptide product peak can be isolated from the synthesis byproduct peak. The UV detector should be connected to a chart recorder to provide a chromatogram for the run.
4. Ensure the Void volume is known by running blue dextran solution through the column and measure how much liquid is collected before the dye elutes. Blue dextran is a massive polysaccharide that will be larger than the cutoff size for any type of gel filtration bead.
5. Dissolve the crude peptide so the concentration is roughly 25 mg peptide/ml of 10% v/v acetic acid. The solution must be refrigerated at 4°C to slow any peptide degradation.
6. Let the column drain down to just the top of the Sephadex bed and layer the sample evenly across the top. The size of the applied sample will vary depending on the column specifications. A 3 cm diameter column will accommodate a 3-5 ml sample volume. A 9 cm diameter column can handle the entire volume of a 2 g crude peptide extract from a small scale SPPS synthesis in a single run.

7. Let the sample drain down to the top of the Sephadex bed and establish a head space of 10% acetic acid atop the bed.
8. Start the peristaltic pump and let the eluent flow through the UV detector and pool the liquid until the void volume is reached; all of the liquid collected up to that point will be waste. The second void volume should be the primary peptide, followed closely by failed sequences that are slightly less massive than the desired sequence due to missing amino acid residues. The third void volume will be leftover synthesis reactants and the scavengers left over from the hydrofluoric acid cleavage.
9. Due to the concentrated nature of the crude peptide sample, the absorbance in the flow cell UV detector will maximize at the upper end of the detection range and plateau out until most of the sample has eluted.
10. After collection has stopped, the fraction tubes can be processed by running them individually in a spectrophotometer at 280 nm (or 220 nm) to determine the true absorbance values where the sample is the most concentrated. 1/10 dilutions can be used if the absorbance of the neat samples are too high.
11. Once the absolute absorbance values are known, use them to determine the time from where the first peak starts to elute to where the absorbance starts to rapidly fall. This range will contain the purest amount of desired product. Pool everything within that range and label it the 'A' Peak. Everything after that to where the absorbance falls back down to baseline levels will mostly contain worthless products; this can be labeled the 'B' Peak and pooled.

12. Freeze the samples in Lyophilizer flasks by inserting them into an isopropanol solution chilled to -80°C using dry ice. Rotate the flasks to coat the sides with a thin, frozen film of acetic acid and product. Place the flasks in shallow pans filled with an isopropanol/dry ice mixture, connect the flasks to the lyophilizer and freeze dry the samples under vacuum to sublime off the frozen acetic acid. The crude product can then be subject to characterization by analytical HPLC and processed in bulk by preparatory HPLC.

C.2.2 Preparatory Reversed Phase High Performance Liquid Chromatography with a C18 Column

1. The peptide mixtures should be dissolved prior to HPLC analysis or purification in 10% acetic acid, ensuring that the concentration is no higher than 10 mg peptide/ml. The analyte solution should be refrigerated at 4°C to slow down any peptide degradation until it is lyophilized to dryness. Just prior to a RP-HPLC run, inject up to 5 ml of the sample into the sample loop.
2. Run the 5% acetonitrile/95% water/0.1% TFA mobile phase through the column until the baseline absorbance on the UV detector stabilizes. Zero out the detector and start the run by switching the valve to inject the loaded peptide product in the sample loop. For step gradient runs, change out the reservoir bottles every time a higher concentration of acetonitrile is required. Make sure to mark on the chromatogram exactly when each new mobile phase concentration begins. At the end of the run, in order to flush the column free of any residual products; the highest concentration of mobile phase used should always be set to 95% acetonitrile/5% water/0.1% TFA and run until the

absorbance reaches the baseline level. Test runs with small amounts of peptide can be used to develop a gradient method capable of achieving baseline separated peaks for each new peptide sequence.

3. After elution has stopped, process the eluent fraction tubes into sub-groups representing three distinct zones: baseline absorbance outside of peaks, the first five fractions of a peak, and the tail end of a peak. Baseline absorbance zones will not usually contain any usable peptide, the leading edges and peak regions will have products of the highest purity, and the tailing edges will contain impure products. One way to assign peaks is to start with the prep column run code followed by letter indicating the order in which each peak eluted during a run. For example, label 4C can refer to the third peak on the fourth prep run. Concentrate pooled fractions on a Rotovap® until all the acetonitrile is removed, and then place the samples into 15 or 50 ml plastic centrifuge tubes.
4. Freeze the pooled and purified samples in centrifuge tubes by inserting them into an isopropanol slurry. Rotate the tubes to coat the sides of the tubes with a thin, frozen film of sample. Use a thumbtack to poke pinholes in the plastic caps to allow the vapor to escape during lyophilization. Place the tubes inside lyophilizer flasks, and then cool the flasks in shallow pans filled with an isopropanol/dry ice slurry. Afterwards, connect the flasks to the lyophilizer to freeze dry the samples under vacuum to sublime off the acetic acid. The pooled fractions are characterized by MALDI-TOF mass spectroscopy to determine if they contain the peptide of interest.

C.3 Mass Spectroscopy

C.3.1 Matrix Assisted Laser Desorption Ionization-Time of Flight

1. Prepare a sample of 2 ug/ml of a known mass standard used to calibrate the MALDI-TOF. Dissolve single crystals of dried peptides in 35 μ l of 10% v/v acetic acid. Make tenfold dilutions of the samples using a diluent mixture (50% acetonitrile/49.95% water/0.05% TFA). Spot the sample plate with 1 μ l of 10 mg sinapic acid dissolved in the same diluent to make up the sample matrix; then pipet 1 μ l of the peptides samples on a metal chip within the center of the matrix droplets, and let the samples dry thoroughly.
2. Place the chip in the MALDI-TOF sample holder and expose it to high vacuum conditions. Scan the MW standard first and correct any deviations from its known mass; this serves to calibrate the machine to accurately record charge/mass ratios for all the other samples.
3. Scan the rest of the samples with the laser beam and save the detector results. Label the relevant peaks. Pure samples will typically only have one well-defined peak of the desired mass. Impure samples will have multiple peaks.
4. Use the determined charge/mass values to pool the peptide samples across multiple RP-HPLC runs into appropriate fractions of the synthetic peptide. Pure samples can be used directly for antimicrobial testing. Other samples can be re-purified if more product is needed at a later date.

C.3.2 Liquid Chromatography-Electrospray Ionization-Mass Spectroscopy

1. Dissolve single crystals of dried peptides in 20 μ l of HPLC Buffer A (50% acetonitrile/49.95% water/0.05% formic acid). Inject 1 μ l of the dissolved peptides samples into the LC column.
2. Note the results in terms of Retention Peaks, Total Ion Chromatograms, and Selected Ion Chromatograms. This information is used to determine m/z ratios for various charges (+1, +2, etc). The m/z ratios can be deconvoluted to determine the overall mass of the uncharged compound.
3. If no major peaks are found, repeat steps 1 and 2 with a 10 μ l injection to increase peptide sample amounts.

C.4 Antimicrobial Assays

C.4.1 Antimicrobial 96-Well Plate Activity Assay

1. Soak any contaminated glassware must overnight in an equal volume of 6% bleach solution, to kill all microorganisms. Wash with soap and water and let them air dry.
2. Use Mueller-Hinton agar for plates, Nutrient agar for slants, and Mueller-Hinton media for broth. Set up broth cultures from slants by disinfecting the work surface with 70% isopropanol. Then set up 4 slant cultures: *Esherichia coli*, *Enterococcus faecalis*, *Staphylococcus aureus*, and *Pseudomonas aeruginosa*. Transfer sterilized broth media to 150 ml Erlenmeyer flasks. Add a loopful of slant growth to the matching labeled flask. Always do

Staphylococcus aureus last as it is easy to cross-contaminate other cultures with it. Place flask overnight in 37°C incubator shaking at 200 RPM.

3. Set up the subcultures by disinfecting the work surface with 70% isopropanol. Next, set up 4 broth cultures: *Esherichia coli*, *Enterococcus faecalis*, *Staphylococcus aureus*, and *Pseudomonas aeruginosa*. Transfer sterilized broth media to 150 ml Erlenmeyer flasks. Add a loopfull of broth growth to the matching labeled flask. Always inoculate *Staphylococcus aureus* last. Place flask overnight in 37°C incubator shaking at 200 RPM; repeat the procedure if necessary.
4. Determine optical density (OD) by turning on a Spec20 spectrophotometer and let it warm up for 30 minutes. Adjust the wavelength knob until the reading is for 630 nm. Set the left (% Transmittance) knob to 0%, and then insert a Mueller-Hinton blank, and turn the right (Absorbance) knob to 0. Read the samples by placing 3 ml of the sample into a 1x10 cm tube, vortex it, and insert it into the spectrophotometer.
5. Adjust the optical density to ensure logarithmic growth for the bacterial culture; the best value is an OD₆₃₀ of 0.120. If the OD is too high, dilute it down with sterilized Muller-Hinton broth to 1/2, 1/5, and 1/10 dilutions until it is around 0.120. Once the OD is reasonable, use the following equations to set up the amount of bacterial broth to use, then measure the diluted OD:

$$(5 \text{ ml}) (0.120/\text{Determined OD}) = x (\text{Volume of bacterial broth}) \quad (1)$$

$$(5 \text{ ml} - x) = \text{Amount of Muller-Hinton broth to add} \quad (2)$$

6. Suspend the AMP in solution of Hancock Diluent to make a working concentration of 5 mg/ml. Take an aliquot from this sample to make a 1:10 dilution, and do a second serial dilution to 1:100. Set up the chemical antibiotic so its working concentration is 0.1 mg/ml. Set up sterile 8-well broth trays. Use at least 5 ml of the bacterial suspension as well as 10 ml of Muller-Hinton broth. Use the first 3 rows for Muller-Hinton broth, skip a row, and use the next 3 rows for the diluted bacterial broth. Set up the 8-arm multipipetter for 150 μ l aliquots. Apply even pressure to properly seat the tips.
7. Set up the 96-well plate. Each well can accommodate 300 μ l of liquid. The plate has 8 rows which give 8 replicate results for each column. There are 12 separate columns for different conditions. The conditions are as follows:
Media (Mueller-Hinton broth only), Bac (*Escherichia coli*, *Enterococcus faecalis*, *Staphylococcus aureus*, or *Pseudomonas aeruginosa*), Dil (Dilution), AMP, Antibio (active antibiotic), 6 M NaOH (total cell kill solution).
8. Make sure all the wells contain 300 μ l of volume. Fill up the wells in the 96-well plate. Columns 2-6, 8-9, and 11 get 150 μ l of the bacterial broth. For the Mueller-Hinton media: column 3 gets 130 μ l, columns 4/8/9 get 140 μ l, and columns 1/7/10 get 300 μ l. Add 20 μ l of the neat AMP solution to Column 3, and 10 μ l to column 4. Add 2 μ l of the 1:10 AMP dilution to column 5 and 2 μ l of the 1:100 AMP dilution to column 6. Add 10 μ l of 6M NaOH to column 9 as 'kill' conditions. 10 μ l of the antibiotic is added to column 8.
9. Use the 96-well plate reader by turning on the device, and the attached computer. Make sure the SoftMax Pro® or an equivalent program is running

and ready to collect data. Set up wavelength to 630 nm, insert the plate into reader, and take a measurement. In between measurements, store the plates on a shake platform at 37°C. Take a reading every half hour for 3 hours, and then after the plate has incubated overnight. Save files as X-PDA format (Softmax only) or open source/ASCII X.csv/x.txt format that can be imported into any analytical software.

C.4.2 Procedure for Antimicrobial peptide Hemolytic Assay Protocol

1. To follow Biohazard protocol, soak any contaminated glassware overnight in 6% bleach solution, to kill all microorganisms. Wash with soap and water and let them air dry. Any blood contaminated sharps must be placed in a properly marked Biohazard container for disposal.
2. Draw whole human blood samples into 3.5 ml tubes containing an anticoagulant, such as Heparin, to prevent blood clot formation, and to facilitate intact red blood cell isolation. Gently mix the samples, spin them down at 800 x g, and wash them several times with filter-sterilized PBS Buffer (100 mM NaCl, 80 mM Na₂HPO₄, 20 mM NaH₂PO₄, pH 7.4) until the supernatant becomes clear. Dilute the washed RBCs with PBS Buffer to a final concentration of 8% (v/v).
3. One type of Hemolysis Assay uses a total of five peptide dilutions. The stock peptide concentrations would be 5 mg/ml (1.71 mM) for LM7-1 and 5 mg/ml (1.67 mM) for LM7-2. Tubes 1-3 get 150 µl of the 8% (v/v) RBC suspension, and Tubes 4-5 get 750 µl. For the AMP solution: Tube 1 (50 µl), Tube 2 (40

μl), Tube 3 (20 μl), Tube 4 (10 μl), and Tube 5 (1 ul). For the PBS Buffer solution: Tube 1 (100 μl), Tube 2 (110 μl), Tube 3 (130 μl), Tube 4 (740 μl), and Tube 5 (749 ul).

4. After making up the assay tubes, make a positive hemolysis control with 750 μl of RBC and 750 μl of 0.020% aqueous Triton X-100 solution to osmotically lyse the RBCs. Make a negative hemolysis control with 750 μl of RBC and 750 μl of PBS buffer to ensure that the buffer does not damage the cells during the course of the assay. Incubate the samples with constant, gentle agitation at 37°C. At selected time points, up to 24 hours, centrifuge a 60 μl aliquot of each sample at 4000 x g for 10 minutes to pellet the intact RBCs. Withdraw 50 μl of the sample supernatant and pipet it into 450 μl of PBS Buffer to dilute the sample tenfold.
5. Use the Genesys 10UV Scanning UV-VIS spectrophotometer by turning on the device. Allow the bulb to warm up for 30 minutes. Insert a quartz cuvette containing PBS buffer into the device and blank the scan. Scan the samples at 419 nm which is the tallest absorbance peak found in soluble hemoglobin. Calculate percent hemolysis using the formula below:

$$\% \text{ Hemolysis} = \frac{(\text{Abs}_{\text{Peptide}} - \text{Abs}_{\text{PBS}})}{(\text{Abs}_{0.020\% \text{ Triton X-100}} - \text{Abs}_{\text{PBS}})} \times 100 \quad (1)$$

BIBLIOGRAPHY

- Andreu, D.; Ubach, J.; Boman, A.; Wåhlin, B.; Wade, D.; Merrifield, R.B.; Boman, H.G. Shortened cecropin A-melittin hybrids. *Federation of European Biochemical Societies*. **1992**, 296, 190-194.
- Ashcroft, A.E. Protein and peptide identification: the role of mass spectrometry in Proteomics. *Natural Products Report*. **2003**, 20, 202-215.
- Bowman, H.G.; Wade, D.; Boman, I.A.; Wåhlin, B.; Merrifield, R.B. Antimicrobial and Antimalarial Properties of Peptides that are Cercropin-Melittin Hybrids. *FEBS Letters*. **1989**, 259, 103-106.
- Chan, D.I.; Prenner, E.J.; Vogel, H.J. Tryptophan- and arginine-rich antimicrobial peptides: Structures and mechanisms of action. *Biochimica et Biophysica Acta*. **2006**, 1758, 1184–1202.
- Chen, Y.; Mant, C.T.; Farmers, S.W.; Hancock, R.E.W.; Vasil, M.L.; Hodges, R.S. Rational Design of α -Helical Antimicrobial Peptides with Enhanced Activities and Specificity/Therapeutic Index. *The Journal of Biological Chemistry*. **2005**, 280, 12316-12329.
- Chou, P.Y.; Fasman, G.D. Empirical Predictions of Protein Conformation. *Annual Review of Biochemistry*. **1978**, 47, 251-276.
- Cole, A.M.; Weis, P.; Diamond, G. Isolation and Characterization of Pleurocidin, an Antimicrobial Peptide in the Skin Secretions of Winter Flounder. *The Journal of Biological Chemistry*. **1996**, 242, 788-792.
- Goraya, J.; Knoop, F.C.; Conlon, J.M. Ranatuerins: Antimicrobial Peptides Isolated from the Skin of the American Bullfrog, *Rana castesbeiana*. *Biochemical and Biophysical Research Communications*. **1998**, 250, 589-592.
- Habermann, E. Bee and Wasp Venoms. *Science*. **1972**, 177, 314-322.

- Hancock, R.E.W. R.E.W. Hancock Laboratory Methods-MIC Determination by Microtitre Broth Dilution Method.
<http://cmdr.ubc.ca/bobh/showmethod.php?methodid=42> (accessed December 1, 2011).
- Hopp, T.P.; Woods, K.R. Prediction of Protein Antigenic Determinants from Amino Acid Sequences. *Proceedings of the National Academy of Sciences of the United States of America*. **1981**, 78, 3824-3828.
- Jia, X.; Patrzykat, A.; Devlin, R.H.; Ackerman, P.A.; Iwama, G.K.; Hancock, R.E.W. Antimicrobial Peptides Protect Coho Salmon from *Vibrio anguillarum* Infections. *Applied and Environmental Microbiology*. **2000**, 66, 1928-1932.
- Jiang, Z.; Vasil, A.I.; Gera, L.; Vasil, M.L.; Hodges, R.S. Rational Design of α Helical Antimicrobial Peptides to Target Gram-negative Pathogens, *Acinetobacter baumannii* and *Pseudomonas aeruginosa*: Utilization of Charge, 'Specificity Determinants', Total Hydrophobicity, Hydrophobe Type and Location as Design Parameters to Improve the Therapeutic Ratio. *Chemistry Biology Drug Design*. **2011**, 77, 225-239.
- Lai, Y.; Gallo, R.L. AMPed up Immunity: How Antimicrobial Peptides have Multiple Roles in Immune Defense. *Trends in Immunology*. **2009**, 30, 131-141.
- Lebl, M. CSPPS Pharmaceuticals: Peptide Companion Software.
<http://www.5z.com/cspps/comer/pcom/> (accessed on April 1, 2010).
- Lee, T.; Choi, J.; Byun, J.; Lee, Y. Preparation of MBHA resin by benzotriazole mediated amidoalkylation. *Tetrahedron Letters*. **2008**, 49, 5380-5382.
- Lequin, O.; Ladram, A.; Chabbert, L.; Bruston, F.; Convert, O.; Vanhoye, D.; Chassaing, G.; Nicolas, P.; Amiche, M. Dermaseptin S9, an α -Helical Antimicrobial Peptide with a Hydrophobic Core and Cationic Termini. *Biochemistry*. **2006**, 45, 468-480.
- Mather, K. *Statistical Analysis in Biology*; University Paperback/Methusen: London, 1965; pp 42-43.

- Merrifield, R.B. Solid Phase Peptide Synthesis. I. The Synthesis of a Tetrapeptide. *Journal of the American Chemical Society*. **1963**, 85, 2149.
- Mor A.; Nguyen, V.H.; Delfour, A.; Migliore-Samour, D.; Nicolas, P. Isolation, amino acid sequence, and synthesis of dermaseptin, a novel antimicrobial peptide of amphibian skin. *Biochemistry*. **1991**, 30, 8824-8830.
- Mor, A.; Hani, K.; Nicolas, P. The Vertebrate Peptide Antibiotics Dermaseptins Having Overlapping Structural Features but Target Specific Microorganisms. *The Journal of Biological Chemistry*. **1994**, 269, 31635-31641.
- NIST Physics Laboratory Atomic Weights/Isotonic Elemental Composition.
http://physics.nist.gov/cgi-bin/Compositions/stand_alone.pl
(accessed on April 1, 2010).
- Patrzykat, A.; Gallant, J.W.; Seo, J.; Pytyck, J.; Douglas, S.E. Novel Antimicrobial Peptides Derived from Flatfish Genes. *Antimicrobial Agents and Chemotherapy*. **2003**, 47, 2464-2470.
- Sakakibara, S.; Shimonishi, Y.; Kishida, Y.; Okada, M.; Sugihara, H. Use of Anhydrous Hydrogen Fluoride in Peptide Synthesis. I. Behavior of Various Protective Groups in Anhydrous Hydrogen Fluoride. *Bulletin of the Chemical Society of Japan*. **1967**, 40, 2164-2167.
- Sarin, V.K.; Kent, S.B.H.; Tam, J.P.; Merrifield, R.B. Quantitative monitoring of solid phase peptide synthesis by the ninhydrin reaction. *Analytical Biochemistry*. **1981**, 117, 147-157.
- Schiffer, M; Edmundson, A.B. Use of Helical Wheels to Represent the Structures of Proteins and to Identify Segments with Helical Potential. *Biophysical Journal*. **1967**, 7, 121-135.
- Scott, M.G.; Yan, H.; Hancock, R.E.W. Biological Properties of Structurally Related α -Helical Cationic Antimicrobial Peptides. *Infection and Immunity*. **1999**, 67, 2005-2009.

- Simmaco, M.; Mignogna, G.; Canofeni, S.; Miele, R.; Mangoni, M.L.; Barra, D. Temporins, antimicrobial peptides from the European red frog *Rana temporaria*. *European Journal of Biochemistry*. **1997**, 272, 12008-12013.
- Strandberg, E.; Tiltak, D.; Ieronimo, M.; Kanithasen, N.; Wadhvani, P.; Ulrich, A.S. Influence of C-terminal Amidation on the Antimicrobial and Hemolytic Activities of Cationic α -Helical Peptides. *Pure and Applied Chemistry*. **2007**, 79, 717-728.
- Stiener, H.; Hultmark, D.; Engström, Å.; Bennich, H.; Boman, H.G. Sequence and specificity of two antibacterial proteins involved in insect immunity. *Nature*. **1981**, 292, 246-248.
- Toke, O. Antimicrobial peptides: new candidates in the fight against bacterial Infections. *Biopolymers*. **2005**, 80, 717-735.
- Yang, D.; Chen, Q.; Oppenheim, J.J.; Kuusela, P.; Taylor, J.W.; Wade, D. Temporin/VesCP (T/V)-like antibiotic peptides, derived from frogs and wasps, induce migration of human monocytes and neutrophils. *Letters in Peptide Science*. **2003**, 10, 99-110.
- Vicente, M.; Hodgson, J.; Massidda, O.; Tonjum, T.; Henriques-Normark, B.; Ron, E.Z. The Fallacies of Hope: Will We Discover New Antibiotics to Combat Pathogenic Bacteria in Time? *Federation of European Microbiological Societies Microbiology Reviews*. **2006**, 30, 841-852.
- Yount, N.Y.; Bayer, A.S.; Xiong, Y.Q.; Yeaman, M.R. Advances in Antimicrobial Peptide Immunobiology. *Biopolymers*. **2006**, 84, 435-453.
- Zasloff, M. Antimicrobial peptides of multicellular organisms. *Nature*. **2002**, 415, 389-395.